Simplified Sizing and Performance Models for Four-Stroke Spark-Ignition Engines for use in Electric Vehicle Range Extenders

A Thesis

Presented in Partial Fulfillment of the Requirements for the

Degree of Master of Science

with a

Major in Mechanical Engineering

in the

College of Graduate Studies

University of Idaho

by

Jason Tyler Brubaker

May 2014

Major Professor: Dean Edwards, Ph.D.

Authorization to Submit Thesis

This thesis of Jason Tyler Brubaker, submitted for the degree of Master of Science with a Major in Mechanical Engineering and titled "Simplified Sizing and Performance Models for Four-Stroke Spark-Ignition Engines for use in Electric Vehicle Range Extenders," has been reviewed in final form. Permission, as indicated by the signatures and dates below, is now granted to submit final copies to the College of Graduate Studies for approval.

Major Professor:	_____ Dean Edwards, Ph.D.	Date: _____
Committee Members:	_____ Steven Beyerlein, Ph.D.	Date: _____
	_____ Dan Cordon, Ph.D.	Date: _____
Department Administrator:	_____ John C. Crepeau, Ph.D., P.E.	Date: _____
Discipline's College Dean:	_____ Larry Stauffer, Ph.D., P.E.	Date: _____

Final Approval and Acceptance

Dean of the College of Graduate Studies:	_____ Jie Chen, Ph.D.	Date: _____

Abstract

The energy storage limitations that currently hinder the marketability of fully-electric vehicles could be overcome with on-board range extenders that consume conventional fuels to generate additional electrical power when needed. This paper presents two simplified tools intended to streamline the initial design of range extender engines.

The first is a simple physics-based model capable of accurately identifying the peak range extender output requirements for highway-capable electric vehicles. The use of this model is demonstrated for three common vehicle types.

The second is a flexible array-based modeling approach capable of performing in-depth simulations of steady-state engine operation. This approach is used to construct a detailed spark-ignition engine model, and this model is used to evaluate the effect of general engine configuration attributes on operation in a range extender. Finally, the design decisions made during the development of existing range extenders are studied, and compared against the results from the engine model.

Acknowledgements

The author would like to thank Dr. Dean Edwards, Dr. Steven Beyerlein, and Dr. Daniel Cordon for their input and assistance during this undertaking; as well as the rest of the outstanding faculty at the University of Idaho who contributed over the past seven years and three degrees.

Dedication

This work is dedicated to my family, as a small token of thanks for their unflagging love, encouragement, and support.

Table of Contents

List of Figures

List of Tables

Chapter 1. Background

In a time of both booming global motor vehicle ownership and growing concerns about the environmental impact of conventional vehicles (CVs) and hybrid-electric vehicles (HEVs) that are completely or primarily powered by internal combustion engines (ICEs), there is a great deal of interest in replacing these fuel-burning vehicles with electric vehicles (EVs) that operate solely on electrical energy obtained from external sources. Unlike CVs that must perform less-than-ideal onboard conversions of very specific fuels, the energy used by EVs can be obtained from any number of renewable and/or nonpolluting sources. Even fossil fuels can be harnessed more cleanly and effectively at stationary facilities. While electricity has historically had a relatively high specific cost (cost per unit energy) as an energy carrier, the specific energy consumption (energy used per unit distance traveled) of EVs is far lower than competing technologies, making operation much more economical overall [1]. The simplicity of electric drives also makes them more reliable and less maintenance-intensive than modern combustion engines and their stepped transmissions, which are becoming increasingly more complex in an attempt to make up for their inherent performance and efficiency limitations.

But despite these advantages, battery-powered electric vehicles (BEVs) have long struggled with getting started in the transportation industry due in large part to the inherent limitations of battery technology. For portable energy storage, traditional combustible fuels retain many advantages.

For a given mass and volume, a fuel tank stores much greater quantities of energy than conventional batteries. Typical fossil fuels contain around 12 kWh/kg, and while much of that energy is wasted due to the efficiency limitations of heat engines, several kWh of usable mechanical energy can still be extracted from each kilogram of fuel [2]. The energy densities of current battery technologies are far lower; current high-energy lithium-based cells top out at 180 Wh/kg, while most other chemistries fall below 100 Wh/kg.

And while there's no inherent limit on the rate at which liquid or gaseous fuel can be delivered to an ICE, power density for batteries is more limited, and for most chemistries comes at the expense of energy density, meaning a battery designed for maximum capacity will deliver that energy at a reduced rate, while a battery designed for high power will have reduced capacity [1]. Also, fuel storage tanks are fairly simple and inexpensive to manufacture, and require very little maintenance over the operating life of the vehicle. Batteries are much more expensive to produce, and degrade with use. If a battery pack's

performance drops below a certain point within the vehicle's service life, the owner is faced with considerable replacement costs.

Perhaps the biggest hindrance with current EV batteries is the issue of restoring the stored energy after it is depleted. A BEV's operating range is limited by the capacity of its battery just as the range of an ICE-powered vehicle is limited by the capacity of its fuel tank; but fuel tanks can easily be refilled in minutes using either well-established fueling infrastructure or simple portable containers, while recharging an EV battery is inherently a much slower process, especially without dedicated charging infrastructure. This is not a major concern for vehicles used for normal short-range commuting and errand-running, as they can be recharged during daily periods of extended non-use, but the prospect of hours-long recharging waits every hundred kilometers or so severely limits the long-range capabilities of current BEVs. This makes them difficult to market to consumers who are accustomed to the freedom afforded by CVs and their established fueling infrastructure. Quick-charging technology is improving, but these chargers are still unable to fully restore an EV battery as quickly as a CV can be refueled, and such advanced charging infrastructure is far from achieving widespread standardization and implementation. Alternate approaches such as physically changing an EV's entire battery pack out for a fresh unit have been proposed and demonstrated, but this type of concept is obviously limited by a number of logistical hurdles that may never be adequately overcome.

A wide variety of experimental and conceptual electrical storage devices and technologies have been proposed for addressing these limitations, but these are largely unproven, under-developed, or otherwise impractical for large-scale implementation in the near future. Limited to conventional technology, manufacturers often upsize EV batteries in order to meet the single-charge range requirements (both actual and perceived) of their customers and extend the pack's service life. The award-winning Model S electric sedan from Tesla Motors was initially offered with three battery options, including an entry-level 40 kWh pack that was estimated to give the vehicle a practical 260 km range for $10,000 less than the mid-level 60 kWh, 370 km battery. Despite the potential savings with the lower-capacity pack, perception of its performance limitations, exacerbated by the scarcity of Tesla's proprietary fast-charging stations, led to such low customer interest in the 40 kWh option that Tesla could not justify the cost of its production. The 40 kWh option was eventually abandoned, and the 60 kWh battery was made the basic option for the Model S. [3]

The Tesla Model S was built and marketed as a luxury vehicle, but for many other market segments, the added expense and mass of a larger pack and its support systems can be as detrimental to a BEV's marketability as range anxiety. To customers looking for practical transportation, an EV with a small battery can be undesirable because of real or perceived operating limitations, while an EV with a large battery is undesirable due to the increased purchase price and reduced daily-driving performance. The initial purchase price of current EVs and HEVs are significantly higher than those of competing CVs due primarily to the cost of the battery, and even if that added expense will pay for itself through reduced lifetime operating and maintenance costs, the more imposing initial investment still hinders a BEV's marketability [4]. Battery prices are expected to decrease as technologies and manufacturing infrastructure are improved, but such progression will be slow unless these vehicles can attain more widespread market acceptance.

A very promising alternative to an overly-expensive, high-capacity battery pack is a range extender (REX). Also called an Auxiliary Power Unit (APU) in certain applications, a range extender is an alternate on-board source of electrical power that runs on conventional and readily-available fuels to extend the operating range of a BEV beyond that afforded by a single battery charge when desired. A BEV equipped with a range extender becomes an Extended-Range Electric Vehicle (EREV).

Unlike other parallel or dual-mode hybrid-electric drivetrain concepts that have limited electric-only capabilities and depend heavily upon an ICE for direct drive power, the ICE in a REX is never used to drive the vehicle directly; it only serves as a prime mover for a generator, and in some cases other secondary accessory systems. As an EREV's battery pack and drive system are similar or identical to those of an equivalent BEV, it is able to achieve full performance without any assistance from the REX as long as the battery is charged. This distinguishes an EREV from other series-hybrid configurations that have similar power flow arrangements, but reduced-power or low-capacity batteries, and frequently require contribution from an active APU for certain types of driving. Thus, an EREV offers the same electric-only range and performance of a BEV, but with the same long-range freedom as a conventional automobile on the rare occasions it is needed.

The self-contained REX and strong electric drive system also allow for a great deal of design freedom and modularity. A single vehicle model can very easily be offered to customers in both BEV and EREV configurations that share a common battery and electric drive. A series-HEV variant with a smaller, lighter battery could also be useful for certain short-range, high-mileage fleet applications such as city taxi vehicles. This adaptability has a

great deal of potential to increase consumer acceptance and market penetration of full-electric drivetrains, and to provide manufacturers with real commercial motivation to improve BEV technologies.

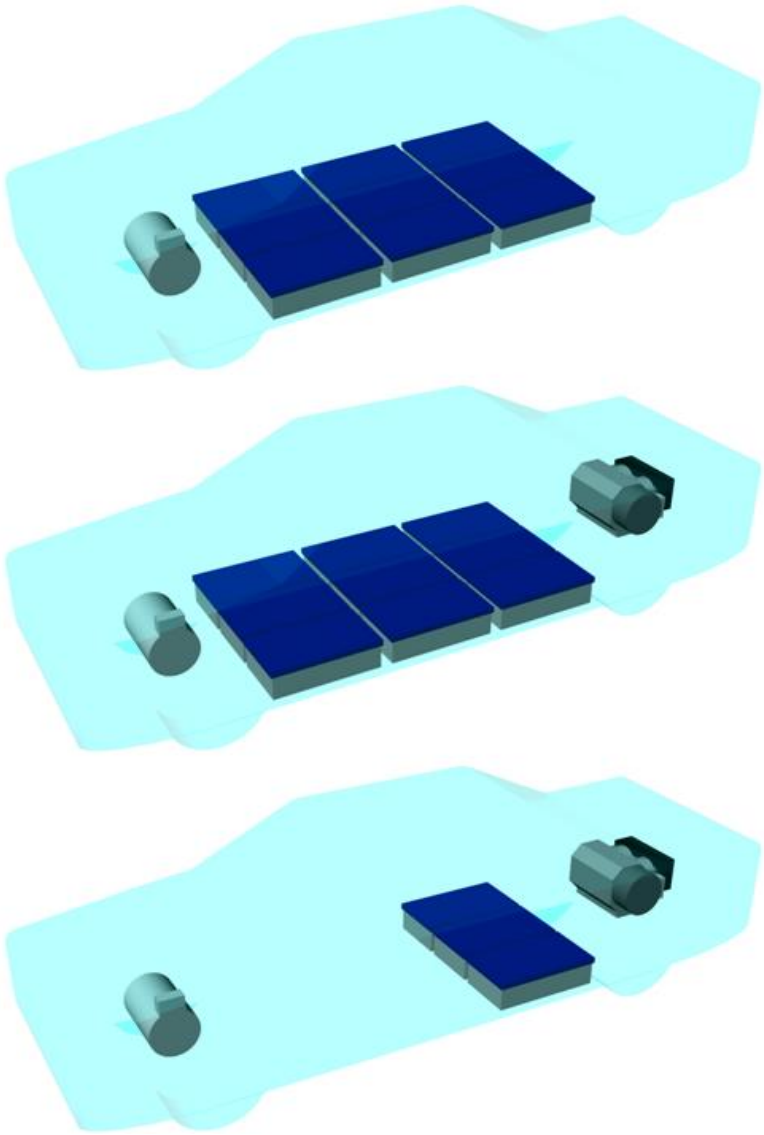

Figure 1.1. Three electric and hybrid-electric vehicle configurations using the same base vehicle with a front-mounted electric drive motor, central battery units, and optional rear-mounted REX. BEV (top), EREV (middle), and series-HEV (bottom).

4-stroke spark-ignition (SI) engines are the most sensible choice for near-term REXs, offering a better balance of specific power, fuel efficiency, and raw pollutant output than other conventional 2- and 4-stroke ICEs [5]. Alternate engine concepts such as microturbines or rotary engines offer potential advantages in REX applications, but currently lack the technological refinement and broad industry support needed to make them realistic options.

4-stroke SI engines have been widely used in transportation and other small-scale mechanical power applications for over a hundred years, so they are well-understood and cost-effective to manufacture.

The construction fundamentals and basic working principles of all 4-stroke SI engines are very similar, but the operating requirements and design priorities of automotive engines used for motive power are inherently more complicated than those of engines used as dedicated prime movers for a generator. ICEs used for direct mechanical propulsion in a vehicle must operate at speeds that are a function of the vehicle's road speed, and produce usable drive torque over the vehicle's entire design speed range. Even with complex multi-ratio mechanical transmissions, this still requires the engine to balance efficiency, steady-state performance, transient response, and emissions over a very wide range of speeds and loads. Hybrid-electric vehicles with operating modes that mechanically tie the ICE to the wheels benefit from electric assists at operating points where their engines are especially inefficient or short on power, but the design and construction of their engines is still as complex as CV engines, often even more so.

The engines in EREVs and full-time series-HEVs, conversely, are completely independent of the road. There is no mechanical link between the crankshaft and the driving wheels, the engine's output is only used to generate electrical power via a matched generator, and occasionally drive accessories. This allows it to be designed for constant-speed operation within a greatly constrained speed and load range, or even at one single operating point. There is no need to prioritize transient response, low-speed torque, high-speed volumetric efficiency, or other performance attributes that have led to such complexity in modern automotive ICEs.

Sizing is fundamentally different as well. While the ICEs in conventional vehicles and many hybrids must be sized for the vehicle's maximum anticipated power and torque needs, an EREV's large battery pack acts as an energy buffer, leveling the fluctuating road-load power demand and only requiring an average power output from the mechanically-independent REX. This allows a much smaller and lighter engine to be used in a REX without limiting the vehicle's performance, and again, alters and simplifies the design process.

So while the operating principles of 4-stroke SI REX engines are much the same as those used for direct drive power, and can benefit from existing design and analysis tools, their fundamentally different and greatly simplified operating requirements could permit initial sizing and configuration to be accomplished using much simpler tools and techniques. The

goal of this paper is to explore this by examining the operating principles and design priorities of 4-stroke SI ICEs specifically intended for use in REXs, developing straightforward math-based models for sizing these engines and simulating their operation, and comparing those tools and the conclusions drawn from them against existing REX concepts.

Chapter 2 will introduce and expand upon various aspects of REX design and operation, to provide a background for the rest of this work. Chapter 3 will present a simplified sizing model that can be used to calculate the maximum required REX power needed for any specific EREV. Chapter 4 will introduce a steady-state engine model developed to simulate the operation of REX engines, which will then be applied in chapter 5 to study the impact of different aspects of ICE design on performance and efficiency in REX roles. In chapter 6, these model-based conclusions will be compared to the design decisions made for various existing REX engines, in order to test the applicability of the model in its current state, and identify areas that should be improved or functionality that should be added. Chapter 7 will conclude this work with suggestions and ideas for refining these models.

References

[1] Pistoia, G, "Electric and Hybrid Vehicles," Elsevier, Oxford, ISBN 978-0-444-53565-8, 2010.

[2] Heywood, J, "Internal Combustion Engine Fundamentals," McGraw-Hill, New York, ISBN 978-1-25-900207-6, 1988.

[3] Pagliery, J, CNN Money, "Tesla expects its first-ever profit," http://money.cnn.com/2013/04/01/news/companies/tesla-profit, April 2013.

[4] "Total Cost of Ownership Model for Current Plug-in Electric Vehicles," EPRI, Palo Alto, CA, 2013, 3002001728.

[5] Turner, J., Blake, D., Moore, J., Burke, P. et al., "The Lotus Range Extender Engine," SAE Int. J. Engines 3(2):318-351, 2010, doi:10.4271/2010-01-2208.

Chapter 2. REX Design and Operation

In this chapter, various aspects of REX design and operation will be introduced and discussed. These principles incorporate preexisting research in addition to original concepts and conclusions in order to establish the design priorities and operating principles that will later be used as a basis for the construction and analysis of models.

2.1. Accessory Integration

While a REX's primary role as a source of electrical power has already been introduced, the waste heat and mechanical power produced by an active REX engine can also be used directly by other vehicle systems. Taking advantage of this to reduce the electrical accessory load can have a measurable impact on an EREV's total energy consumption, and will affect how a REX should be operated to maximize its usefulness.

Heating and cooling systems constitute a major part of a BEV's total accessory power draw. In addition to temperature control of the passenger compartment, a BEV's large, high-power battery pack requires active thermal management to maintain the cells within a proper operating temperature range. Some types of electric drive motors also incorporate liquid cooling systems. In very hot or cold environments that require continuous operation, heating and cooling systems can consume multiple kilowatts of battery power [1]. In an EREV, there are opportunities to reduce or offset these electrical loads when the REX is active, which will reduce the total electrical output that the REX must supply in order to enable sustained driving.

Some of the most significant potential improvements involve heating systems. When active, a REX that uses a liquid-cooled ICE as a prime mover will generate a considerable amount of waste heat that is easily harnessed by routing engine coolant through accessory heat exchangers just as in a CV, though an EREV will still require electric heating systems for when the REX is inactive. Lacking this reliable supply of waste heat, electric BEV heating systems commonly employ resistive heating elements (simple, but wasteful) or electrically-driven heat pumps (better performance, but more complex) that consume far more power than what would be required to circulate engine coolant.

There is also the potential for installing a fuel-fired heater that uses conventional fuel (available from an EREV's existing REX fuel system) to provide heat when the REX is inactive. Fuel-fired heaters have been offered on past EVs to reduce battery power

consumption in cold climates. Depending on the local fuel and electricity prices, regulations concerning emissions and fuel use, and the performance of the electric heating system it would replace, these heaters can offer economy and performance advantages over electric heating [1].

Cooling systems in EVs typically employ compressors driven by electric motors, sometimes as part of a more advanced heat pump system that performs both heating and cooling. Electrically-powered compressors for cooling systems or heat pumps can demand multiple kilowatts, and could potentially benefit from integration with a REX. While the presence of a REX will not fundamentally alter the power requirements of these devices, efficiency gains can be achieved by using the REX engine to directly drive these accessories, eliminating electrical losses as illustrated in figure 2.1. This would obviously reduce the torque available to power the REX's generator, but for the same accessory drive power requirement, the total demand on the engine would be reduced.

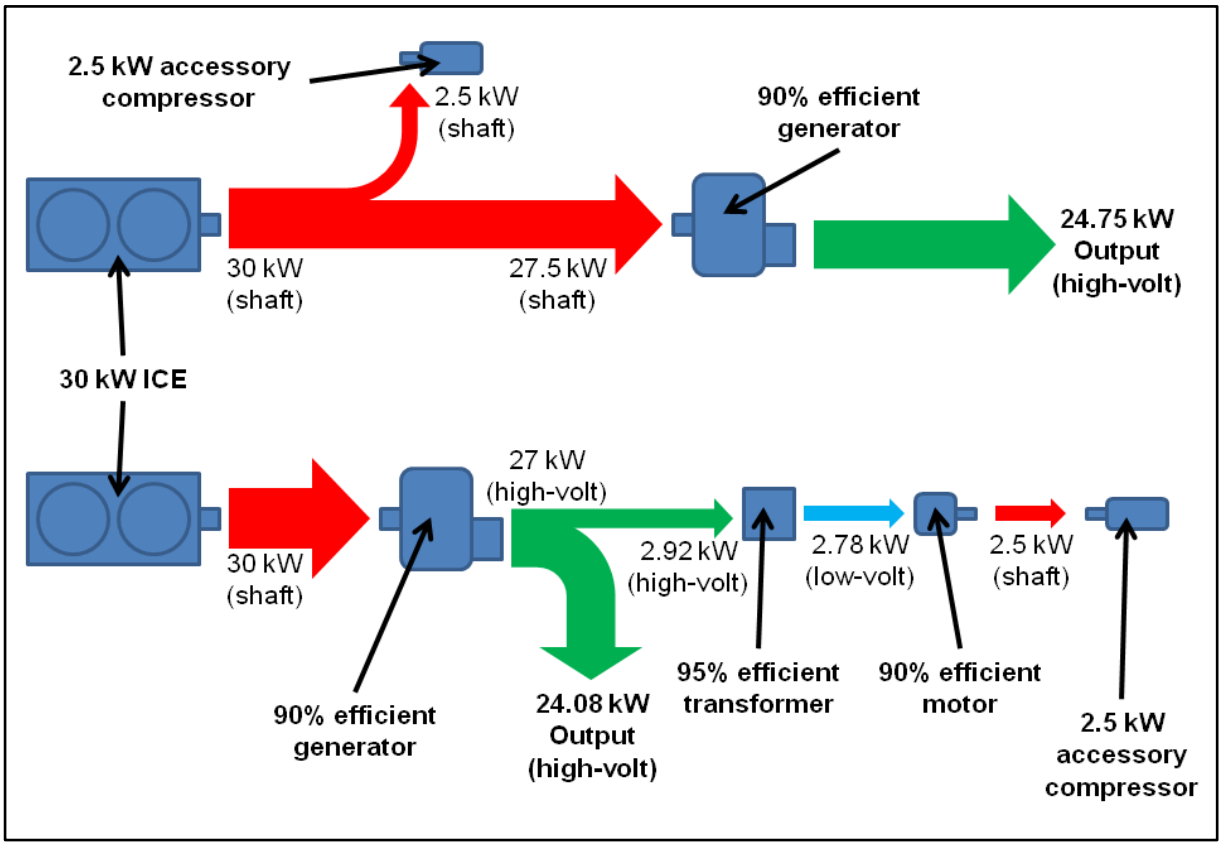

Figure 2.1. REX power flow diagrams and final electrical output with a 2.5 kW accessory compressor that is directly driven (top) and electrically driven (bottom). Adjusted for losses, the electrically-driven compressor effectively consumes 3.24 kW of the engine's brake power.

This can be accomplished with a dual-drive system, where one device can be mechanically driven by both the REX and an electric motor, or by incorporating secondary accessory devices and systems into the REX. Both approaches result in some amount of added weight, complexity, and cost that must be considered along with the potential benefits.

The efficiency of other accessory systems that require a source of mechanical power, such as hydraulic pumps for power brakes and steering, could also be improved by connecting them directly to the REX engine. However these would probably not be worth integrating in most cases, as they do not consume a large amount of power, and often only need to run intermittently. Even many modern CVs use electric motors to drive these devices [1].

2.2. REX Operating Points

The engine in a CV or parallel hybrid must be able to operate effectively over a wide range of speeds and loads since it is mechanically linked to the driving wheels. Because of this, modern ICEs used for mechanical drive power adopt a great deal of complexity in order to ensure satisfactory performance and transient response over the required speed and torque ranges. There is some potential for using lighter, more efficient, smaller-displacement engines, but it is limited by the reduced ability of these smaller engines to produce usable torque over suitable speed ranges.

As discussed in chapter 1, an EREV's electric drive system meets the varying motive torque demand, freeing the REX engine to simply run constantly at fixed operating points to generate the average power needed for a given drive cycle. This allows ICEs designed for REX applications to do away with much of the complexity that conventional automotive engines adopt to expand their effective operating ranges.

The simplest way to take advantage of this is to design a REX to operate at one single, highly-optimized point that provides the maximum desired power output. When reduced power is called for, this type of REX must run intermittently, switching on and off at regular intervals and using the battery as a buffer to achieve the desired average power output. For example, to meet a 21 kW demand, a REX with a single 30 kW operating point would have to be operated on a 70% duty cycle. If the duty cycle has a 20-minute period, the REX would run for 14 minutes and then switch off for the next 6.

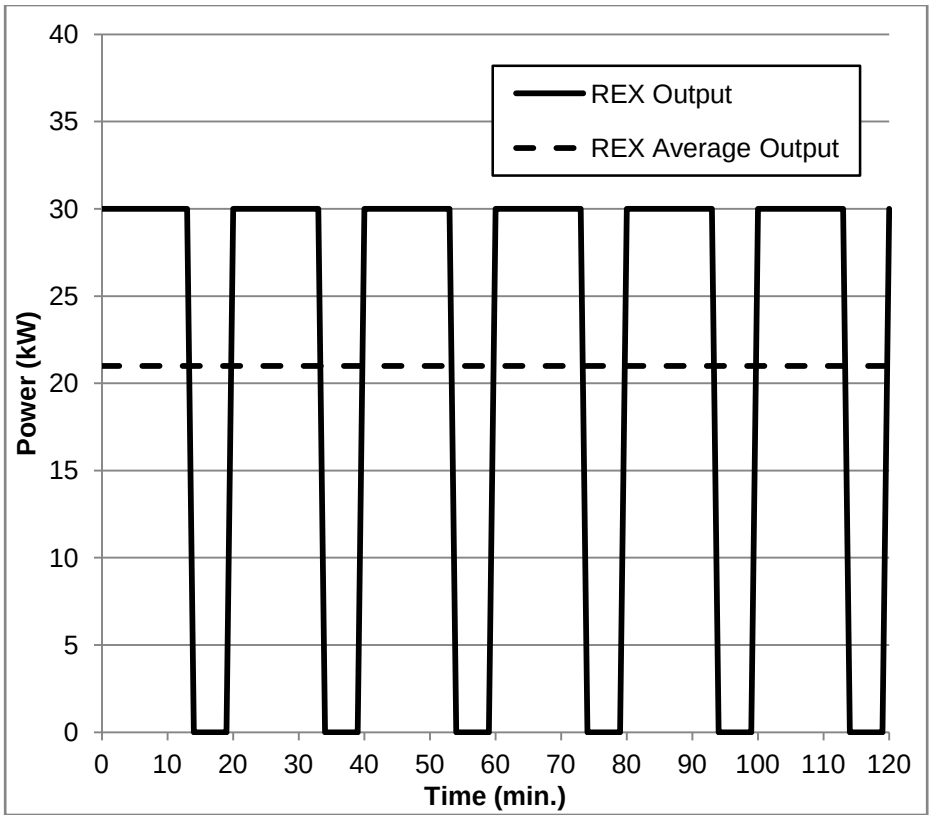

Figure 2.2. Power output versus time for a 30 kW REX meeting an average 21 kW power demand using a 70% on/off duty cycle.

One single operating point allows the ICE, generator, and control system to be very simple and precisely-tuned, but there are a number of disadvantages. Small piston ICEs generally achieve their best specific fuel consumption at low-to-mid speeds, but provide their maximum power at high speeds [2]. If minimizing fuel consumption is a design priority, a REX with a single operating point must use an engine with a displacement large enough for its maximum efficiency point to coincide with the required maximum output - even if it will rarely operate at that point with a 100% duty cycle. The frequent start/stop cycles of a strictly binary on/off duty cycle can also increase fuel consumption, engine part wear, and emissions. The same average REX output could be achieved with fewer start/stop cycles by increasing the period of the duty cycle, but then the battery will be cycled more severely. Finally, a REX operating on a binary duty cycle will not provide continuous accessory heat and mechanical power.

To improve upon these shortcomings, range extenders are often designed with multiple fixed operating points or a constrained range of operating speeds that offer different output levels. When discrete operating points are used, an effective output anywhere

between two points can be met by alternating between them in a high/low duty cycle, again using the battery to smooth out the delivered power. For example, a REX with a max-power 30 kW point and a max-efficiency 15 kW point could meet the 21 kW desired average output from the previous example by running 40% of the time at the 30 kW point, and 60% at the 15 kW point.

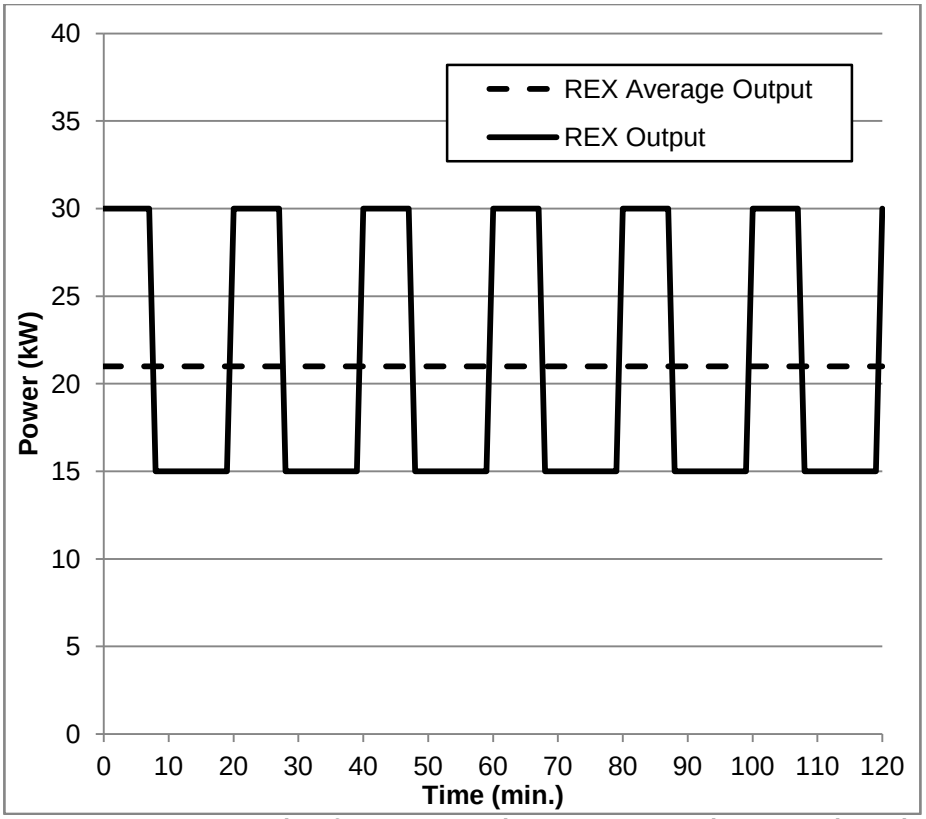

Figure 2.3. Power output versus time for a REX meeting an average 21 kW output by switching between 30 kW and 15 kW operating points on a 40%/60% high/low duty cycle.

This type of duty cycle causes less stress to the battery than a strict on/off cycle, reducing wear and extending its life. While designing and tuning an engine and generator for multiple operating points is slightly more involved than just one, it should still be achievable with a simple engine design, especially if the operating speeds are not wildly different, and prioritize power and efficiency differently.

Continuously-variable load-matched operation within a range of speeds minimizes battery wear as much as possible, but changing speed too frequently in an attempt to precisely match a variable power demand can reduce efficiency, and if a wide speed range is desired, some additional complexity may have to be adopted to ensure effectiveness.

However, good performance and efficiency can generally be achieved without too much added complexity if the speed range is sufficiently narrow.

Both types of multi-speed REX operation will have fewer start/stop cycles, can provide an uninterrupted source of heat and mechanical power for accessory systems, and can meet a maximum output level when necessary without sacrificing specific fuel consumption or being oversized when a reduced output is desired. A less-ideal on/off duty cycle will still have to be adopted if an output less than the minimum operating point is desired, but there will be little need for this if the operating points or ranges are selected to bracket a majority of the vehicle's anticipated power needs. Situations requiring very low REX output would likely be limited to brief periods of low-speed driving, where overall fuel conversion efficiency and extended battery cycling are not major concerns.

2.3. REX Operating Modes

When active, a REX can extend an EREV's range in two distinct ways: charge-sustaining operation, during which the REX meets the vehicle's entire power demand and maintains the battery pack at a more-or-less constant state of charge (SoC), and charge-depleting operation, where the REX output is less than the total power demand, and the battery SoC is allowed to decrease over time. Both have certain advantages.

2.3.1. Charge-Sustaining

In charge-sustaining mode, the REX allows an EREV to operate indefinitely as a series-hybrid vehicle as long as it is kept fueled. This requires a REX that can at least slightly exceed the vehicle's average road-load power requirements over anticipated driving cycles in order to compensate for imperfect regeneration and bring the battery back up to the desired SoC after periods of elevated power consumption.

Most commonly, the REX is simply programmed to maintain the battery above a specific minimum SoC, usually 35% or less [1]. This low-SoC charge-sustaining operation is often the default strategy in REX control software. The EREV operates as a BEV using only battery power until the SoC drops below the predetermined threshold, and then the REX is automatically activated to bring the battery SoC back to - or slightly above - the predetermined minimum and maintain it there. This strategy prioritizes the consumption of electrical energy over fuel by treating the REX as a backup that is used only when the battery

is nearly depleted. While this helps to minimize fuel consumption over any trip, extended driving with the pack at such a low SoC can degrade it more rapidly, and will limit its peak power capabilities. With a REX sized only for an EV's average power, this can lead to lackluster performance when additional power is desired for climbing hills, rapid acceleration, or even higher-speed cruising. The reduced power and harsher battery treatment would likely be acceptable for short periods of lower-speed operation when an EREV unexpectedly needs to be pushed just slightly past its electric-only capabilities, such as an emergency errand in the evening after the vehicle's battery is mostly discharged by the normal daily commute, but few drivers would want to attempt long-range travel this way.

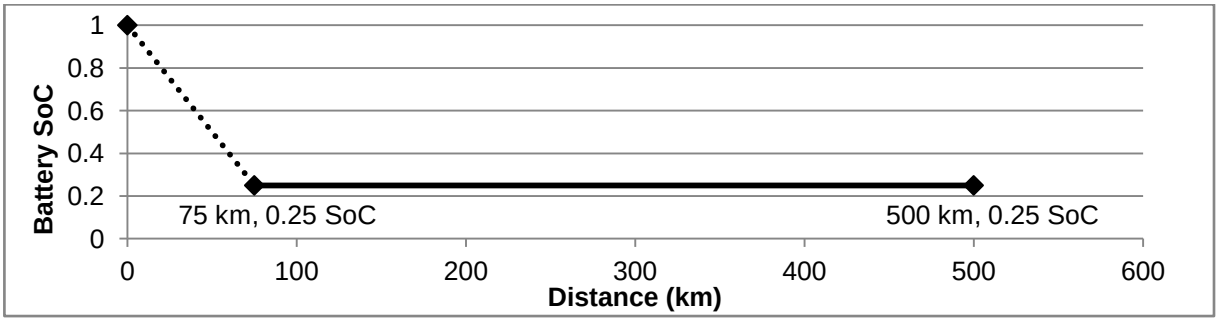

Figure 2.4. Battery SoC versus distance traveled for a long-range trip using low-SoC charge-sustaining REX operation. The dotted line indicates electric-only driving, while the solid line indicates charge-sustaining operation with an active REX.

If it is known ahead of time that the vehicle's electric-only range will be exceeded, the REX can be activated early in the trip, and set to maintain the battery at a high SoC such as 70 or 80%. This leaves some room for effective regeneration and load leveling without risking overcharging the pack, while still providing a large energy buffer that can meet temporarily increased power demands without sacrificing performance, requiring an oversized REX, or overstressing the battery.

High-SoC charge-sustaining operation is often implemented as an optional mode that can be manually activated at the discretion of the driver whenever the battery is below a certain maximum threshold SoC. This strategy may seem unattractive for prioritizing the use of fuel over battery power, but it is not necessarily less fuel-efficient than low-SoC charge-sustaining operation if employed intelligently. If the REX is activated early on to sustain a high SoC during an extended trip, it can still be switched off later on to consume battery energy before the trip is completed. With proper planning, the final battery SoC and total REX running time at the end of the trip will be the same as if a low-SoC strategy was used, but the performance limitations and increased battery wear of extended low-SoC operation will be largely avoided.

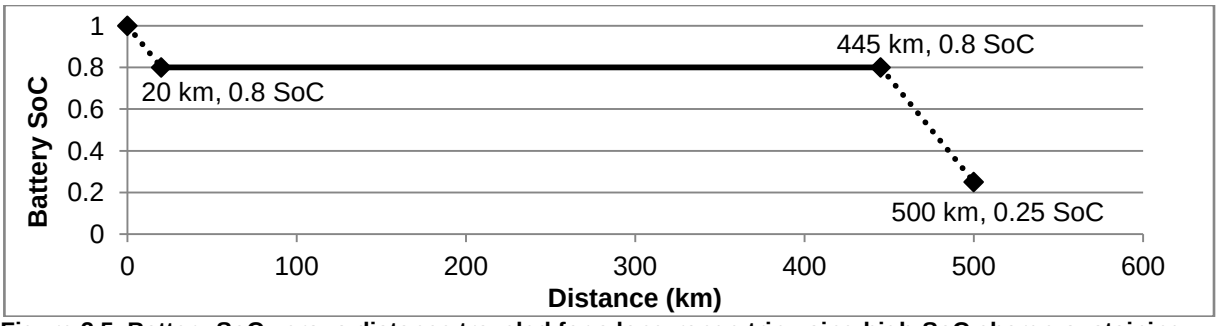

Figure 2.5. Battery SoC versus distance traveled for a long-range trip using high-SoC charge-sustaining REX operation. Note that the final battery SoC and total REX running time with this strategy are identical to the low-SoC strategy shown in figure 2.4, but the battery SoC is kept high for nearly the entire trip.

The trip's total energy consumption (fuel and electricity combined) may be slightly higher if the improved performance is taken advantage of, but most drivers would likely consider this an acceptable trade-off, and maximum-economy driving habits could still be employed if desired.

A potential issue with attempting to minimize fuel consumption with a high-SoC charge-sustaining strategy is that it typically relies on the driver to manually deactivate the REX once the destination is near enough to be reached on the current battery charge. This optimal switch-off time could be difficult to gauge, and erring on the side of caution would tend to lead to late REX deactivation, reducing the battery utilization and increasing the amount of fuel used. A proactive driver could avoid this by purposefully switching off the REX slightly early, allowing the battery to run down, and then finishing the final few kilometers of a trip in low-SoC charge-sustaining mode if necessary. Alternatively, integrating the REX controller with an onboard navigation system could allow the REX switch-off to be automated and better-timed.

Even though high-SoC charge-sustaining operation will not increase fuel use if employed correctly, the idea of allowing drivers to burn fuel when there is still energy in the battery is sometimes discouraged by regulatory organizations seeking to reduce fuel use and emissions. This can affect manufacturers attempting to gain credit for producing electric vehicles, or customers who expect financial incentives when purchasing electric vehicles. As a result, EREV manufacturers may not allow drivers to activate the REX before the battery is depleted, or they may lock out that feature in certain markets for compliance [3].

2.3.2. Charge-Depleting

An alternative to charge-sustaining REX operation is charge-depleting operation, where the average power output from the REX is less than the vehicle's average energy consumption, and the battery charge is depleted over time as it supplies the difference. Because EV-only driving can also be considered to be charge-depleting operation, controlled charge-depleting operation with an active REX is often referred to as blended or hybrid charge-depleting operation to distinguish it. For brevity, the term "charge-depleting" will always refer to REX-assisted operation in this paper, not to EV-only operation where the REX is switched off completely.

In charge-depleting mode, the REX is employed not to facilitate indefinite series-hybrid operation, but to offset a portion of the road-load power and "stretch" the battery's charge. For example, if an EREV requires a constant 24 kW of power while driving, a contribution of 12 kW from the REX will double the vehicle's driving range. If the REX can provide 16 kW, it will triple the range. At 18 kW, the range will be quadrupled.

When a long trip can be planned out ahead of time, charge-depleting strategies maintain a reasonable energy buffer in the batteries and provide uninterrupted accessory power by allowing the REX to operate over the entire trip, while minimizing fuel consumption by ensuring full utilization of the battery's charge by the end of the journey. REX engines are often more efficient when operating at less than maximum output, which can further reduce fuel consumption. As with high-SoC charge-sustaining operation, advanced control software that interfaces with onboard navigation can assist the driver in selecting the proper charge-depleting REX output for a given trip.

In addition to potential efficiency gains, charge-depleting operation could allow a REX to significantly extend an EV's range even in driving situations that exceed its maximum output. For example, a smaller REX sized to provide indefinite range during level highway cruising could still contribute during extended mountain driving or at very high speeds, stretching the battery's capacity far enough to still provide an acceptable driving range between charging stops. An application of this concept will be presented in section 3.4.

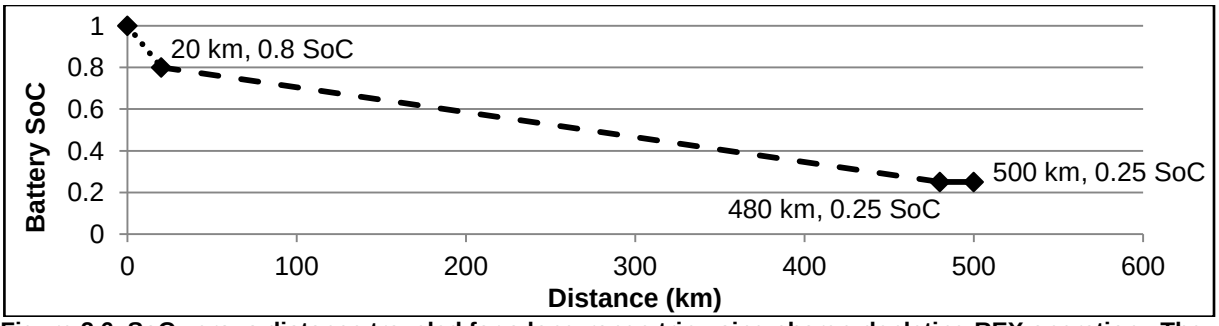

Figure 2.6. SoC versus distance traveled for a long-range trip using charge-depleting REX operation. The dotted and solid lines again represent electric-only and charge-sustaining modes, respectively. The dashed line represents charge-depleting REX operation.

Charge-sustaining and charge-depleting operation can also be combined. For example, the EV-only sections in the charge-sustaining operating strategies discussed previously could be replaced with blended charge-depleting operation. This would allow the REX to provide accessory heat and power over the entire trip and reduce the amount of time spent in a less-efficient high-power mode, but still make full use of the charge in the battery pack by the end of the trip.

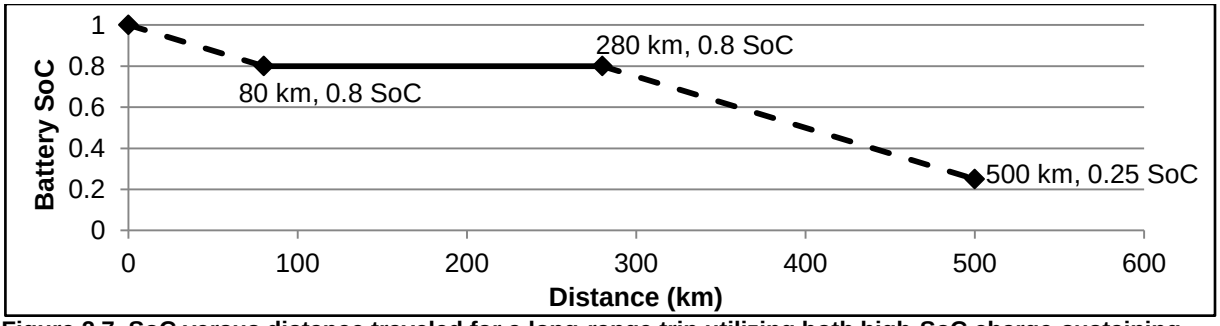

Figure 2.7. SoC versus distance traveled for a long-range trip utilizing both high-SoC charge-sustaining and blended charge-depleting REX operation. Note that, compared to the trip shown in figure 2.5, the final battery SoC and total REX energy consumed are the same, but the REX spends more time in a lower-output mode that can allow for improved fuel conversion efficiency and less component wear.

2.3.3. Other Modes

It is common for a REX to have additional operating modes that are not intended specifically for power generation. These can include startup, diagnostic, and idling modes where the engine is operated at low speed and no load, or partial-load engine warm-up and catalyst light-off modes intended to produce high-temperature exhaust with minimal pollutants in order to bring the engine and catalytic converter up to their proper operating temperatures [4][5].

2.4. REX Trailers

A primary downside of the integral REX in an EREV is that its added mass is always present, and in most cases the vehicle and REX must be specifically designed or adapted for each other. An alternative to an integral REX is a range-extending trailer that incorporates a genset, fuel tank, cooling & support systems, emissions controls, power electronics, and other systems into a self-contained unit that can be towed behind a variety of BEVs. While a REX trailer will add more mass to the overall vehicle system than an integral REX, and will have a greater impact on its aerodynamics, this is offset by the fact that these trailers can be easily removed in minutes when not needed. This could allow BEV owners to simply rent these trailers when needed, rather than paying the full price for an EREV or REX trailer that is only required once or twice a year.

Other advantages to the trailer platform are that it allows for greater standardization; two or three common trailer models with different power outputs could extend the range of a wide variety of BEVs with compatible trailer hitches and electronic connections. And as separate, self-contained units, these trailers offer a flexible platform that could easily be used to explore other range-extending concepts such as improved ICE designs, microturbine or rotary engine gensets, fuel cell APUs, or supplemental battery packs; and implement them with any compatible BEV with no modifications to the vehicles themselves.

An excellent proof of this concept is the LongRanger series of prototype range-extending trailers (RXTs) developed by AC Propulsion between 1992 and 2001.

Figure 2.8. An AC Propulsion LongRanger RXT attached to a Toyota RAV4 BEV.

The 3rd generation trailers were built around a 2-cylinder, 489 cm^3 Kawasaki EX500 motorcycle engine that operated at 7000 RPM to supply 20 kW of continuous electrical

power to the vehicle towing it. Fuel was stored in a 34-liter tank that was sealed against evaporation, and the entire package was contained in a streamlined housing set with supplemental brake and indicator lights. The alternator was based on an AC Propulsion 70 kW AC-150 traction motor that was shortened and modified for the reduced-power 20 kW operation. It was able to run at over 90% efficiency, and many of its parts and production steps remained the same as the base motor, presenting obvious manufacturing advantages.

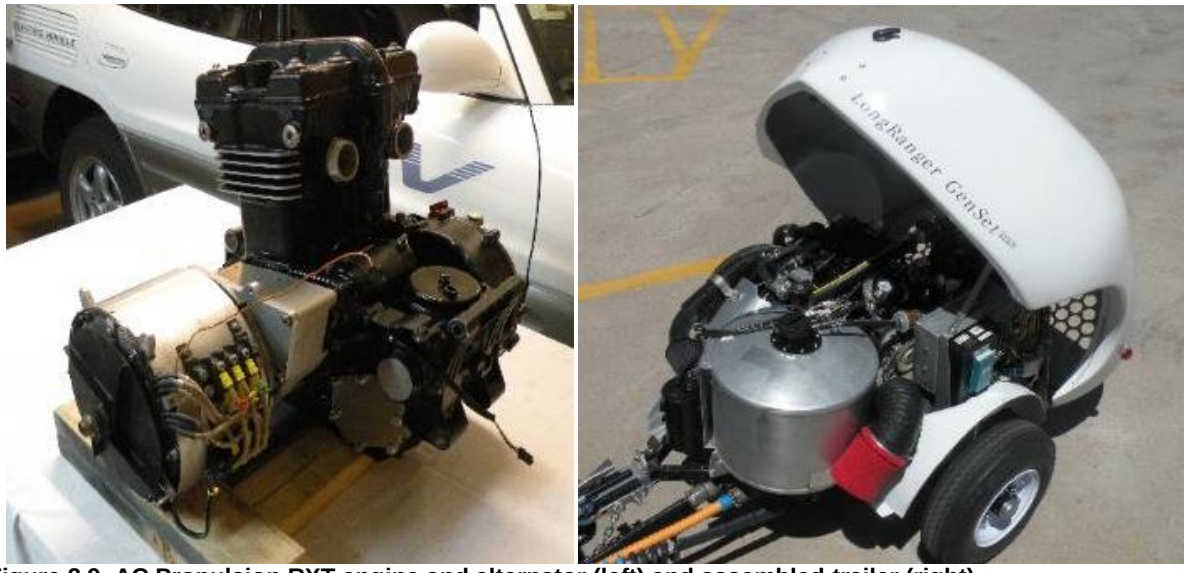

Figure 2.9. AC Propulsion RXT engine and alternator (left) and assembled trailer (right).

These trailers also offered solutions to secondary technical and logistical issues with the range-extending trailer concept. With a mass of only 160 kg and a length of 1220 mm, these low-sitting trailers had a minor impact on vehicle performance and were easy for a single person to move around when separated from the vehicle, but the short length, wheelbase, and height also made it difficult to control during certain maneuvers and potentially unstable at high speeds. To address this, an intelligent steering system was devised that sensed the yaw angle at the hitch, and automatically adjusted the angle of the trailer's wheels to maintain stability and position during both forward and reverse driving.

The 3rd-generation RXT has seen over 5000 kilometers of road testing with multiple BEVs, as well as laboratory emissions testing. Its overall specific fuel consumption (including generator efficiency) at full output was measured at 370 g/kWh [5].

Figure 2.10. ACP LongRanger III RXT attached to an ACP TZero BEV sports car.

This demonstrates the efficiency advantages inherent to EREVs. Despite the relatively high BSFC, it was still able to meet a typical road-load power demand of 125 Wh/km with an effective charge-sustaining fuel mileage of 5.5 l/100 km (38 mpg), and mileage below 2.9 l/100 km (80+ mpg) with charge-depleting strategies [5].

An updated design incorporating a purpose-designed REX genset could offer even better mileage, and allow automakers to broadly improve the market appeal of an entire line of BEVs without the production challenges of designing and manufacturing separate EREV variants of each individual vehicle.

2.5. REX Design Priorities and Considerations

The following is a brief overview of major REX design priorities and considerations. These priorities are arranged in a typical order of importance for a REX design, but this order may change depending on the specific application.

2.5.1. Mass

The mass of a REX is a primary concern, as a vehicle's energy consumption is directly related to its total mass. Even when inactive, the added mass of an integral REX and its support systems, or an attached REX trailer will make an EV less efficient than an otherwise-equivalent BEV. The effective added mass of a REX can be even greater than the total mass of its components if a BEV requires significant structural reinforcements or suspension enhancements in order to accommodate it. In addition, the more a BEV has to be modified to accept a REX, the more complex and expensive it will be to produce BEV and EREV versions of the same vehicle.

Mass can be saved by using lightweight materials such as aluminum or magnesium for large engine components, and by employing advanced structural design techniques that

reduce the amount of material used. The mass of a REX can also be offset if its installation allows a smaller, lighter battery pack to be used, though the vehicle still needs to have a usable range and sufficient power in EV-only mode.

The quantitative relationships between vehicle mass and energy use will be studied in greater detail in the next chapter.

2.5.2. Cost

As a REX and its associated systems are additions to a BEV, not replacements for any entire system, their added expense is a major factor in the marketability of an EREV. The payback period for a REX depends on how frequently it is used, so since an EREV will do most of its driving on battery power alone, a REX will tend to justify its cost rather slowly. The payback period of a REX will also be extended by the engine's need for periodic oil changes, replacement parts, and other added maintenance that is not normally required for normal BEVs.

Another factor that can increase the purchase price of an EREV over an equivalent BEV is government regulations and incentives. Financial incentives for HEVs and especially EVs are currently very common, but their value for a given vehicle can vary depending on how it is classified by local agencies. If EREV and BEV variants of the same vehicle model are classified differently, and the EREV is not awarded the same financial incentives, the difference is effectively added to the cost of the REX. Both the design parameters (output power, efficiency, emissions, fuel storage capacity) and operation (running modes, degree of driver control, prioritization of fuel vs. battery energy) may play a part in how an EREV is categorized.

Due to all this, it is important to make a REX as cost-effective as possible, and there are many opportunities for accomplishing this. The role's straightforward operating requirements allow purpose-designed REX engines to be much smaller and simpler than modern CV engines, reducing development and production costs. Alternatively, retrofitting existing production engines, electric machines, and other components can reduce the effective cost of a REX, especially during production start-up.

As with mass, the cost of adding a REX to a BEV can also be offset if it allows a smaller, less-expensive battery pack to be marketed to customers without incurring range anxiety. Turner et al. [6] estimated in 2010 that the assembled cost of EV batteries would be $300 per kWh or greater for near-future production vehicles. In the case of the Tesla Model

S discussed in chapter 1, customers were overwhelmingly willing to pay $10,000 extra for the 370 km, 60 kWh battery over the 260 km, 40 kWh battery (which comes to $500 per kWh) [7]. Given that studies estimate the average daily driving distance of household vehicles in the US to be merely 63.6 km, and 93% of US vehicle total daily driving distance (on days they are used) to be below 161 km [8], this can largely be attributed to range anxiety. Even if it is rarely used, the security of having a REX just in case it's needed can help increase market acceptance of EV drivetrains, especially among first-time customers.

2.5.3. NVH

Noise, vibration, and harshness (NVH) are undesirable side effects of the reciprocating internals and combustion processes inherent to SI engines. High NVH can have a negative impact on the comfort of the vehicle's occupants, and can be disturbing to nearby individuals outside the vehicle as well. As smoothness and low noise are selling points for electric vehicles, high NVH from a REX can be especially jarring and unpleasant.

A large amount of unwanted engine noise is a result of its combustion and exhaust processes. Sound from these sources can be reduced by lowering the operating speed of the engine, and by effectively muffling or silencing the exhaust. Since a REX engine typically operates at fixed loads and predetermined speeds or narrow speed ranges, mufflers tuned for a specific frequency range can be very effective. Another common measure is to have the REX shut off or run at a reduced speed during low-speed or stop-and-go driving where engine noise would be most noticeable to occupants or bystanders, and where maximum REX output is rarely called for anyway. During high-speed driving situations where peak REX output is necessary, engine noise inside the vehicle is camouflaged by increased road and wind noise, and the comfort of nearby pedestrians is not a major concern.

Vibration can be more difficult to alleviate than noise for REX engines, as many cylinder arrangements used for small-displacement applications are inherently unbalanced (this will be discussed in greater detail in chapter 5). Unbalanced ICEs used in motor vehicles often employ accessory balance shaft systems to counteract out-of-balance forces and moments, but these systems can increase the cost, friction, and mass of an ICE. Out-of-balance vibrations can be reduced by operating the engine at lower speeds, choosing a better-balanced cylinder arrangement and crank design, and reducing the mass of the reciprocating components. If these measures can reduce out-of-balance forces enough, the remainder can often be acceptably absorbed by vibration-dampening engine mounts that

isolate the REX from the vehicle's structure. This is especially applicable in EREVs since the REX does not need to be rigidly connected to the driveline as the engine in a CV does.

2.5.4. Size

The spatial volume taken up by a REX and its support systems is an important, though often secondary design consideration. Whenever possible however, a small REX package volume is desirable, especially if it will be used to convert a pre-existing BEV that was not initially designed to accommodate a REX. The shape of the REX must be considered along with its total volume, though the optimal shape will obviously depend on the specific application. Both volume and package shape are largely influenced by the displacement and cylinder configuration of the engine. Other factors include the dimensions of the generator, the design of the intake and exhaust systems, and the structural elements used to mount the REX. Items such as the fuel tank and cooling system also take up space in the vehicle, but these components are much more flexible because they need not be integral to the REX's core engine/generator assembly (or genset), and have fewer inherent geometric design constraints.

Compact cylinder arrangements, close-fitting or cast-in manifolds, low-profile overhead valvetrains, and a reduced-length generator are effective methods for decreasing the total volume of a REX.

2.5.5. Efficiency

The total brake fuel conversion efficiency of a REX engine is given much attention, but it is not generally a top priority. If a REX will only be used occasionally, the consequences of reduced fuel efficiency are greatly diminished. This gives any EREV an advantage from an emissions regulations standpoint, and since the customer will have to purchase very little fuel compared to a CV, the theoretical fuel mileage is less of a concern. Beyond that, a REX engine already enjoys significant efficiency advantages over engines in CVs due to its greater design flexibility and how it is operated [6]. Even after electrical losses, an EREV's charge-sustaining fuel mileage (the amount of fuel consumed per distance traveled) will generally be equal to or greater than that of similar CVs and HEVs. When charge-depleting modes are used, the effective fuel mileage can be much higher [5].

So while improving the efficiency of a REX engine is desirable, and will receive much attention in later chapters, cost-effectiveness, NVH, and mass are generally higher priorities.

References

[1] Pistoia, G, "Electric and Hybrid Vehicles," Elsevier, Oxford, ISBN 978-0-444-53565-8, 2010.

[2] Heywood, J, "Internal Combustion Engine Fundamentals," McGraw-Hill, New York, ISBN 978-1-25-900207-6, 1988.

[3] Voelcker, J., Green Car Reports, "2014 BMW i3 Electric Car: Why California Set Range Requirements, Engine Limits," http://www.greencarreports.com/news/1087888_2014-bmw-i3-electric-car-why-california-set-range-requirements-engine-limits, Oct. 2013.

[4] Bassett, M., Hall, J., OudeNijeweme, D., Darkes, D. et al., "The Development of a Dedicated Range Extender Engine," SAE Technical Paper 2012-01-1002, 2012, doi:10.4271/2012-01-1002.

[5] Gage, T.B., Bogdanoff, M.A., "Low-Emission Range Extender for Electric Vehicles," AC Propulsion Inc.

[6] Turner, J., Blake, D., Moore, J., Burke, P. et al., "The Lotus Range Extender Engine," SAE Int. J. Engines 3(2):318-351, 2010, doi:10.4271/2010-01-2208.

[7] Pagliery, J, CNN Money, "Tesla expects its first-ever profit," http://money.cnn.com/2013/04/01/news/companies/tesla-profit, April 2013.

[8] van Haaren, R., " Assessment of Electric Cars' Range Requirements and Usage Patterns based on Driving Behavior recorded in the National Household Travel Survey of 2009," Earth and Environmental Engineering Department, Columbia University, July, 2012.

Chapter 3. REX Sizing Model

One of the very first steps in developing an engine for a specific application is determining the maximum output power needed to fulfill that role. For any type of automotive application, the required engine power is directly dependent on the tractive power needed for the vehicle to achieve its desired performance capabilities, but the specific performance capabilities that drive a REX engine's maximum required output are significantly different from those that drive the maximum required output of a CV engine. The software-based drive cycle simulation techniques currently used to size automotive engines, while applicable to some aspects of EREV design, are overly-complex for simply calculating the maximum output requirements of their REXs. There exists potential for the development of more direct and streamlined tools and techniques that can be used to size REX engines for specific EREVs.

In this chapter, a simple, math-based approach to REX sizing will be presented and demonstrated. First, the general road-load power relationships that form the basis for this approach will be introduced, and the performance criteria that dictate the maximum power requirements for a REX engine will be defined, with some discussion on how they differ from the critical requirements for CVs. Then, these principles will be used to study the sensitivity of those power requirements to various design, environmental, and operating factors for typical EREV classes. Based on that study, a set of applicable performance criteria will be developed, and used to determine the maximum required REX engine power for various EREVs.

3.1. General Road-Load Power Relationships

The theoretical tractive force required to propel a vehicle with a given speed and acceleration is equal in magnitude to the sum of the forces opposing that behavior [1][2]. When discussing them, these forces will be regarded as resistive forces, with a positive sign indicating a force that opposes the velocity of the vehicle. The four types of resistive forces that must be overcome by a road vehicle's tractive force are rolling resistance, aerodynamic drag, gravity, and inertia.

3.1.1. Rolling Resistance

Rolling resistance represents the energy absorbed by cyclical tire deformation and friction in and between the wheels, wheel bearings, and road surface while the vehicle is in motion. As such, this force always opposes a vehicle's motion. Rolling resistance can change significantly due to environmental conditions, tire construction and pressure, and vehicle weight. It also varies with speed, but this effect is relatively minor, and rolling resistance forces for typical road vehicles can be modeled as independent of speed during normal operation. The total resistive force will be calculated here as the product of an empirical constant based on wheel and tire design, and the total normal force between the wheels and the road surface. This normal force is often simply assumed to be the weight of the vehicle, but on inclined roads the vehicle's weight can be multiplied by the slope's cosine to arrive at a more accurate value [3].

$$F_{rr} = C_{rr} * m_v * g * \cos(\alpha) \tag{3.1}$$

where

C_{rr} = coefficient of rolling resistance
m_v = vehicle mass in kg
g = gravitational acceleration in m/s^2
α = angle of slope relative to horizontal

3.1.2. Aerodynamic Drag

Aerodynamic drag is caused by fluid friction and pressure effects that resist the relative movement of a vehicle through the surrounding air. While total fluid drag incorporates multiple interactions that behave differently at different speeds, the total drag force for typical road vehicle shapes and speeds can be well-approximated with a simplified model in which the vehicle's shape is characterized by a constant drag coefficient determined through experiments or simulations. The drag force is proportional to the density of the surrounding air, the frontal area of the vehicle, and the square of the vehicle's relative velocity through the air. This relative velocity is often assumed to be equal to the vehicle's

road speed, but here the effect of a sustained head-wind is included for later sensitivity analyses. Aerodynamic drag always opposes a vehicle's relative motion, and thus will always be a positive restive force except in the case of a sustained tail-wind (which would be entered here as a negative head-wind) that is faster than the vehicle's road speed.

$$F_{ad} = .5 * \rho_a * C_{sd} * A_f * (V + V_w)^2 \quad (3.2)$$

where

ρ_a = air density in kg/m^2
C_{ad} = the aerodynamic drag coefficient for the vehicle's shape
A_f = vehicle frontal area in m^2
V = vehicle road speed in m/s
V_w = opposing wind speed in m/s

3.1.3. Gravity

When a vehicle is operated on an inclined surface, with a velocity component in the vertical direction, a portion of the vehicle's weight will directly oppose or encourage its motion. The gravitational force can be a positive or negative resistance depending on the vehicle's direction of travel, and its magnitude is proportional to the vehicle's weight, and to the sine of the angle between the vehicle's velocity vector and the horizontal plane. To ensure that the force will have the proper sign, upward travel on a slope is described by a positive angle.

$$F_g = m_v * g * \sin(\alpha) \quad (3.3)$$

When a grade is defined as a ratio or percentage of rise-to-run, its exact angle can be calculated by taking the inverse tangent of that ratio. For typical road grades of 10% or less, the rise-to-run ratio is also approximately equal to both the slope's angle in radians, and to the sine of that angle, but the more precise relation will be used here.

$$\alpha = \tan^{-1}\left(\frac{rise}{run}\right) \tag{3.4}$$

3.1.4. Inertial Forces

Inertial forces arise due to a gain or loss of linear and rotational kinetic energy when the vehicle's speed changes, and will have the same sign as the vehicle's acceleration. Inertial resistance is simply the product of the vehicle's inertial mass and its first time-derivative of velocity.

$$F_i = m_v * \dot{V} \tag{3.5}$$

In addition to the rest mass of the vehicle, a precise model will also include the rotational inertia of the wheels, engine, transmission, and all other rotating components that are directly tied to the road through the wheels. This, however, requires very detailed information (or assumptions) about the vehicle being studied.

3.1.5. Total Road-Load Power

The sum of all external forces can be directly equated to the responding motive force that must be exerted by the vehicle's propulsion system. A positive net resistive force requires a positive drive force, while negative external resistance will require a negative braking response.

$$F_r = F_{rr} + F_{ad} + F_g + F_i \tag{3.6}$$

where

F_r = total resistive force in N

The tractive power demanded at the wheels can be calculated by multiplying the road speed of the vehicle by the total demanded tractive force.

$$P_r = F_r * V \tag{3.7}$$

where

P_r = ideal road-load power in kW

This theoretical drive power must be adjusted by the overall efficiency of the drive system to account for losses between the engine or battery and the wheels, and combined with the additional power draw of any non-tractive accessory systems to determine the vehicle's total power demand.

$$P_{total} = \frac{P_r}{\eta_{drive}} + P_{acc} \tag{3.8}$$

Dividing this total power by the vehicle's road speed in kilometers per hour will give the energy consumption per unit distance traveled. The reciprocal of energy consumption gives the distance traveled per unit energy. Both figures are useful for judging a vehicle's efficiency and range.

$$E_{Wh/km} = \frac{P_{total}}{V_{kph}} \tag{3.9}$$

3.2. REX Sizing Criteria

The maximum tractive power requirements for road vehicles are usually determined by their desired maximum speed, gradeability, or acceleration; with the latter often requiring the highest maximum power for typical passenger vehicles that are not designed for very high-speed driving or hauling heavy loads [3]. For CVs and HEVs with direct-drive engine modes, these peak instantaneous power demands are what their ICEs must be sized for, even though those peaks represent a very small portion of their operation. But in an EREV, all tractive power comes from the electric drive, and the substantial battery levels out any

power peaks, so the REX need only be sized relative to the average energy consumption over the most power-intensive drive cycle it is expected to be used in.

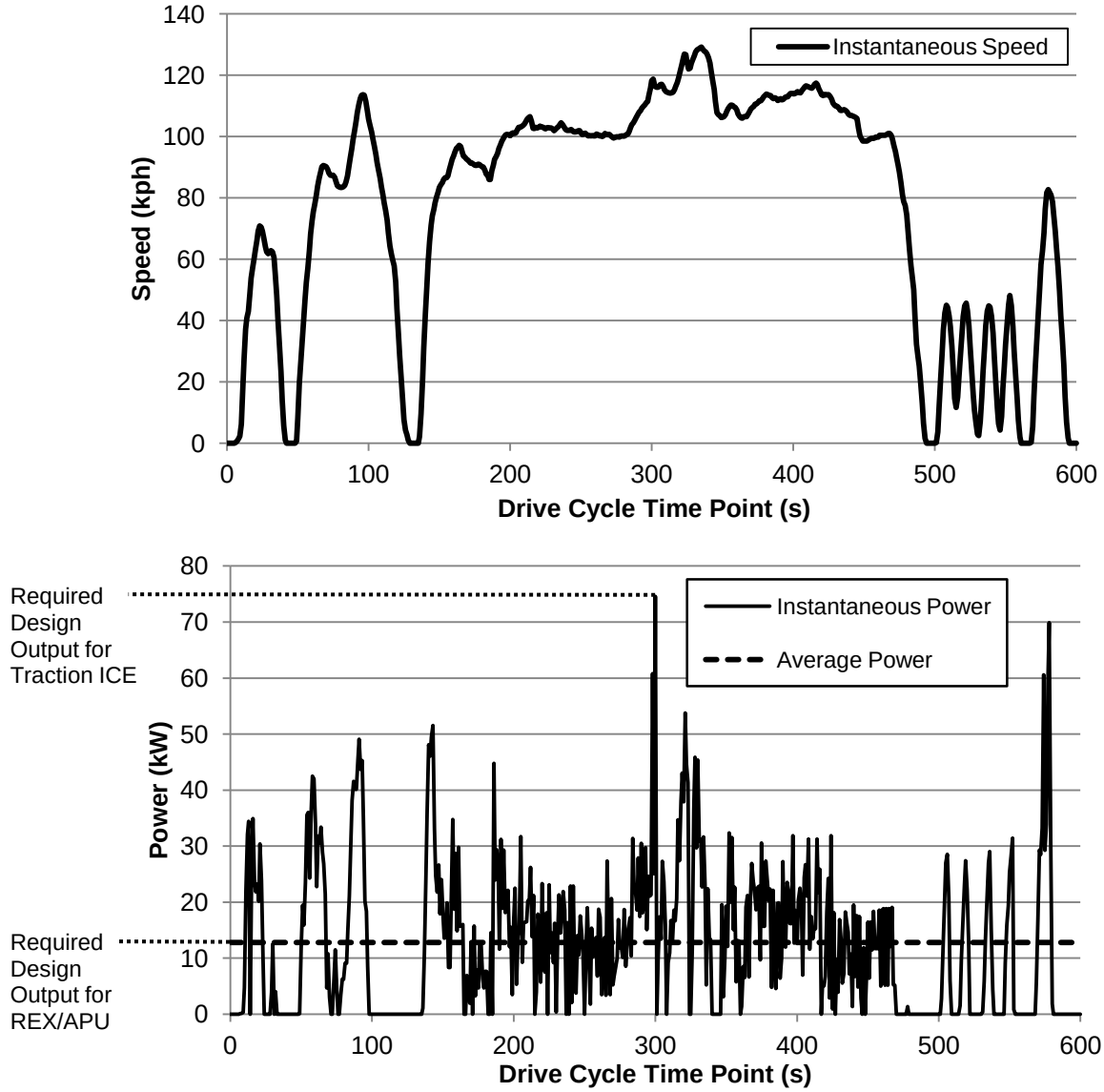

Figure 3.1. Plots of instantaneous speed (top) and power (bottom) for a vehicle operating over an aggressive drive cycle.

In 2010, Basset et al. [4] presented the results of an in-depth study that examined the auxiliary power needed for effective range-extension of EREVs over a variety of drive cycles. Their simulations showed that charge-sustaining operation during constant-speed cruising at high speeds required similar or higher REX output than other standard drive cycles.

Time-step simulations over standard drive cycles are still useful for sizing an EREV's electric drive system and predicting its energy consumption and effective range during real-world driving, but sizing the REX can be accomplished with a much simpler examination of road-load power during high-speed driving. This simplifies calculations to straightforward steady-state relationships that do not require advanced software, integration over complex driving cycles, or detailed information about a specific vehicle's regenerative capabilities or inertial characteristics.

3.3. Road-Load Power Sensitivity Analysis

This section will study the relative importance of aerodynamic drag, rolling resistance, grade, and accessory power demands on constant-speed road-load power for common classes of EREVs, and examine the sensitivity of road-load power to various environmental and operating parameters. The results from these simulations will aid in establishing the specific performance criteria that will be used to determine the exact REX power requirements for each type of vehicle.

Based on the relationships presented in the preceding section, the total power equation for constant-speed operation is as follows:

$$P_{total} = \left(F_{rr} + F_{ad} + F_g\right) * \frac{V}{\eta_{drive}} + P_{acc} \tag{3.10}$$

This equation neglects inertial forces, since the time derivative of velocity will always be zero if speed is held constant. It also does not properly calculate reverse power flows during regenerative braking, as that is not particularly relevant here, and would require additional assumptions about the design of the drive system and a more complex model.

Representative vehicles from three common classes of EREVs were selected for study here, a compact vehicle, a mid-size sedan, and a mid-sized SUV. Inputs for each vehicle type are summarized in table 3.1, and were based on PHEV models generated by the EPRI for drive cycle simulations [5][6].

Vehicle Type	Mass (kg)	C_rr	A_f (m^2)	C_ad (base)	C_ad (optimized)	Base Accessory Load (W)	AC/Heating Accessory Load (W)	Usable Battery Capacity (kWh)
Compact	1381	0.008	1.974	0.315	0.19	400	1000	15.45
Mid-Size Sedan	1782	0.008	2.174	0.327	0.24	500	2000	17.94
Mid-Size SUV	2546	0.006	2.84	0.41	0.3	600	2500	23.37

Table 3.1. Input parameters for the vehicle types simulated.

The base aerodynamic coefficients selected by the EPRI for these vehicles were not based on the current state-of-the-art, so to study the potential of improved body design, optimized drag coefficients were selected from similar existing EVs that were specifically designed for reduced drag. For the compact vehicle, the GM EV1's coefficient of .19 was selected [7]. For the sedan, a coefficient of .24 was borrowed from the current-production Tesla Model S [8]. For the SUV, a coefficient of .3 was selected from the 2014 Toyota RAV4 EV [9].

3.3.2. Baseline Road-Load Power

The baseline power demands for each vehicle type were calculated for constant-speed driving at up to 150 kph (93.2 mph) on a dry, level road with a low accessory power draw. All simulations assumed a gravitational acceleration of 9.81 m/s^2, an air density of 1.2 kg/m^3, and electric drive systems that were 90% efficient at all speeds. The resultant total and component power demands are plotted relative to road speed in figure 3.2.

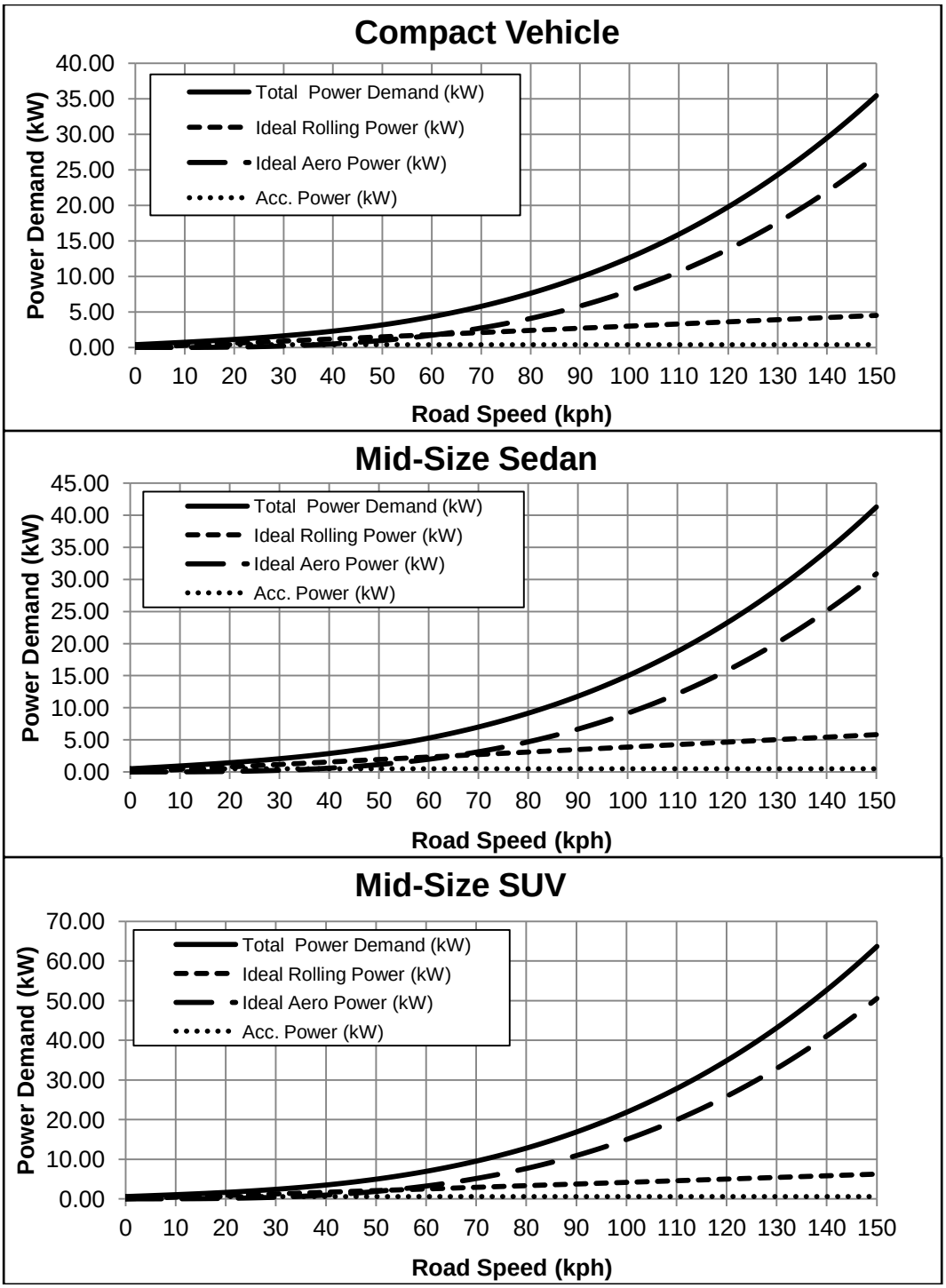

Figure 3.2. Break-down of total baseline power requirements for each vehicle type during constant-speed driving in ideal conditions.

In each case, aerodynamic drag was clearly the dominant component at higher speeds, especially for the SUV with its large frontal area and high drag coefficient. The effect of drag power scaling with the cube of velocity explains why high-speed driving is more

energy-intensive than other drive cycles for EVs, which have more consistent drive efficiencies than CVs, and do not lose as much energy during idling and braking.

3.3.3. Aerodynamic Optimization

Because aerodynamic drag forces were so overwhelmingly dominant at highway speeds, the potential benefits of aerodynamic improvements warranted examination. Total speed-power curves were generated for base and low-drag versions of each vehicle type, with all other model inputs kept at their base values. As expected, the improved aerodynamics significantly reduced the high-speed power demand for each vehicle.

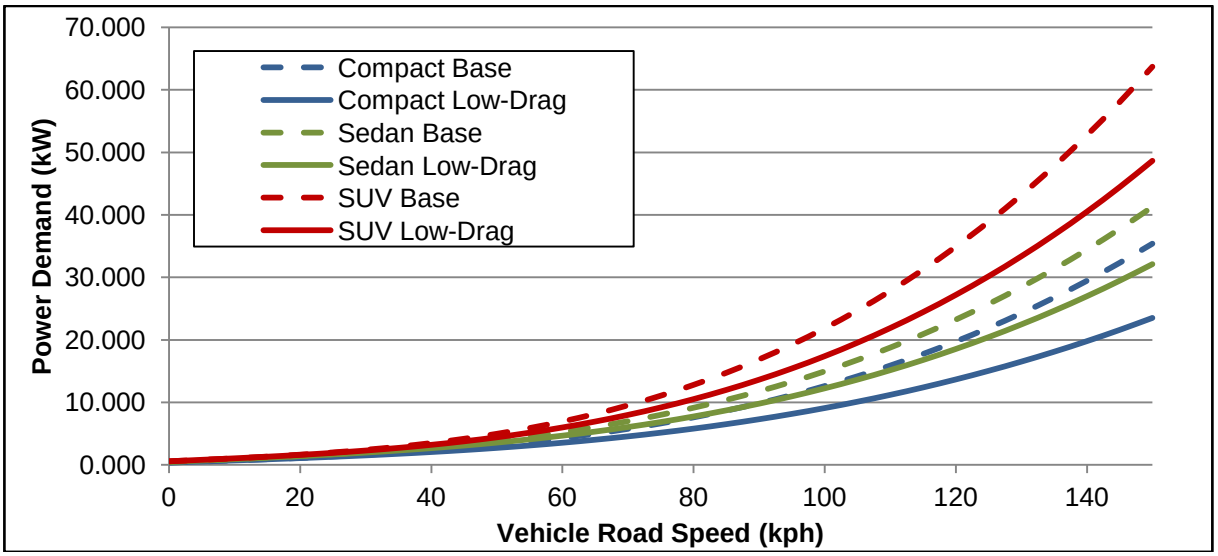

Figure 3.3. Speed-power curves for each vehicle type with base and improved drag coefficients.

3.3.4. High Accessory Load

To simulate constant use of a power-intensive heating or cooling system, road-load power was calculated with the same ideal road conditions as the base scenario, but with the additional AC/heating accessory load from table 3.1 added to the base accessory power demand for each vehicle. This resulted in a speed-independent increase in road-load power. While the relative impact of the increased accessory power draw was severe at low speeds, and could significantly reduce EV range during urban driving cycles, the relative change at highway speeds was much less significant.

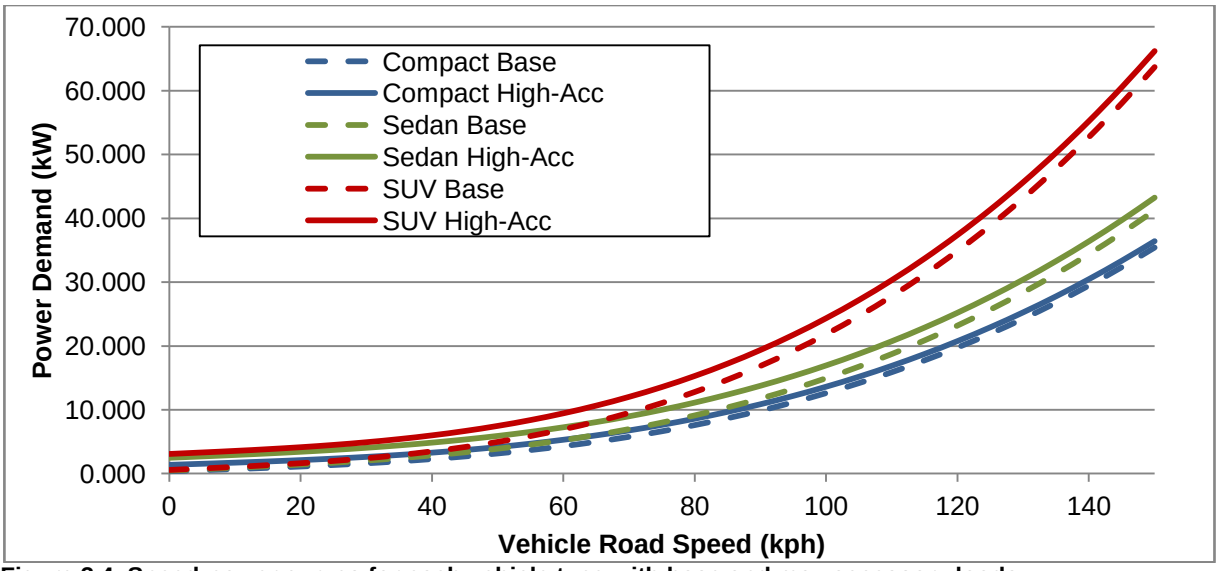

Figure 3.4. Speed-power curves for each vehicle type with base and max accessory loads.

3.3.5. Increased Rolling Resistance

Road-load power response to non-ideal road conditions was studied by increasing the rolling resistance coefficient by 20%, simulating a wet or rough road surface [3]. While certain surfaces and conditions can increase rolling resistance by much more than 20%, it is assumed that the vehicle would be operated at a significantly reduced speed in such extreme conditions. The increased resistance had little impact on total energy consumption at high speeds where drag forces were dominant, generally increasing total road-load power by less than 5%.

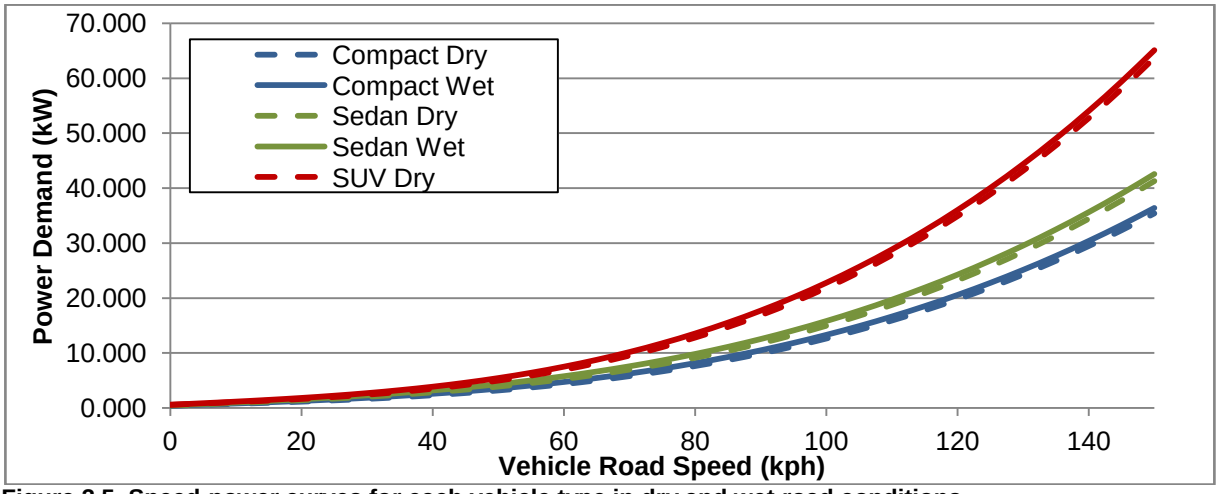

Figure 3.5. Speed-power curves for each vehicle type in dry and wet road conditions.

3.3.6. Wind

As discussed earlier in this chapter, the drag force experienced by a moving vehicle is proportional to the square of the vehicle's relative velocity through the air, which is not necessarily equal to its road speed. For simplicity, drag force is frequently calculated using the vehicle's road speed in models, with the assumption that any wind is transitory, and averages out as stationary relative to the road.

This is a reasonable assumption for many applications of road-load simulations, but when attempting to identify the maximum continuous power demand during high-speed operation, a sustained head- or tail-wind should be considered, as highways and other roads used for long-distance driving often run through geographical features that encourage regular winds. The stretch of US Interstate 84 that runs through the Columbia River Gorge is an excellent example. As the only major low-elevation passage through the Cascade mountain range, sustained winds regularly flow through the gorge from the east in the winter and from the west in the summer. An average wind speed of 15.4 kph has been recorded at the western end of the gorge, and surface wind speeds inside the gorge exceed 60 kph several times per year [10].

For each vehicle, sustained head-winds of 10, 20, and 30 kph were modeled as increases to vehicle air speed when calculating the drag force. All other variables were kept at their base values. As expected, sustained headwinds had a severe impact on the road load, typically increasing the power demand at highway speeds by 12% - 15% for every 10 kph increase in headwind speed. The relative change in power demand was more severe at lower speeds between 55 and 70 kph, where energy consumption was increased by about 15% - 20% per 10 kph increment.

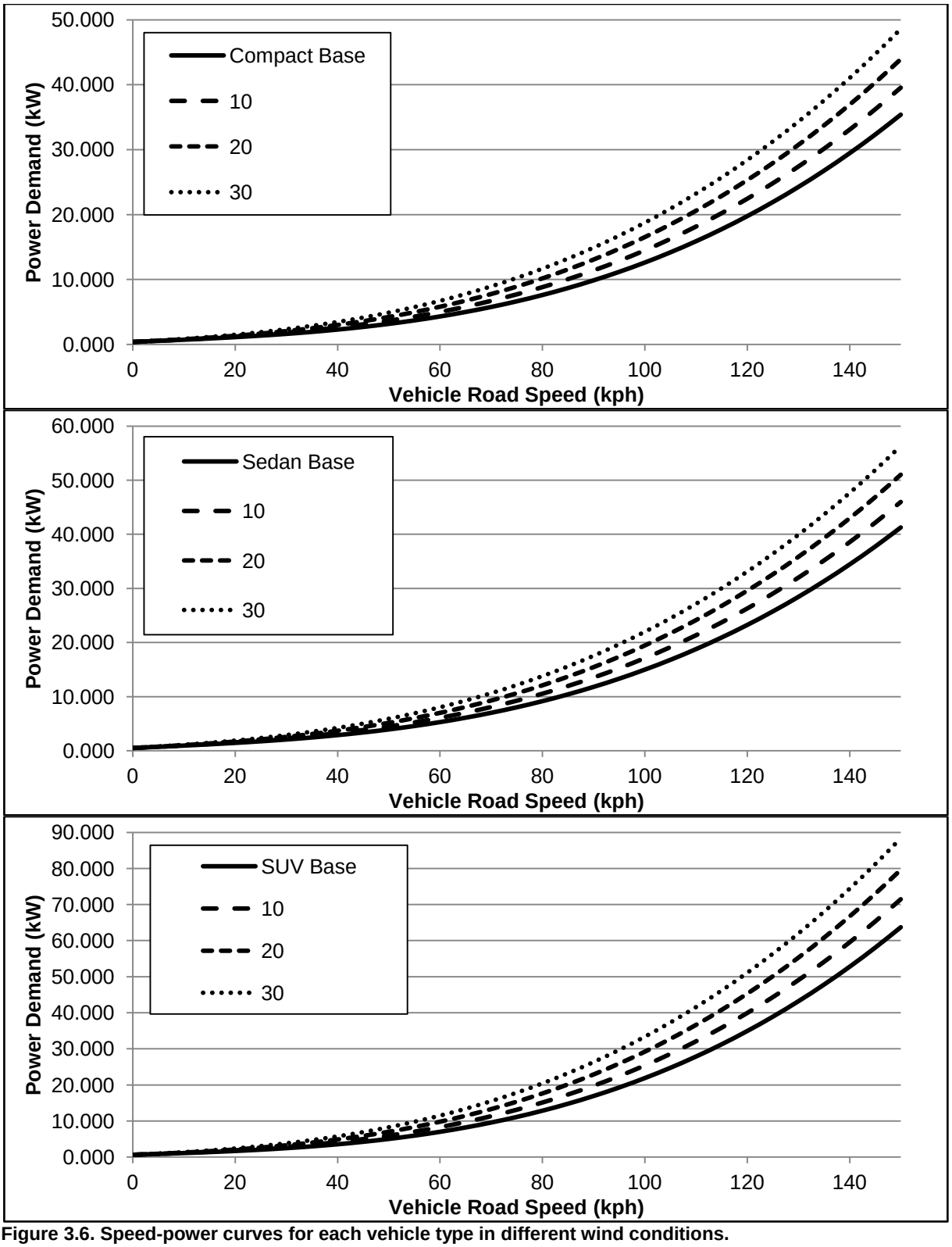

Figure 3.6. Speed-power curves for each vehicle type in different wind conditions.

3.3.7. Grade

Positive (uphill) grades of up to 7% were simulated for each vehicle type, with all other variables kept at their base values. The resultant speed-power curves are shown in figure 3.7.

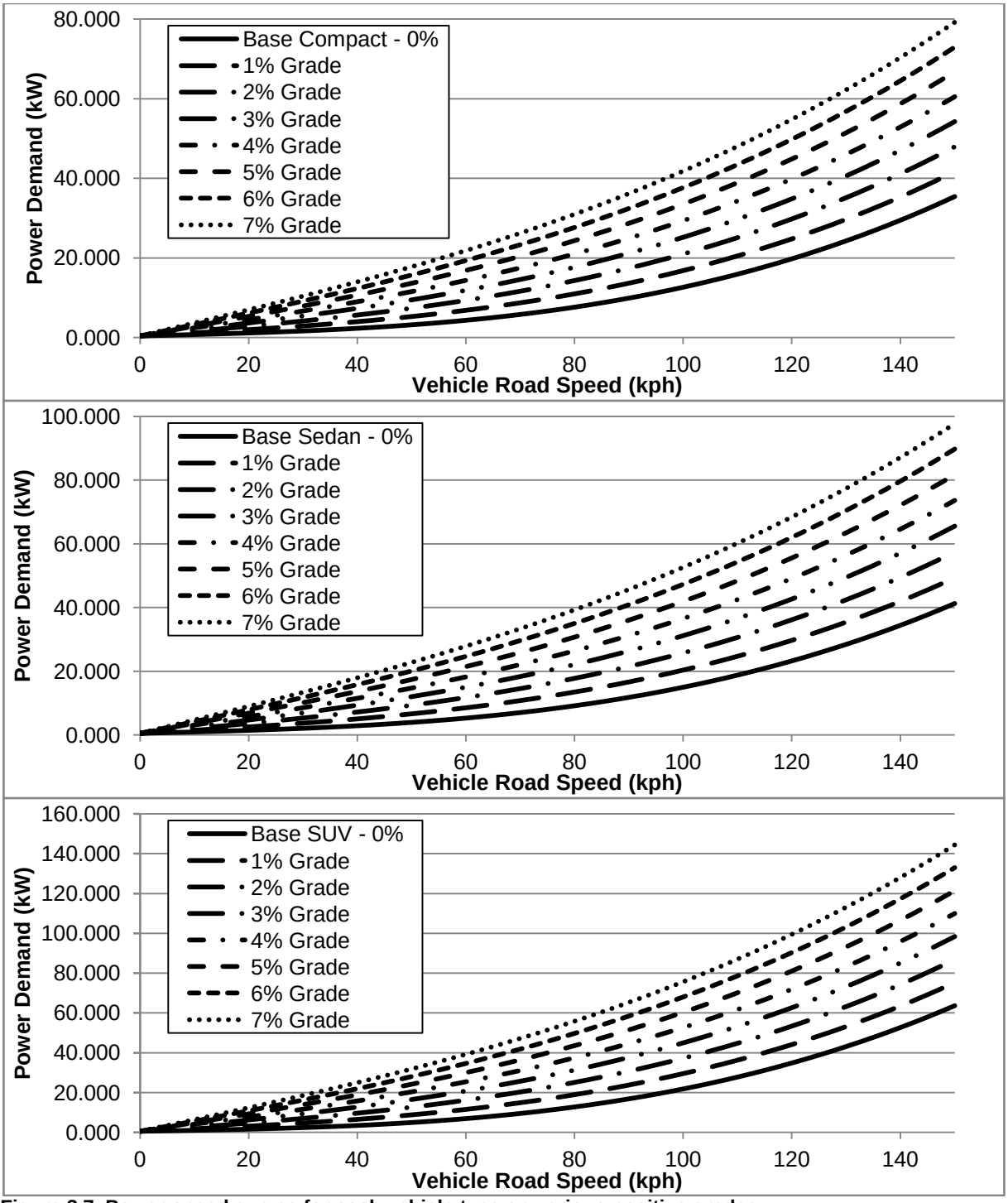

Figure 3.7. Power-speed curves for each vehicle type on various positive grades.

During uphill driving, the change in demanded power was severe. At highway speeds, mild 2% grades increased the total road load power by 10 kW or more, and at grades of around 4%, climbing power began to overtake aerodynamic drag as the largest component of road load. The steepest 7% grades resulted in high-speed road load power values that were double or triple their base values.

A REX designed to meet the total road-load when climbing a steep grade is not feasible, as it would require an excessively large and powerful engine and generator, but this does not necessarily mean that gradeability should not be considered in the design of the REX. An active REX will help offset the total energy consumption during charge-depleting uphill driving situations. This will limit the extent to which the battery is discharged, thus extending the vehicle's climbing capabilities, decreasing cycle wear on the battery, and - during charge-sustaining operation - reduce recovery time once the hill is crested and the REX is once again able to shoulder the entire road load and bring the battery back up to the desired SoC.

Aside from total energy use, the reduced instantaneous power demand makes things easier on the battery. Most battery chemistries are only able to supply their peak rated power in short bursts; the continuous power levels that can be sustained over longer periods of time are generally much lower [1]. Both peak and continuous power capabilities are strongly dependant on the battery's SoC. The reduced pack draw should not be used to justify a lower-power battery that depends on the REX for certain types of driving, as a true EREV must be able to achieve full performance in EV mode, but there are other potential benefits. Even if the pack is capable of supplying high sustained power, lowering the demand on it will reduce stress and extend its operating life. In addition, internal resistances in the battery pack cause some of the transferred energy to be lost as waste heat during discharging, with higher currents resulting in greater proportional losses [3]. A lower discharge rate will not only make the batteries operate more efficiently, it will also reduce the amount of heat that the battery thermal management system must work to remove.

3.4. Determination of REX Output Requirements

To determine the REX output requirements for each vehicle, it is necessary to first establish performance criteria that the REX must be able to meet. The following shows the development and application of an example set of criteria for sizing REXs for effective range extension on US highways for each type of EREV introduced earlier. There were three

components to each criteria; the environmental and road conditions, the driving speed, and the specific tasks that the REX must be able to accomplish.

3.4.1. Selection of Driving Conditions

Based on the results of section 3.3, three different driving condition scenarios were established. Scenario one represents high-speed driving in good conditions on a level road. Rolling resistance coefficients are assumed to be at their base values, and there is no relative head- or tail-wind. Accessory power demand is assumed to be high, to account for driving in cold or hot weather and/or active battery thermal management.

Scenario two represents high-speed, level driving in poor conditions. In addition to a high accessory power demand, a 10kph sustained headwind and a 20% increase in rolling resistance are included to simulate weather that is less than ideal, but not so severe as to strictly necessitate reduced-speed driving.

Scenario three represents climbing a steep grade at highway speeds. Road conditions are identical to scenario one, except that the road has a 7% upward slope, which is the maximum grade generally allowed for interstates [11]. A high accessory power level is assumed due to the likely need for active battery cooling.

3.4.2. Selection of Driving Speeds

Driving speeds used to determine the required REX output were based on design standards for the US Interstate Highway System. Prescribed interstate design speeds range from 80 kph minimums in urban and mountainous areas to maximums of 120 kph, with speed limits of up to 130 kph in certain areas [11].

	Metric						U.S. Customary						
	Design Speed (km/h)						Design Speed (mph)						
	80	90	100	110	120	130	50	55	60	65	70	75	80
Type of Terrain	Grades (%)*						Grades (%)*						
Level	4	4	3	3	3	3	4	4	3	3	3	3	3
Rolling	5	5	4	4	4	4	5	5	4	4	4	4	4
Mountainous	6	6	6	5	–	–	6	6	6	5	5	–	–

* Grades up to one percent steeper than the value shown may be provided in urban areas with crucial right-of-way constraints or where needed in mountainous terrain.

Figure 3.8. AASHTO Interstate design speeds and standards for grades [11].

Speeds of 100, 110, and 120 kph were selected for this study. 110 kph will be treated as a target for indefinite charge-sustaining operation in good conditions. At 120 kph, low rates of battery depletion will be acceptable. 100 kph will be considered a "fallback speed" that will enable faster battery replenishment or ensure charge-sustaining operation in less-than-ideal conditions without significantly inflating travel times or disturbing traffic flow. 100 kph will also be considered as the maximum design speed for steep grades.

3.4.3. Performance Goals for Scenarios and Speeds

At the chosen speeds and in the selected conditions, the REX should be able to meet certain requirements. These may vary depending the intended use for a specific EREV, but the performance goals chosen here are an example of what would be desirable in a typical passenger vehicle that is suitable for long range highway travel.

In scenario one conditions, the REX should be able to completely meet the power demand and indefinitely maintain the battery charge at 110 kph or less. At 100 kph, the REX should be able to meet the road load and provide Level 2 or greater battery charging. The US Level 2 charging standard corresponds to the power available from a 240-volt AC outlet, which for the purposes of this work will be considered with a maximum 30-amp current for a nominal power supply of 7.2 kW [1]. At 120 kph, charge-depleting operation will be acceptable so long as the REX is able to stretch the usable energy in a fully-charged battery to ensure a minimum blended range of 400 km, corresponding to the approximate 99th percentile of US vehicle daily travel distance [12].

In scenario two conditions, the REX should be able to ensure indefinite charge-sustaining operation at 100 kph. At 110 kph, the REX should provide a 400 km minimum blended range from a full battery. There are no specific performance goals for 120 kph operation in scenario two conditions.

Performance goals for scenario 3 conditions only concerned 100 kph driving, as this is the maximum interstate design speed recommended for 7% grades. When climbing a constant 7% grade at 100 kph, the REX must ensure that less than 50% of the usable battery capacity will be consumed after 20 kilometers. This criteria is meant to limit discharge depth and maintain a healthy energy reserve when the vehicle starts out with a high battery SoC at the bottom of the slope, or ensure acceptable grade performance if the vehicle starts with a lower SoC.

3.4.4. Results

For base and low-drag versions of each vehicle, the minimum electrical power output required from the REX to meet each performance goal was calculated. The resultant electrical power requirements and the corresponding brake engine outputs (with an assumed 90% generator efficiency and rounded up to the nearest whole kilowatt), are presented in table 3.2.

	Goals	Scenario 1 - 100 kph CS operation & minimum 7.2 kW charging power	Scenario 1 - 110 kph CS operation	Scenario 1 - 120 kph 400 km blended range	Scenario 2 - 100 kph CS operation	Scenario 2 - 110 kph 400 km blended range	Scenario 3 - 100 kph 50% battery discharge or less after 20 km
Minimum REX Power (kW)	Compact	20.83	16.91	17	16.17	16	5
	Sedan	24.18	20.77	20	19.97	20	10
	SUV	31.57	30.34	31	28.79	30	20
Rounded REX Engine Power (kW)	Compact	24	19	19	18	18	6
	Sedan	27	24	23	23	23	12
	SUV	36	34	35	32	34	23
Minimum REX Power (low-drag) (kW)	Compact	17.31	12.21	11	11.9	11	1
	Sedan	21.47	17.17	16	16.7	16	8
	SUV	27.1	24.4	23	23.39	23	16
Rounded REX Engine Power (low-drag) (kW)	Compact	20	14	13	14	13	2
	Sedan	24	20	18	19	18	9
	SUV	31	28	26	26	26	18

Table 3.2. REX power outputs required to meet driving scenarios.

The maximum brake power required from a REX engine to meet all the performance criteria for the base vehicles was 24 kW for compacts, 27 kW for mid-sized sedans, and 36 kW for mid-sized SUVs. With improved aerodynamics, the required REX engine power dropped to 20, 24, and 31 kW for the compact, sedan, and SUV, respectively.

For each vehicle type, the criteria of Level 2 charging at 100 kph in scenario one conditions proved to be the most power-intensive, especially for the compact and sedan,

where that power requirement tended to exceed the next-highest criteria by 4 - 5 kW. On the other end of the range, the REX power needed to satisfy the grade requirement for each vehicle was very low compared to the other criteria. All other criteria produced very similar power requirements.

Because of this, the 100 kph charging rate could be relaxed by a significant amount before meeting any of the other criteria becomes an issue. This could allow for increased standardization or further downsizing. For example, if 5 kW of charging power at 100 kph would still provide adequate SoC recovery for the base compact car and sedan models studied here, smaller 19 and 22 kW REXs could be used to save space, weight, and cost; or a single 22 kW REX could be used in both vehicles to simplify and economize development and production.

3.5. Conclusions

The procedure demonstrated in this chapter allows for a REX's peak power requirement to be identified using simple algebra rather than specialized software or complex simulations. Though simple, it gives very precise and accurate results for specific vehicles, and can be used with whatever steady-state design criteria are judged to be important for a specific application.

This sizing approach is not intended to replace more advanced drive cycle simulation tools and techniques, which will still be needed for sizing an EREV's electric drive, and for simulating and predicting their performance during typical daily driving. It also has limited applicability for EREVs and series-HEVs that are not intended to operate at highway speeds for extended periods of time. For short-range or low-speed series-hybrid vehicles such as city busses or utility vehicles, simulations over urban drive cycles will be more relevant.

References

[1] Pistoia, G, "Electric and Hybrid Vehicles," Elsevier, Oxford, ISBN 978-0-444-53565-8, 2010.

[2] Heywood, J, "Internal Combustion Engine Fundamentals," McGraw-Hill, New York, ISBN 978-1-25-900207-6, 1988.

[3] Guzzella, L., Sciarretta, A., "Vehicle Propulsion Systems," Springer, Berlin, ISBN 978-3-540-25195-8, 2005.

[4] Bassett, M., Fraser, N., Brooks, T., Taylor, G. et al., "A Study of Fuel Converter Requirements for an Extended-Range Electric Vehicle," SAE Int. J. Engines 3(1):631-654, 2010, doi:10.4271/2010-01-0832.

[5] "Comparing the Benefits and Impacts of Hybrid Electric Vehicle Options," EPRI, Palo Alto, CA: 2001. 1000349.

[6] "Comparing the Benefits and Impacts of Hybrid Electric Vehicle Options for Compact Sedan and Sport Utility Vehicles," EPRI, Palo Alto, CA: 2002. 1006892.

[7] Wing, K., Kimble, D., CNET Car Tech, "General Motors EV1 - Driving Impression," Motor Trend, June 1996.

[8] Cunningham, W., "Tesla Model S first drive: Quiet Satisfaction," http://www.cnet.com/news/tesla-model-s-first-drive-quiet-satisfaction/, June 2012.

[9] Toyota, "RAV4 EV Features & Specs," http://www.toyota.com/rav4ev/features.html, 2014.

[10] Sharp, J., Mass, C.F., " Columbia Gorge Gap Winds: Their Climatological Influence and Synoptic Evolution," Weather and Forcasting, May 2004.

[11] American Association of State Highway and Transportation Officials, "A Policy on Design Standards Interstate System," Rev. Jan. 2005.

[12] van Haaren, R., " Assessment of Electric Cars' Range Requirements and Usage Patterns based on Driving Behavior recorded in the National Household Travel Survey of 2009," Earth and Environmental Engineering Department, Columbia University, July, 2012.

Chapter 4. Steady-State REX Engine Performance Model

As discussed in previous chapters, the operating requirements and priorities for REX engines are significantly different from those of engines used for propulsion in CVs and HEVs. REX engines primarily operate at full or nearly-full loads within a constrained speed range to run a matched generator. Thus, the design of these engines is mainly focused on constant-speed operation at these specific brake operating points, rather than the plethora of opposing priorities and requirements that drive the design of CV engines.

ICE performance simulations are often accomplished using either very broad correlative models that provide little useful detail, or very intensive time-step simulations that require advanced programming and a great deal of detailed information about the specific engine being simulated. This chapter will present the development and application of an engine modeling process that takes advantage of the constant-speed focus of genset engines to simulate engine performance over a wide operating range using straightforward math-based operations that can be as simple or advanced as required.

Using this approach, a model will be developed that will simulate constant-speed engine operation and study the performance and efficiency of 4-stroke SI engines based simply on general design parameters such as displacement, bore & stroke, number of cylinders, compression ratio, and basic valvetrain type. In the next chapter, this model will be used to examine the applicability of various engine configurations to REX applications.

4.1. Overview of Array-Based Engine Modeling Approach

This model was based on an approach presented by I. N. Bishop [1] in which steady-state performance parameters are calculated for a wide range of individual operating points defined by geometry-independent speed and indicated load values, and then interpolation is used to remap parameters of interest to operating points defined by brake mean effective pressure (BMEP) and crank speed. Bishop's original model defined indicated load with speed-corrected values that needed to be multiplied with a correction factor from a table to arrive at the actual indicated load. In the model developed here, this was streamlined, and the operating points and governing equations used the actual indicated mean effective pressure (IMEP), while speed was defined by the crankshaft speed in RPM. Together, these parameters were used to frame operating point arrays that represented all combinations of a wide range of IMEP and speed values.

ISCF (g/(kW*hr))

IMEP (kPa)	N (RPM)	400	600	800	1000	1200	1400	1600	1800	2000	2200	2400	2600	2800	3000	3200	3400	3600
	2000	245.53	233.91	227.49	223.31	220.32	218.05	216.26	214.8	213.57	212.53	211.63	210.84	210.15	209.52	208.96	208.46	207.9
	1950	245.87	234.16	227.7	223.49	220.48	218.2	216.39	214.92	213.69	212.64	211.73	210.94	210.24	209.61	209.05	208.54	208.0
	1900	246.22	234.42	227.91	223.67	220.64	218.34	216.53	215.04	213.8	212.75	211.84	211.04	210.34	209.71	209.14	208.63	208.1
	1850	246.58	234.69	228.13	223.86	220.81	218.5	216.67	215.17	213.93	212.86	211.95	211.15	210.44	209.8	209.23	208.72	208.2
	1800	246.95	234.96	228.36	224.06	220.98	218.65	216.81	215.31	214.05	212.98	212.06	211.25	210.54	209.9	209.33	208.81	208.3
	1750	247.34	235.25	228.59	224.26	221.16	218.82	216.96	215.45	214.18	213.11	212.18	211.36	210.64	210	209.43	208.9	208.4
	1700	247.74	235.55	228.83	224.47	221.35	218.98	217.12	215.59	214.32	213.23	212.3	211.48	210.76	210.11	209.53	209	208.5
	1650	248.16	235.86	229.09	224.68	221.54	219.16	217.28	215.74	214.46	213.37	212.42	211.6	210.87	210.22	209.63	209.1	208.6
	1600	248.6	236.18	229.35	224.91	221.74	219.34	217.44	215.9	214.6	213.5	212.55	211.72	210.99	210.33	209.74	209.21	208.7
	1550	249.06	236.52	229.62	225.15	221.95	219.53	217.62	216.06	214.75	213.65	212.69	211.85	211.11	210.45	209.86	209.32	208.8
	1500	249.53	236.86	229.91	225.39	222.17	219.73	217.8	216.23	214.91	213.8	212.83	211.99	211.24	210.58	209.98	209.43	208.9
	1450	250.03	237.23	230.21	225.65	222.39	219.93	217.99	216.4	215.08	213.95	212.98	212.13	211.38	210.7	210.1	209.55	209.0
	1400	250.54	237.61	230.52	225.91	222.63	220.15	218.18	216.58	215.25	214.11	213.13	212.27	211.52	210.84	210.23	209.68	209.1
	1350	251.09	238.01	230.84	226.19	222.88	220.37	218.39	216.77	215.43	214.28	213.29	212.43	211.66	210.98	210.37	209.81	209.3
	1300	251.66	238.43	231.18	226.49	223.14	220.61	218.6	216.97	215.61	214.46	213.46	212.59	211.81	211.13	210.51	209.95	209.4
	1250	252.26	238.87	231.54	226.79	223.41	220.85	218.83	217.19	215.81	214.64	213.64	212.75	211.98	211.28	210.65	210.09	209.5
	1200	252.89	239.33	231.92	227.12	223.7	221.11	219.07	217.41	216.02	214.84	213.82	212.93	212.14	211.44	210.81	210.24	209.7
	1150	253.56	239.82	232.31	227.46	224	221.38	219.32	217.64	216.24	215.05	214.02	213.12	212.32	211.61	210.97	210.4	209.8
	1100	254.27	240.34	232.74	227.82	224.32	221.67	219.58	217.88	216.47	215.26	214.22	213.31	212.51	211.79	211.15	210.57	210.0
	1050	255.02	240.89	233.18	228.2	224.66	221.98	219.86	218.14	216.71	215.49	214.44	213.52	212.71	211.98	211.33	210.74	210.2
	1000	255.83	241.47	233.65	228.61	225.02	222.3	220.16	218.42	216.97	215.74	214.67	213.74	212.92	212.18	211.53	210.93	210.3
	950	256.68	242.09	234.16	229.04	225.4	222.65	220.48	218.72	217.24	216	214.92	213.97	213.14	212.4	211.73	211.13	210.5
	900	257.6	242.76	234.7	229.5	225.81	223.02	220.82	219.03	217.54	216.27	215.18	214.22	213.38	212.63	211.95	211.34	210.7
	850	258.59	243.48	235.28	230	226.25	223.41	221.18	219.37	217.85	216.57	215.46	214.49	213.64	212.87	212.19	211.57	211.0
	800	259.67	244.25	235.91	230.53	226.72	223.84	221.57	219.73	218.19	216.89	215.76	214.78	213.91	213.14	212.44	211.82	211.2
	750	260.83	245.1	236.59	231.11	227.23	224.3	222	220.12	218.56	217.23	216.09	215.09	214.21	213.43	212.72	212.08	211.5
	700	262.11	246.01	237.33	231.74	227.79	224.8	222.46	220.55	218.96	217.61	216.45	215.43	214.53	213.74	213.02	212.37	211.7
	650	263.51	247.02	238.14	232.43	228.4	225.35	222.96	221.01	219.4	218.02	216.84	215.8	214.89	214.07	213.34	212.68	212.0
	600	265.06	248.14	239.03	233.2	229.07	225.96	223.51	221.53	219.88	218.47	217.26	216.21	215.28	214.45	213.7	213.03	212.4
	550	266.81	249.38	240.03	234.05	229.82	226.63	224.13	222.1	220.41	218.98	217.74	216.66	215.71	214.86	214.1	213.41	212.7
	500	268.77	250.78	241.16	235	230.66	227.39	224.82	222.74	221.01	219.54	218.27	217.17	216.19	215.33	214.55	213.84	213.1
	450	271.03	252.38	242.44	236.09	231.61	228.25	225.61	223.47	221.69	220.18	218.88	217.74	216.74	215.85	215.05	214.33	213.6
	400	273.66	254.24	243.92	237.35	232.72	229.24	226.51	224.3	222.47	220.91	219.57	218.4	217.37	216.46	215.63	214.89	214.2
	350	276.78	256.43	245.66	238.82	234.01	230.4	227.57	225.28	223.38	221.77	220.39	219.18	218.11	217.16	216.31	215.54	214.8
	300	280.57	259.08	247.77	240.6	235.57	231.8	228.85	226.46	224.48	222.8	221.36	220.1	218.99	218.01	217.12	216.33	215.6
	250	285.37	262.4	250.39	242.81	237.5	233.53	230.43	227.92	225.84	224.08	222.56	221.25	220.08	219.05	218.13	217.29	216.5
	200	291.71	266.76	253.82	245.69	240.01	235.77	232.47	229.8	227.59	225.72	224.12	222.72	221.49	220.4	219.42	218.53	217.7
	150	300.79	272.91	258.62	249.7	243.5	238.89	235.3	232.4	230.01	227.99	226.26	224.75	223.43	222.25	221.19	220.24	219.3
	100	315.64	282.77	266.24	256.02	248.97	243.76	239.71	236.45	233.77	231.51	229.57	227.89	226.41	225.1	223.93	222.87	221.9
	50	348.46	303.69	282.09	269.02	260.13	253.62	248.6	244.59	241.3	238.54	236.18	234.14	232.35	230.76	229.35	228.08	226.9

Figure 4.1. Example IMEP/speed array for indicated specific fuel consumption (ISFC).

Identically-sized and defined IMEP/speed arrays were created for each relevant operating parameter that varied with speed and/or load, and parameter values for each operating point were calculated using identical functions of model inputs, crank speed, IMEP, and values with the same speed/load "coordinates" from other arrays.

The general modeling process is as follows. For each IMEP/speed point, the cycle efficiency and ISFC are calculated first. Then, the manifold pressures and friction MEP losses are computed for each operating point, and used to calculate corresponding BMEP, BSFC, and mechanical and brake efficiency values.

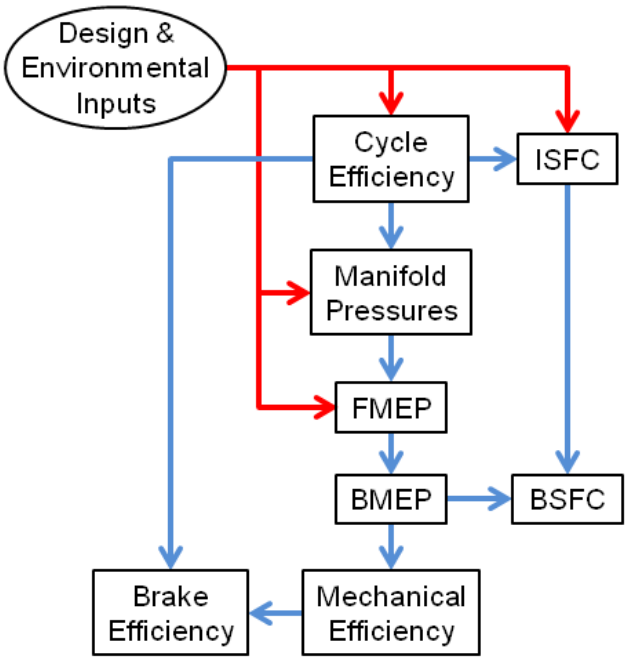

Figure 4.2. Data flow diagram of a model for simulating steady-state brake performance and efficiency using IMEP/speed arrays. Blue arrows indicate the flow of calculated parameter data between arrays.

Once all of the IMEP/speed arrays are populated, including the IMEP/speed array for BMEP, parameters of interest are remapped to arrays defined by BMEP and speed so that the engine's performance and efficiency can be studied in terms of its brake output. The remapping process is accomplished by first constructing BMEP/speed arrays for each parameter of interest. These arrays do not need to match the dimensions of the IMEP/speed arrays. It is beneficial to use speed values that have already been explicitly solved for in the IMEP/speed arrays in order to simplify the interpolation process, but not every speed needs to be included. For the BMEP values, any range and interval can be used so long as those operating points can be found in the IMEP/speed arrays.

Once defined, each operating point in a parameter's BMEP/speed array is populated using a double-interpolation process. First, the IMEP/speed array for BMEP is interpolated to approximate the value of IMEP that would result in the brake operating point's BMEP at the same speed. Then, the IMEP/speed array for the parameter being remapped is interpolated to estimate that parameter's value at the approximate IMEP and speed of the brake operating point, and that value is inserted in the BMEP/speed array. This process is repeated for each operating point in that parameter's BMEP/speed array.

Linear interpolation is the most straightforward way to carry out this process, but more advanced polynomial or spline interpolation could be used to reduce error when interpolating

IMEP/speed arrays that do not have many data points, which may be an issue for models that incorporate experimental data. With purely math-based models however, the limitations of linear interpolation can be alleviated by simply solving for a sufficient number of intermediate IMEP values in the IMEP/speed arrays. If enough discrete IMEP values are solved for, an extremely simple nearest-neighbor interpolation technique could also be used with satisfactory results. While linear interpolation will always be more accurate, nearest-neighbor functions could be a better choice in especially bare-bones software, or as a simplified placeholder while a model is being built.

If supported by the software being used, a recommended addition to the remapping process is a logical check that will skip a BMEP/speed point or return a null value if a specific BMEP value cannot be located in the IMEP/speed array. Basic "if-then-else" conditionals are an effective way to implement this, and are widely supported in computational software.

If desired, operations can be performed between BMEP/speed arrays the same way they are with IMEP/speed arrays. For example, once BMEP/speed arrays for indicated and mechanical efficiency are populated with interpolation, a BMEP/speed for brake efficiency can be filled in using those two existing BMEP/speed arrays. This can cut down on the amount of interpolation necessary, though there are some limitations and drawbacks, and certain parameters are best calculated in IMEP/speed arrays.

4.2. Advantages and Disadvantages of Array-Based Engine Modeling

There are a number of advantages to this modeling approach. A key one is its flexibility; each step toward brake performance can be as complex or simple as desired without affecting the underlying structure of the model.

For example, the FMEP block in figure 4.2 could consist of anything from a single polynomial of engine speed to a highly detailed break-down that separately models every individual source of mechanical loss based on dozens of design inputs. Largely independently, the manifold pressures block could be implemented using simple functions of speed and load, more involved functions incorporating data from the cycle efficiency block, or detailed pressure maps based on tests or simulations of specific manifold designs. It could even be omitted entirely if none of the subsequent equations require manifold pressure values.

And because the relationships between arrays are purely mathematical, and any parameter equations that incorporate values from other arrays only use values from

elements with the same IMEP/speed "coordinates", these arrays can be lumped together or broken up very easily. For example, mean piston speed is an important operating parameter that varies with design inputs and operating speeds, and is frequently used in equations for mechanical losses and manifold pressures:

$$V_p = \frac{L * N}{30000} \tag{4.1}$$

where

V_p = mean piston speed in m/s
L = piston stroke in mm
N = crankshaft speed in RPM

If V_p will only be used a few times in the entire model, it is easily replaced with equation 4.1 in any other equation. But if it will be used in a large number of equations, it could be calculated by itself in a separate IMEP/speed array that would then be referenced whenever V_p is needed by other equations. While this would require an additional IMEP/speed array, it would also simplify the equations in other arrays and streamline computations in large or complex models.

As another example, if FMEP is calculated with a highly-detailed, multi-component model, each component or sub-component can be calculated on its own in separate arrays, and then added together to give the total FMEP. This would break up and simplify the friction equations, helping to avoid, identify, and remedy any errors. It would also allow any specific friction component or group of components to be individually remapped to BMEP & speed in order to investigate their specific behavior and response to input changes.

This approach is also very adaptable from a programming standpoint. While this type of model could be implemented in any number of conventional programming environments, its straightforward mathematical nature makes it well-suited to spreadsheets and other table- or array-based computational programs. A spreadsheet permits all parameter values to be organized and presented in a straightforward, visual format; and automatic recalculation provides nearly instantaneous response to changes in model inputs. Spreadsheet programs are widely available, inexpensive or even free to obtain, and easy to work with, requiring little to no knowledge of advanced programming languages or proprietary software packages.

But while this modeling approach is very powerful and flexible, it is strictly limited to steady state performance analysis, as all parameter values for each operating point are calculated independently of time and adjacent operating points. So this type of model, at least on its own, is completely unsuited to studying transient performance, and it cannot incorporate dynamic effects such as changes in friction and cycle equations as an engine heats up to its operating temperature.

4.3. REX Engine Model

Many different phenomena figure into the overall brake efficiency of an ICE. Work loses due to heat transfer, pumping work, gas flow effects, rubbing friction from a variety of diverse mechanical interactions; all of these factors are influenced by aspects of an engine's design and operation, but all respond to changes in those inputs in different ways. Properly incorporating all these relationships and realistically modeling the overall efficiency of different engines required a complex model that could separate and organize all these different interactions, and accurately model their response to input changes.

At the same time, this model needed to be able to accomplish all this with a relatively small number of relevant inputs. When more detailed design information is required, those details needed to either be established and kept constant, or extrapolated based on other inputs. This is not only important for keeping the model manageable, it also ensures that comparisons between different engine configurations are made on a "like-to-like" basis.

Based on a review of existing work on steady-state engine modeling and operating principles, a model was constructed that could allow different engine configurations to be easily compared. The operating parameters were computed using the array-based process described above, and were organized according to the diagram shown in figure 4.2. The individual equations used to calculate each parameter are as follows:

4.3.1. Indicated Performance

Based on engine geometry inputs, the indicated fuel conversion efficiency was first calculated for each speed/load point using a relation developed by Wu et al. [3]:

$$\eta_i = \eta_{ifa} * \eta_c * (1 - Q) \quad (4.2)$$

where

η_i = indicated fuel conversion efficiency
η_{ifa} = indicated fuel-air cycle efficiency
η_c = overall combustion efficiency (assumed to be .95 based on Wu et al. [3])
(1-Q) = the ratio of cycle work retained after heat transfer losses.

The indicated fuel-air cycle efficiency was approximated using a correlation developed by Muranaka et al. that produced more realistic results for stoichiometric operation than the idealized thermodynamic formula for the constant-volume cycle [4]

$$\eta_{ifa} = .4178 - .0012 * (R_c - 8)^2 + .0202 * (R_c - 8) \quad (4.3)$$

where

R_c = the geometric compression ratio

The heat loss ratio Q was developed by Wu et al. to realistically approximate the proportion of ideal cycle work lost to cylinder walls via heat transfer as a function of cylinder pressure, engine speed, and general combustion chamber geometry. Wu et al. assembled a correlation based on previous studies, engine performance data, and thermodynamic principles to model this heat loss [3]. Here, the heat loss ratio was rearranged as a torque ratio (1-Q) that represented the proportion of cycle work retained after heat losses. This value could be multiplied together with other efficiencies and the ideal cycle work to compute the actual indicated cycle work. The modified correlation and constants used produced the equation:

$$(1-Q) = 1 - .13 * \left(\frac{350}{IMEP}\right)^{.2} * \left(\frac{1800}{N}\right)^{.5} * \left(\frac{(S/V)_{tdc}}{250}\right) \quad (4.4)$$

where

$(S/V)_{tdc}$ = the surface-to-volume ratio of the combustion chamber in m^{-1} with the piston at top dead center, calculated by:

$$(S/V)_{tdc} = \frac{(R_c - 1)}{L} + \frac{4000}{B} \quad (4.5)$$

where

B = Cylinder bore diameter in mm
L = Piston stroke in mm

With the indicated fuel conversion efficiency calculated, the indicated specific fuel consumption (ISFC) in grams per kWh for each speed and load could be computed using a relationship established by Heywood [2] without having to explicitly solve for fuel- or air-flow rates or attempt to model complex exchange phenomena:

$$ISFC = \frac{3.6 * 10^9}{\eta_i * Q_{hv}} \quad (4.6)$$

where

Q_{hv} = the fuel heating value in J/kg

4.3.2. Manifold pressures

As several sources of friction and pumping losses are influenced by the intake and exhaust manifold pressures, values for these parameters had to be estimated for each operating point. Bishop [1] showed that intake manifold pressure p_i could be approximated reasonably well for a variety of naturally-aspirated engines as a linear function with a slope proportional to IMEP:

$$p_i = IMEP * \frac{Z}{12.8} + 10 \tag{4.7}$$

where Z is a correction factor that decreases to unity as the reciprocal of crank speed approaches zero to account for speed-dependant work losses due to heat transfer. This factor is equal to the ratio of speed-corrected IMEP without heat transfer losses to actual IMEP with heat losses. Bishop demonstrated that the same Z value could also relate observed thermal efficiency to speed-corrected thermal efficiency without heat losses:

$$Z = \frac{IMEP_{corrected}}{IMEP_{observed}} = \frac{\eta_{corrected}}{\eta_{observed}} \tag{4.8}$$

With this relationship established, Z can be equated to the reciprocal of the torque ratio (1-Q) from equation 4.4, allowing Bishop's expression for absolute intake manifold pressure to be written as:

$$p_i = \frac{IMEP}{12.8 * (1 - Q)} + 10 \tag{4.9}$$

With the intake manifold pressures defined, the firing exhaust manifold pressures were estimated using a correlation developed by Sandoval et al. based on production engines:

$$p_e = .178 * \left(\frac{p_i * V_p}{p_a}\right)^2 + p_a \tag{4.10}$$

where

p_a = ambient atmospheric pressure
V_p = mean piston speed in m/s

These correlations produced acceptably realistic manifold pressure responses to changing load and speed. The exact relationships between manifold pressures, IMEP, and crank speed are much more complex, especially when tuning or forced induction are

employed. Precisely matching the manifold pressure behavior of specific engines will generally require detailed design information or advanced flow models. While this model can easily be modified with more complex correlations or pressure maps to better represent a specific engine design, such complexity is beyond the scope of this study. This linear correlation was considered to be adequate for general examinations of engine geometry.

4.3.3. Friction

Mechanical losses due to engine friction and pumping work were broken up into five major components and a number of sub-components as established by Bishop [1]:

$$FMEP_{total} = FMEP_{crankcase} + FMEP_{piston} + PMEP_{throttling} + PMEP_{valve\ flow} + PMEP_{blowby} \quad (4.11)$$

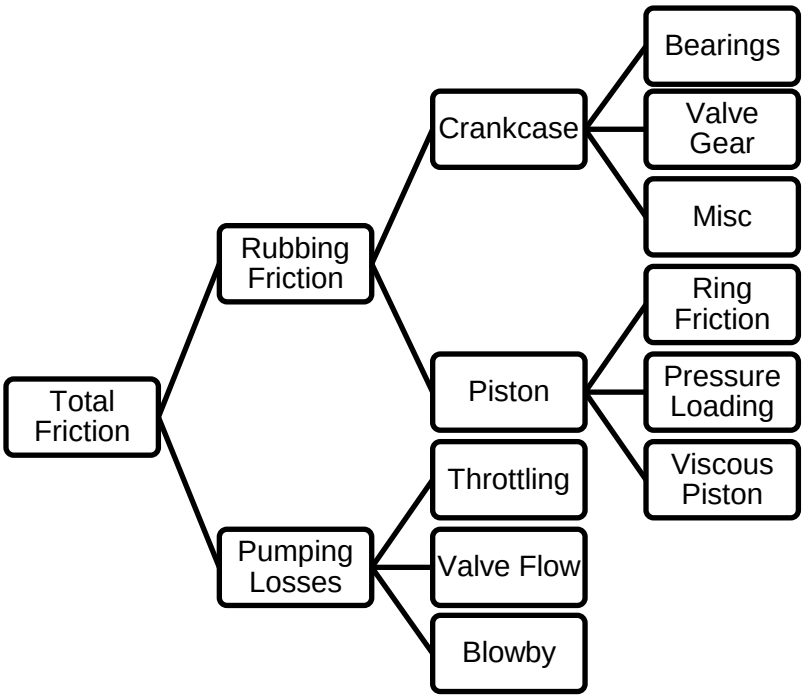

Figure 4.3. Organization of friction components and sub-components as used in this model.

The friction model was organized according to Bishop's original model in order to simplify the design inputs, but the individual equations were largely updated or replaced using expressions and information adapted from a 2003 friction model developed by Daniel Sandoval and John Heywood [5]. All MEP values discussed here are in units of kPa.

4.3.3.1. Crankcase Friction

Crankcase friction encompasses all mechanical losses that are not caused by piston motion. It is further subdivided into bearing friction, valve gear friction, and miscellaneous friction, all of which are independent of load.

$$FMEP_{crankcase} = FMEP_{bearings} + FMEP_{valve\ gear} + FMEP_{misc} \tag{4.12}$$

Bearing friction includes losses from all crank, rod, and accessory bearings; and is modeled here using Bishop's original correlation [1] rather than the updated Sandoval et al. model [5], as the latter required bearing dimensions for all shafts to be individually specified.

$$FMEP_{bearings} = 41.3686 * \left(\frac{B}{L}\right) * \left(\frac{N}{1000}\right) * K \tag{4.13}$$

where K is a dimensionless bearing size coefficient equal to .14 for typical SI engines [2].

Valve gear friction accounts for losses in the engine's valvetrain. The relevant elements of the Sandoval et al. model were adapted and simplified with some basic assumptions to produce:

$$FMEP_{valve\ gear} = C_{ff} * \left(1 + \frac{500}{N}\right) * \frac{n_v}{L} + C_{rf} * \left(\frac{N * n_v}{L}\right) + C_{oh} * \left(\frac{.058 * N^{.5} * n_v}{L}\right) + C_{om} * \left(1 + \frac{500}{N}\right) * \frac{.15 * B * n_v}{L} + 4.12 \tag{4.14}$$

where

n_v = the number of valves per cylinder

and C_{ff}, C_{rf}, C_{oh}, C_{om} are constants that depend on the valvetrain configuration, and are given in table 4.1 [5]:

Valvetrain Type:	**Cam Follower Flat (C_{ff})**	**Cam Follower Roller (C_{rf})**	**Cam Oscillating Hydrodynamic (C_{oh})**	**Cam Oscillating Mixed (C_{om})**
SOHC finger follower	600	0.0227	0.2	42.8
SOHC rocker arm	400	0.0151	0.5	21.4
SOHC direct acting	200	0.0076	0.5	10.7
DOHC finger follower	600	0.0227	0.2	25.8
DOHC direct acting	133	0.005	0.5	10.7
OHV	400	-	0.5	32.1

Table 4.1. Friction coefficients for various valvetrain configurations, given by Sandoval et al [5].

Miscellaneous friction accounts for mechanical losses due to accessory systems such as oil and water pumps. The 2003 Sandoval et al. correlation for accessory FMEP was used here.

$$FMEP_{misc} = 8.32 + 1.86 * 10^{-3} * N + 7.45 * 10^{-7} * N^2 \quad (4.15)$$

4.3.3.2. Piston Mechanical Friction

Piston mechanical friction encompasses the reciprocating friction of the piston and rings in the cylinder. It is broken up into viscous and non-viscous components, with the non-viscous component split up further into friction due to ring tension, and friction due to gas pressure loading.

$$FMEP_{piston} = FMEP_{ring\ friction} + FMEP_{pressure\ loading} + FMEP_{viscous\ piston} \quad (4.16)$$

Load-independent piston friction due to ring and skirt drag in boundary and mixed lubrication regions was correlated to crank speed and bore size by Sandoval et al. [5].

$$FMEP_{ring\ friction} + 406008\left(1 + \frac{500}{N}\right) * \left(\frac{1}{B^2}\right) \quad (4.17)$$

Additional piston ring friction due to pressure loading is correlated to intake manifold pressure. The Bishop and Sandoval et al. functions for pressure-dependant piston friction used the same structure, but Bishop's function included the additional geometric term (L/B^2), which accounted for the effect of varying bore and stroke dimensions [1]. This term was retained here, but the coefficients were modified to account for reduced liner roughness in modern engines as recommended by Sandoval et al. [5].

$$FMEP_{pressure\ loading} = \left(\frac{p_i}{p_a}\right) * \left(\frac{L}{B^2}\right) * \left(36.2162 * R_c + 74.9018 * R_c^{\left(1.33 - .0238 * V_p\right)}\right) \quad (4.18)$$

Viscous piston friction includes the combined hydrodynamic drag of the piston and rings. The term developed by Sandoval et al. [5] was:

$$FMEP_{viscous\ piston} = \frac{294 * V_p}{B} \quad (4.19)$$

4.3.3.3. Throttling Losses

Throttling losses account for pumping losses due to pressure differentials that the piston must work against during the intake and exhaust strokes. When defined as a mean effective pressure, the total pumping work can simply be equated to the differential between the intake and exhaust manifold pressures [2]:

$$PMEP_{throttling} = p_e - p_i \quad (4.20)$$

where

p_e = exhaust manifold pressure (kpa absolute)
p_i = intake manifold pressure (kpa absolute)

This pressure difference can also be calculated using gauge values so long as both inlet and exhaust pressures are defined that way, but manifold pressures are defined in

absolute terms in this model for simplicity. In most cases, p_e will be greater than p_i, resulting in pumping losses. However, this can be reversed at operating points where tuning or forced induction is employed.

4.3.3.4. Valve Flow Losses

Valve flow losses account for the additional pumping work required to move intake charge and exhaust gasses through the flow restrictions of valves and ports. The 2003 Sandoval et al. expression for pressure drop through the valves [5] included terms for the number of intake and exhaust valves as well as an improved fit to modern cylinder head and manifold designs.

$$PMEP_{valve\ flow} = 3 * 10^{-3} * \left(\frac{p_i}{p_a}\right)^2 * \frac{{V_p}^2 * B^4}{{n_c}^2} * \left(\frac{1}{{n_{iv}}^2 * {d_{iv}}^4} + \frac{1}{{n_{ev}}^2 * {d_{ev}}^4}\right) \qquad (4.21)$$

where

n_c = number of cylinders
n_{iv} = number of inlet valves per cylinder
n_{ev} = number of exhaust valves per cylinder
and d_{iv} & d_{ev} are the inlet and exhaust valve head diameters in (mm) which were set to automatically scale with bore size using coefficients supplied by Heywood [2]. If desired for modeling a specific engine, these valve sizes can also be entered manually.

Typical Valve Head Diameter/Bore		
Chamber Type:	**Inlet**	**Exhaust**
2-Valve Wedge/bathtub	.43 - .46	.35 - .37
2-Valve Bowl-in-Piston	.42 - .44	.34 - .37
2-Valve Hemispherical	.48 - .5	.41 - .43
4-Valve Pent-Roof	.35 - .37	.28 - .32

Table 4.2. Typical valve size coefficients for various combustion chamber designs [2].

It should be noted that this method for calculating valve sizes is highly simplistic. It provides a reasonable match to existing automotive engines, but for REX engines that operate within a constrained speed and load range, valves are generally sized relative to the

displaced volume of the cylinder rather than its bore diameter alone; and other assumptions and inputs concerning the intake system design and target operating speed are required to optimize the gas dynamics and maximize the volumetric efficiency [6].

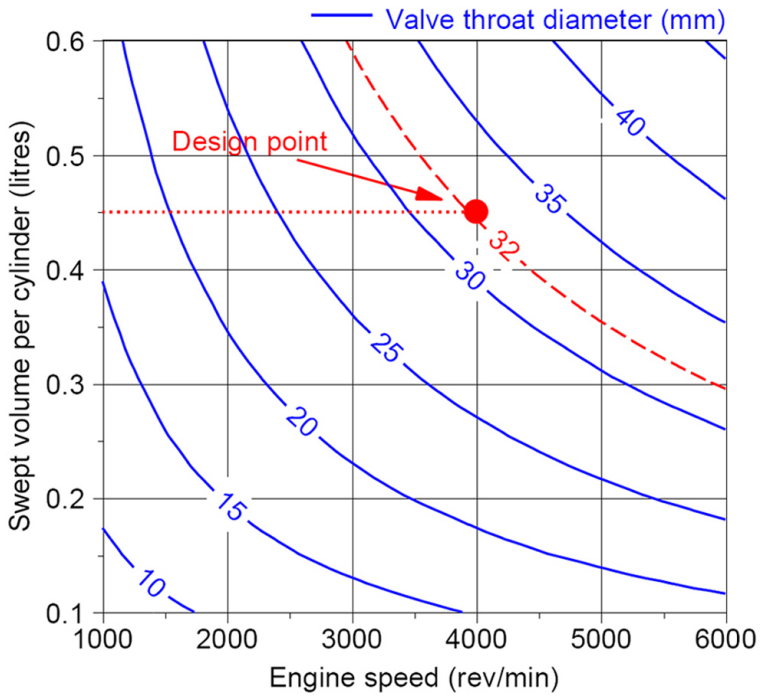

Figure 4.4. Variation in optimal valve throat diameter for various cylinder displacement and crank speed values. Shown is an interpolated design point for a REX engine intended to operate at 4000 RPM [6].

For this model, the decision was made to simply scale the valves relative to the bore or specify the diameter manually in order to aid in validation, and to more easily study and compare parameter curves over wide speed ranges for different engine configurations without having to juggle several additional degrees of freedom. However, this decision precluded a study of different valve arrangements that was initially planned to be included in chapter 5.

4.3.3.5. Blowby

The final component in Bishop's friction model accounted for intake charge and cylinder pressure losses due to leakage around the piston, past the rings, and into the crankcase during the compression and expansion strokes. Bishop developed a correlation for effective blowby FMEP based on data from tests in the 1960s with a single-cylinder laboratory engine [1].

$$PMEP_{blowby} = 6.89476 * \left(\frac{p_i}{p_a}\right)^{.5} * \left(1.72 * R_c{}^{.4} - (.49 + .015 * R_c) * \left(\frac{N}{1000}\right)^{1.185}\right) \quad (4.22)$$

The losses predicted by Bishop's blowby model were much higher than the normal 1% charge loss predicted for more modern engines in proper operating condition [2]. Blowby is a variable, geometry-dependant loss that should increase at higher loads and lower speeds, and could be worth revisiting in a more refined iteration of this model, but its magnitude should be negligible for the purposes of this general study. Therefore, an up-to-date blowby component was not developed for this model, and the blowby IMEP/speed array that used equation 4.22 was disabled during simulations. Currently, the effects of blowby are assumed to be adequately accounted for in the combustion efficiency input η_c, as suggested by Wu et al [3].

4.3.4. Brake performance

Once the total friction MEP values were obtained, BMEP, mechanical and brake efficiencies η_m and η_b, and BSFC were calculated:

$$BMEP = IMEP - FMEP_{total} \quad (4.23)$$

$$\eta_m = \frac{BMEP}{IMEP} \quad (4.24)$$

$$\eta_b = \eta_i * \eta_m \quad (4.24)$$

$$BSFC = ISFC * \frac{IMEP}{BMEP} = \frac{ISFC}{\eta_m} \quad (4.25)$$

Using the BMEP values, the IMEP/speed arrays for BSFC, mechanical, cycle, & brake efficiencies, and other parameters were remapped to BMEP using basic linear interpolation:

$$X_{(BMEP,N)} = X_{(IMEP^-,N)} + \frac{\left(X_{(IMEP^+,N)} - X_{(IMEP^-,N)}\right) * \left(BMEP - BMEP_{(IMEP^-,N)}\right)}{\left(BMEP_{(IMEP^+,N)} - BMEP_{(IMEP^-,N)}\right)} \quad (4.26)$$

where X is the parameter of interest, and BMEP and N describe the brake operating point being populated. A subscript of (BMEP,N) denotes a specific point in the final BMEP/speed array, a subscript of ($IMEP^-$,N) denotes the point in that parameter's IMEP/speed array at the IMEP value that results in the closest BMEP below the target BMEP, and a subscript of ($IMEP^+$,N) denotes the point in that parameter's IMEP/speed array at the IMEP value that results in the closest BMEP above the target BMEP.

To provide a wide range of indicated operating points for interpolation, the IMEP/speed arrays ranged from 50 to 2,000 kPa and 400 to 10,000 RPM in intervals of 50 kPa and 200 RPM. The BMEP/speed arrays used the same speed values, while the BMEP range of interest was adjustable, and could either be defined directly by BMEP, or by total brake torque. In the latter case, the corresponding BMEP values were automatically calculated using the relevant design inputs.

4.4. Results and Validation

Despite the simplifications and assumptions, results for friction and mechanical efficiency from this model were still a good qualitative match with the real-world data and modeled predictions given by Sandoval et al. [5]. Primary validation involved comparing BSFC maps and performance ratings for various production engines to calculated results from this model. An example is shown below in figure 4.5.

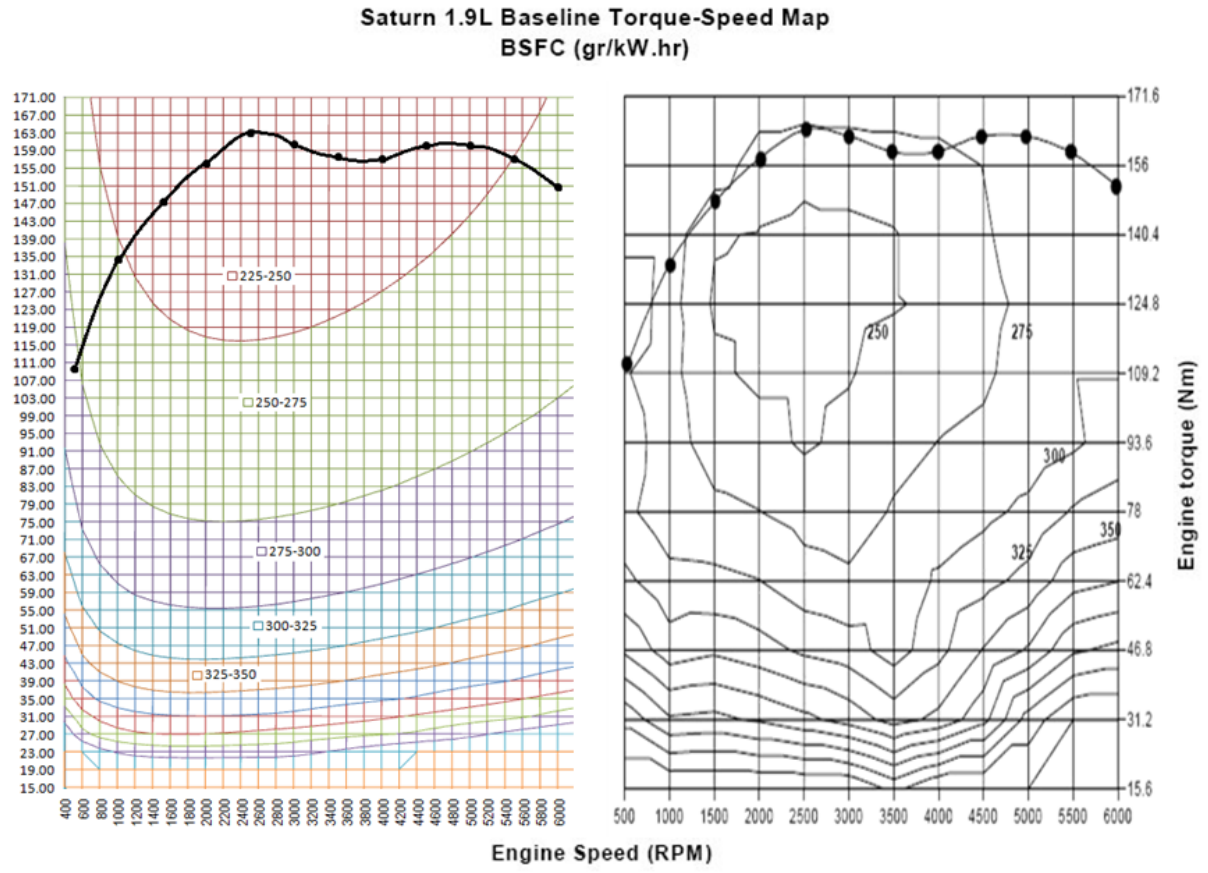

Figure 4.5. Comparison of modeled (left) and published (right) BSFC maps with superimposed peak torque curves for a 1.9 liter, 4-cylinder, DOHC Saturn LL0 engine.

There are some obvious differences when the two are compared; most prominently that the contours produced by the model show ever-decreasing fuel consumption as load is increased, while the published map shows a peak BSFC "island" at less than full load. This is quite typical of automotive SI ICEs, and can be attributed to the fact that most automotive engines change their working air/fuel ratios at different operating points. In particular, it is common for these engines to run rich at higher loads, leading to increased specific fuel consumption at peak torque, and a part-load minimum SFC point [2]. When the fuel/air ratio is held constant, the efficiency of SI engines tends to move to higher loads corresponding to wide-open-throttle (WOT) conditions, where pumping losses in the intake system are generally minimized. The air/fuel ratios of modern automotive engines are usually governed by electronic control systems and pre-programmed fuel maps that are highly specific to a particular engine and application, so it is difficult to account for this factor and precisely match a specific engine's real-world behavior without explicit knowledge of its fuel map.

Other factors that make real-world BSFC contours more complex than those produced by an idealized model include variable ignition and valve timing - both of which are common in modern automotive ICEs - and complex manifold phenomena that influence pumping work, combustion behavior, and volumetric efficiency in ways that are difficult to predict with generalized, steady-state models. This model is capable of being expanded to incorporate these factors, but as with the fuel map, exactly matching test data for a particular engine is difficult without explicit design information.

Finally, SFC is defined as the mass fuel mass consumed per unit of energy produced, so it is directly affected by the energy density of the fuel being used (see equation 4.6). Commercial fuels for 4-stroke SI engines typically contain a variety of additives, which can vary depending on the supplier, and are often blended with various amounts of alcohols, which have very different heating values and other combustion properties [2]. Even the temperature of the fuel will have an effect on its energy density. These details are not always included with BSFC maps, which can lead to discrepancies between modeled results and test data.

Despite these differences though, the model results showed a good qualitative match to published test data, with similar trends in the location and general shape of the BSFC contours relative to speed and load. The non-ideal elements discussed above were intentionally left out or simplified to allow this model to simulate and effectively compare engines of different sizes and configurations, but overall similar design. Some initial attempts were made to incorporate an IMEP/speed array that functioned as a fuel map, but as REX ICEs typically operate at constant air/fuel ratios, this was not fully explored, and all tests simply assumed stoichiometric operation.

While the resultant smooth, idealized efficiency curves are not completely realistic, they present an acceptable qualitative representation of engine behavior, and their simplicity makes for a clearer and more useful basis for general comparisons between engines of similar design and construction.

References

[1] Bishop, I., "Effect of Design Variables on Friction and Economy," SAE Technical Paper 640807, 1964, doi:10.4271/640807.

[2] Heywood, J, "Internal Combustion Engine Fundamentals," McGraw-Hill, New York, ISBN 978-1-25-900207-6, 1988.

[3] Wu, W. and Ross, M., "Spark–Ignition Engine Fuel Consumption Modeling," SAE Technical Paper 1999-01-0554, 1999, doi:10.4271/1999-01-0554.

[4] Muranaka, S., Takagi, Y., and Ishida, T., "Factors Limiting the Improvement in Thermal Efficiency of S. I. Engine at Higher Compression Ratio," SAE Technical Paper 870548, 1987, doi:10.4271/870548.

[5] Sandoval, D. and Heywood, J., "An Improved Friction Model for Spark-Ignition Engines," SAE Technical Paper 2003-01-0725, 2003, doi:10.4271/2003-01-0725.

[6] Bassett, M., Thatcher, I., Bisordi, A., Hall, J. et al., "Design of a Dedicated Range Extender Engine," SAE Technical Paper 2011-01-0862, 2011, doi:10.4271/2011-01-0862.

Chapter 5. Engine Model Results and Analysis

In the early stages of an engine's development, a great deal of effort can be spent making decisions regarding very broad-strokes design characteristics such as the total displacement, the number, shape, and arrangement of the cylinders, and the design of the crankshaft and valvetrain. Settling on the best engine configuration for a specific application can be a substantial endeavor, often involving time- and labor-intensive comparisons between multiple candidate configurations that are performed using disparate and complex simulation and analysis tools.

As with engine sizing, the simplified operation and design of REX engines presents opportunities for streamlining this portion of the design process by using the steady-state modeling techniques introduced in the previous chapter to more expediently predict and compare a number of relevant operating parameters for different engine configurations.

In this chapter, the array-based model developed previously will be used to study the effect of general engine design parameters on performance and efficiency in REX roles. The conclusions drawn here are meant to be qualitative, due to the model's current state of refinement, and to the larger inherent difficulty in precisely predicting the true performance potential of such a wide variety of engines with models of this type. Each section will also include some discussion of other influencing factors that are not explicitly accounted for in the model.

5.1. General ICE Power Relationships

Rotating shaft power is proportional to the product of rotational speed and torque. In an ICE, brake torque is proportional to the product of brake mean effective pressure (BMEP) and total displacement. With some adjustment for units, the shaft power developed by a 4-stroke engine can be defined by a fairly straightforward function of these three basic operating parameters:

$$P = \frac{BMEP * V_d * N}{1.2 * 10^8} \tag{5.1}$$

where

P = brake power in kW

BMEP = brake mean effective pressure in kPa

V_d = total swept volume in cm^3

N = crank speed in RPM

At typical operating speeds, full-load BMEP is generally similar for all engines of the same type. For naturally-aspirated SI engines, full-load BMEP values are usually between 900 and 1100 kPa; higher pressures generally require the use of aggressive tuning or supercharging [1]. Since SI REX engines are usually operated at a more-or-less fixed full or near-full load to minimize pumping losses, speed and displacement are the primary degrees of freedom for achieving a desired engine output.

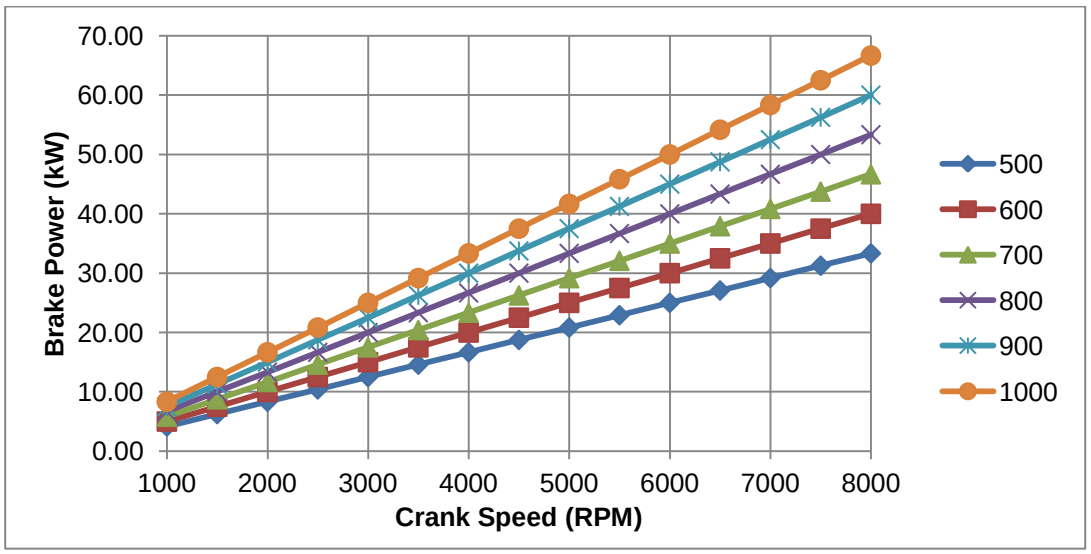

Figure 5.1. Comparison of brake power as a function of crank speed for a variety of engine displacements (in cm^3) operating at 1000 kPa BMEP.

This relationship presents two different approaches for meeting a desired power output. One is to use a small-displacement, high-speed engine in order to minimize the mass and volume of the REX. The high operating speed also allows a smaller and lighter generator to be used [2]. This approach makes a REX easier to integrate into a BEV, and reduces its impact on the vehicle's design and performance, but there are a number of negative trade-offs. SI engines are most efficient at low- to mid-speed operating points;

running at higher speeds reduces total brake efficiency due to increased friction [1]. Effective high-speed operation also requires certain design considerations that tend to increase complexity and work against maximum efficiency at lower outputs. Other downsides include accelerated part wear and increased NVH.

The alternative is to operate the engine at lower speeds that are at or around the its peak efficiency point, and use a larger displacement to increase torque and compensate for the reduced speed. This approach results in a larger, heavier REX that has more of an impact on vehicle design and performance, but the low operating speed can reduce NVH, improve fuel consumption, allow for a simpler and more efficient design, constrain operation to a narrower speed range, and reduce wear.

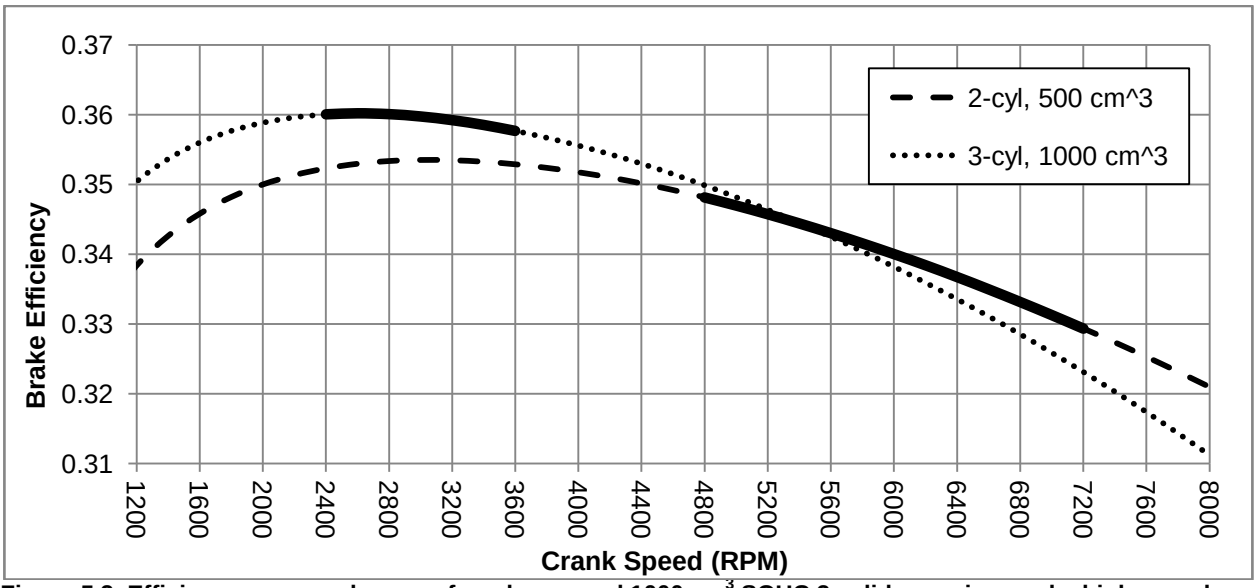

Figure 5.2. Efficiency vs. speed curves for a low-speed 1000 cm^3 SOHC 3-cylider engine, and a high-speed 500 cm^3 DOHC 2-cylinder engine. The highlighted sections of the curves represent speed ranges in which each engine will develop 20 - 30 kW at a BMEP of 1000 kPa.

The chosen approach will affect subsequent configuration decisions, as the following sections will illustrate.

5.2. Bore/Stroke Ratio

An engine's bore/stroke ratio is calculated by dividing the bore diameter by the stroke length. A ratio of 1, in which the bore and stroke are equal, is referred to as a square bore/stroke ratio. Undersquare ratios of less than one reflect a stroke that is longer than the bore, while oversquare ratios greater than 1 describe short-stroke engines with larger bores. Changing the bore/stroke ratio will directly affect many operating parameters.

Efficiency curves were calculated for 2-, 3-, and 4-cylinder engines operating at 1000 kPa BMEP for speeds between 1000 and 6000 RPM. Engine displacements ranged from 500 to 1000 cm^3 in increments of 100 cm^3, and bore/stroke ratios were varied between .6 and 1.2 in increments of .1. All engines were modeled with compression ratios of 10.5, with roller-follower SOHC valvetrains and two valves per cylinder sized relative to the bore as typical for wedge-style combustion chambers [1] (see table 4.2). Combustion efficiency was assumed to be .95, and ambient atmospheric pressure was set at 100 kPa. The resultant curves for the 2-cylinder, 800 cm^3 case are shown here. Curves for other engines are presented in appendix A.

The results showed that high bore/stroke ratios led to improved mechanical efficiency. This was found to be due primarily to the fact that both friction and pumping losses are highly dependent on mean piston speed. For a given displacement and crankshaft speed, a lower bore/stroke ratio results in a longer stroke, and thus a higher mean piston speed. Distributing the total engine displacement across more cylinders increased the number of moving parts, but also reduced the stroke length and mean piston speed. As a result, adding more cylinders reduced the impact of the bore/stroke ratio on mechanical efficiency at higher speeds, but increased it at lower speeds.

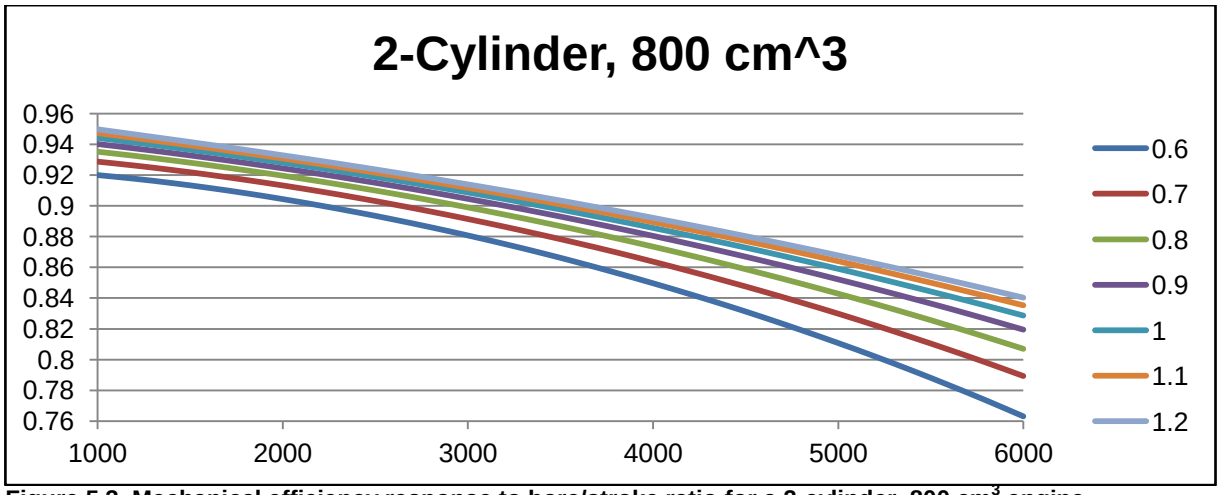

Figure 5.3. Mechanical efficiency response to bore/stroke ratio for a 2-cylinder, 800 cm^3 engine.

Contrary to mechanical efficiency, thermal efficiency favored low bore/stroke ratios due to the dependence of heat loss on the cylinder's surface-to-volume ratio (see equations 4.4 and 4.5). A lower bore/stroke ratio reduced the relative surface area of the combustion chamber, causing less heat to be transferred out of the cylinder during the compression, combustion, and expansion events [1][3]. The effect of the bore/stroke ratio on the cycle

efficiency was most pronounced at low speeds, where more time was available for heat transfer.

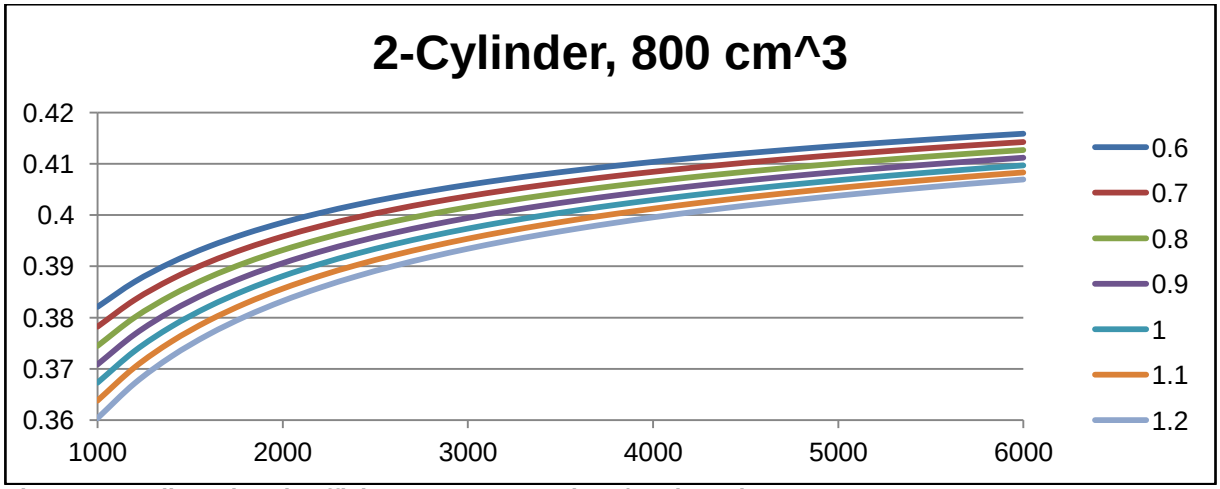

Figure 5.4. Indicated cycle efficiency response to bore/stroke ratio.

Another positive effect of a low bore/stroke ratio on cycle efficiency is that the narrower bore results in a shorter flame path for faster combustion and improved knock resistance. This allows the engine to use a higher compression ratio, lower-octane fuels, and/or more optimal ignition timing [4]. This is not directly accounted for here, as this model assumes no change in timing loss for different bore sizes [3].

When the cycle and mechanical efficiencies were combined into the overall brake efficiency, larger bore/stroke ratios led to peak efficiency at higher speeds, while smaller bore/stroke ratios had lower-speed peak efficiency points in all cases. An undersquare bore/stroke ratio of .8 provided the highest peak brake efficiency in all cases, though the difference between the maximum efficiency values for each ratio was less than 1% of total brake efficiency. Changing the bore/stroke ratio had more of an impact on brake efficiency at speeds well above or below the peak efficiency operating range. Undersquare engines were most efficient at low speeds, though there were diminishing returns on ratios below .8 or .9. At high speeds, high bore/stroke ratios gave the highest brake efficiency, though there were again diminishing returns for ratios above .9 or 1. The variation at high speeds was more pronounced in engines with larger displacements and fewer cylinders.

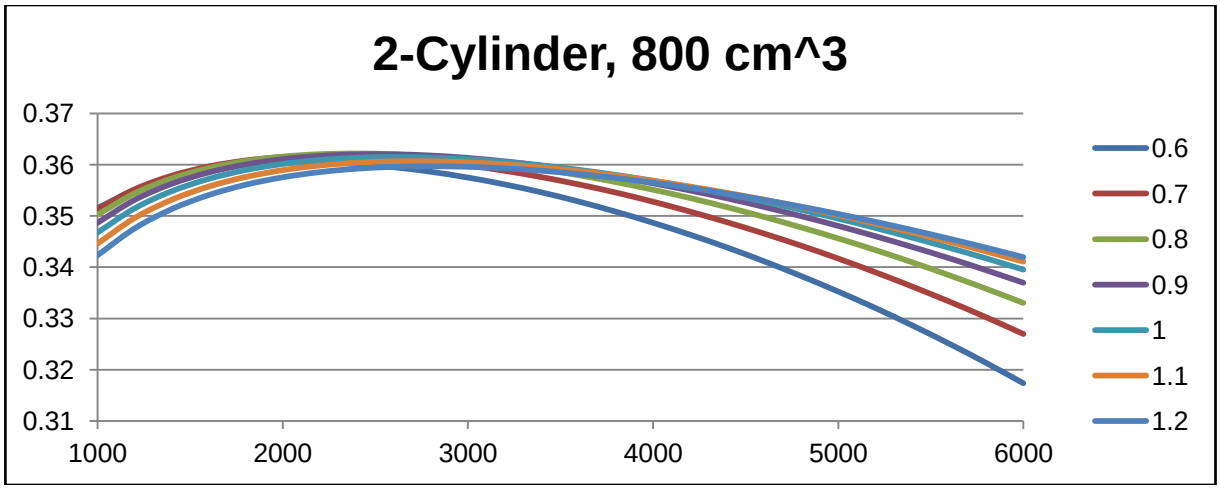

Figure 5.5. Total brake efficiency response to bore/stroke ratio.

Based upon these results, undersquare bore/stroke ratios between .8 and .9 were found to offer the best all-around efficiency for engines in this displacement range that are intended to operate at or around their peak efficiency speed. Lower ratios offered very little improvement at speeds below the peak efficiency point, and had a much more pronounced negative effect at higher speeds. For engines intended to always operate well above their peak efficiency speeds, square ratios were found to be the best-balanced choice. Oversquare ratios offered minor high-speed efficiency gains, but could result in less-effective combustion behavior.

There are other considerations regarding bore/stroke ratio that are not directly related to efficiency, however. A long stroke will increase the height or width of an engine, which can be undesirable if packaging is a design priority [5]. For unbalanced engine configurations, a larger bore may also increase the forces that must be dampened by the engine mounts or counteracted by a balance system. On the other hand, if a dished piston is to be used to achieve the desired combustion chamber volume and/or shape at top dead center (TDC), a narrower bore can complicate the design of the piston [4].

5.3. Number of Cylinders

Efficiency data were gathered for 2-, 3-, and 4-cylinder engines with displacements between 500 and 1200 cm^3 operating at a BMEP of 1000 kPa and at speeds between 1000 and 8000 RPM. All engines used a bore/stroke ratio of .8, and all other model inputs were identical to those of the previous simulations examining bore/stroke ratios. The curves for 800 cm^3 engines are shown here, with curves for other cases presented in appendix B.

For each case, the indicated efficiency improved as the number of cylinders was reduced. As with the bore/stroke ratio, this can be attributed to reduced heat losses due to the reduced total surface area with fewer cylinders. This trend applied to all speeds, but was most pronounced at lower speeds, as would be expected for heat transfer effects [1].

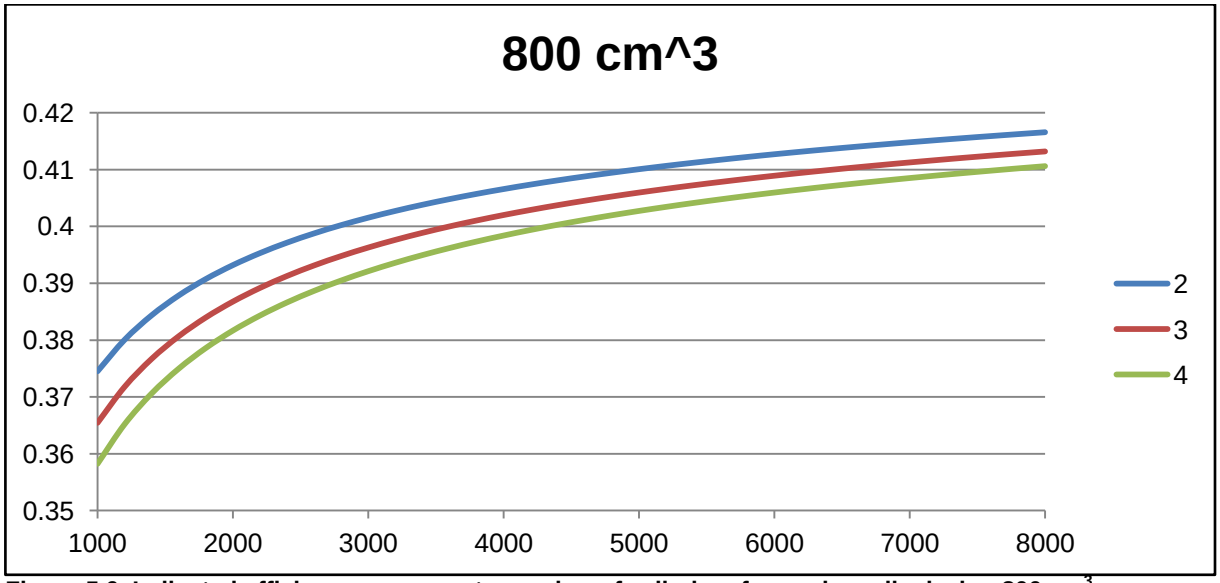

Figure 5.6. Indicated efficiency response to number of cylinders for engines displacing 800 cm^3.

The mechanical efficiency response to the number of cylinders was more complex. Reducing the number of cylinders improved mechanical efficiency at low speeds, but degraded it at high speeds. Investigations of the individual friction components showed that pumping losses were reduced in engines with more cylinders, but mechanical friction was increased. The increase in rubbing friction is easily attributable to the additional valves, bearings, and other points of sliding contact that are added with each new cylinder. While additional cylinders led to a shorter stroke and subsequent reduction in mean piston speed, the friction reduction due to this was not found to be sufficient to offset the increased friction from other sources while the bore/stroke ratio was held constant.

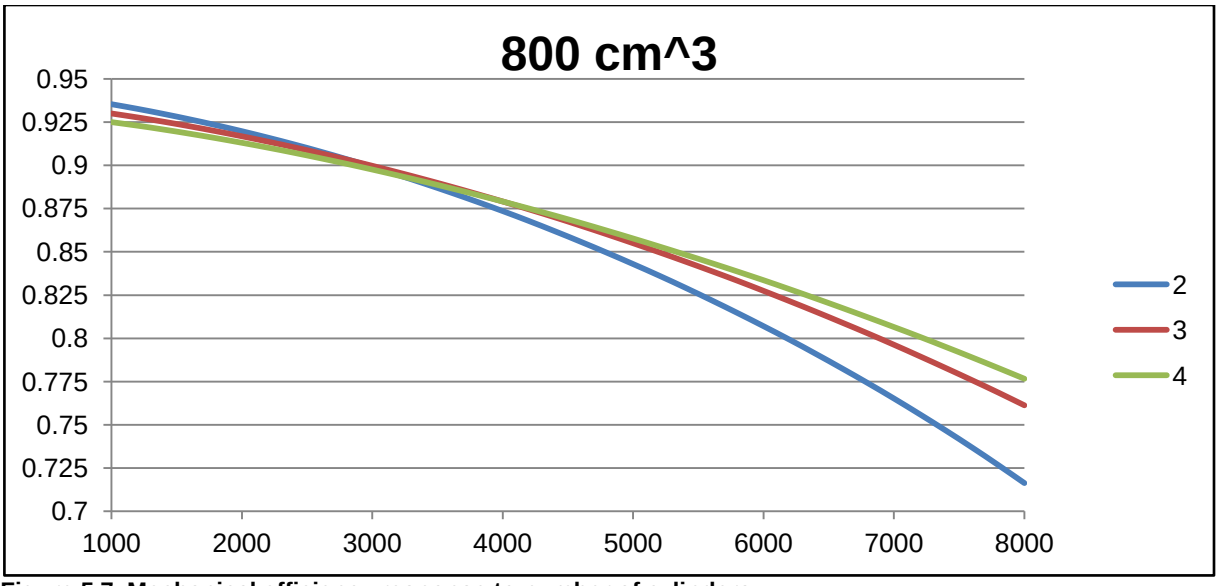

Figure 5.7. Mechanical efficiency response to number of cylinders.

The change in pumping losses with different numbers of cylinders was found to be a result of changes in the geometry of the individual cylinders. The increased mean piston speed in engines with fewer, larger cylinders increased the exhaust manifold pressure, especially at higher speeds, leading to a net increase in pumping work. The valve pumping work also increased due to the higher piston velocity, and the reduced total valve flow area for the same displaced volume. The fact that the ratio of valve flow area to displacement decreases as displacement increases helps to explain why larger-displacement engines had greater high-speed efficiency losses with fewer cylinders.

Combined, the cycle and mechanical efficiencies produced total brake efficiency curves that favored fewer cylinders at lower speeds, and more cylinders at higher speeds. As the displacement was increased, the speeds at which adding another cylinder offered an efficiency advantage were reduced, and the differences in efficiency at high speeds increased. The approximate speed at which the brake efficiency of the 3-cylinder configuration overtook that of the 2-cylinder ranged from 5500 RPM for the 500 cm^3 displacement to just under 3800 RPM for 1200 cm^3. The 4-cylinder configuration overtook the 3-cylinder between 6900 and 5100 RPM, but offered very minor efficiency improvements for all engines simulated. 5- and 6-cylinder engines were modeled as well, but were found to offer negligible benefits for the speeds and displacements studied here, and their complexity would likely make them impractical in this displacement range. For all displacements examined, the 2-cylinder configurations always produced the highest peak efficiency values,

while 3- and 4-cylinder engines had lower peak efficiencies that occurred at slightly higher crank speeds.

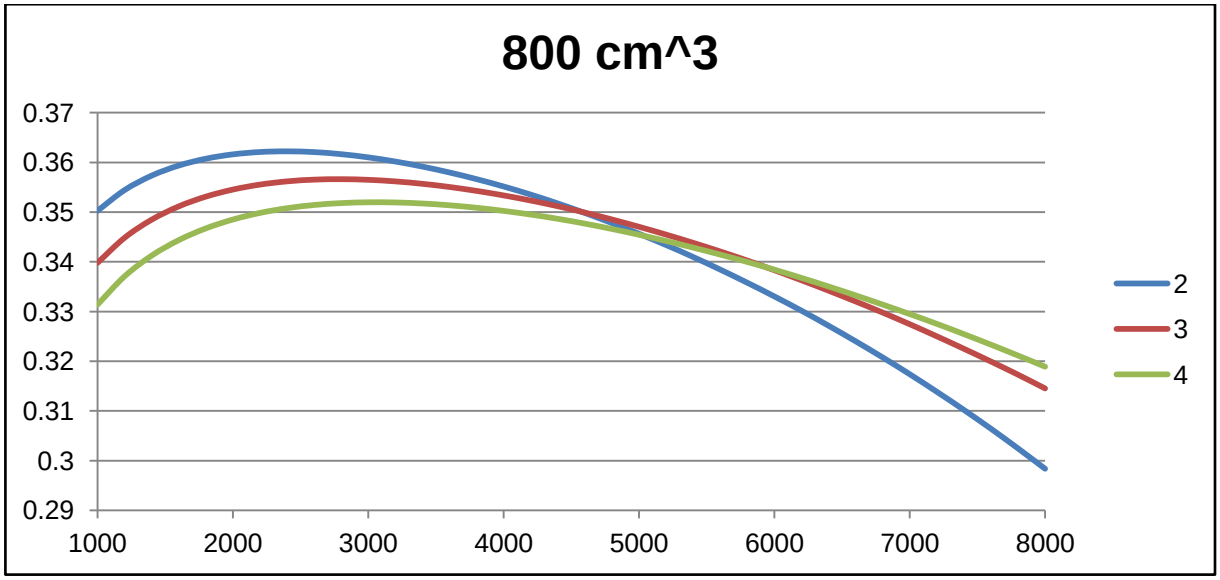

Figure 5.8. Total brake efficiency response to number of cylinders.

This efficiency analysis would seem to indicate that 2-cylinder configurations are the better choice for low-speed engines, and 3- and 4-cylinders should be used in high-speed designs, but the operational nature of REX engines mitigates these efficiency benefits somewhat. As discussed, additional cylinders are most beneficial for larger-displacement engines at high speeds, but high-speed REX engines tend to have small displacements, and larger-displacement REX engines tend to operate at lower speeds that actually favor fewer cylinders.

In addition, increasing the number of moving parts by adding cylinders invariably adds weight and makes the engine more expensive to manufacture. Even at higher operating speeds where additional pistons would theoretically increase brake efficiency, the added expense may not be worth the slight efficiency improvement for REX applications, where the engine is not expected to see frequent use.

On the other hand, 3- and 4-cylinder engines enjoy distinct NVH advantages over two-cylinder engines, which usually have inherent balance issues. To be even-firing, four-stroke inline two-cylinder engines (which require 720 degrees of rotational crank displacement to complete all four strokes) must use a so-called 360-degree crankshaft that causesboth pistons to move up and down together to achieve a power stroke every 360 degrees. This design causes considerable vibrations in a direction parallel to the bore axis, much like the vibrations in single-cylinder engines. There are a number of ways to address

this issue, but all have some downsides. Balance shafts or other reciprocating weights can be used to dampen the vibrations of a 360-degree inline-two, but these also add weight, complexity, cost, and friction [4]. Alternate 180-degree or 270-degree crank designs offer improved, but still imperfect balance, and may still require balance shafts in larger or higher-speed designs if the vibrations cannot be sufficiently reduced or dampened by other means. 180- and 270-degree cranks also force four-stroke inline-two engines to adopt uneven firing sequences that can complicate manifold tuning and increase unwanted NVH [5]. Vee or boxer piston configurations can be better balanced, but are less compact than inline layouts, and they require separate cylinder heads and valvetrains for each cylinder, adding considerable expense and weight [5].

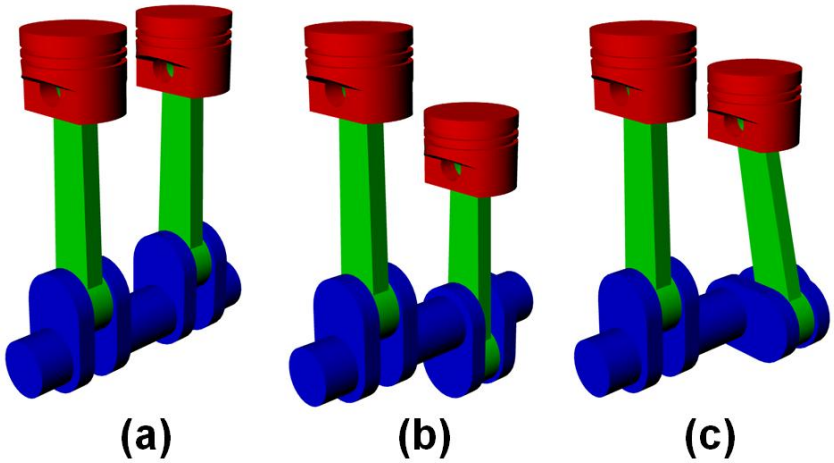

Figure 5.9. Common inline-2 crankshaft designs: 360-degree (a), 180-degree (b), 270-degree (c).

Even-firing inline three- and four-cylinder engines are also inherently imbalanced, but to a less severe degree than even-firing inline-twos. While they can benefit from balance systems, those can often be avoided in the displacement range of REX engines in favor of vibration-dampening engine mounts [4].

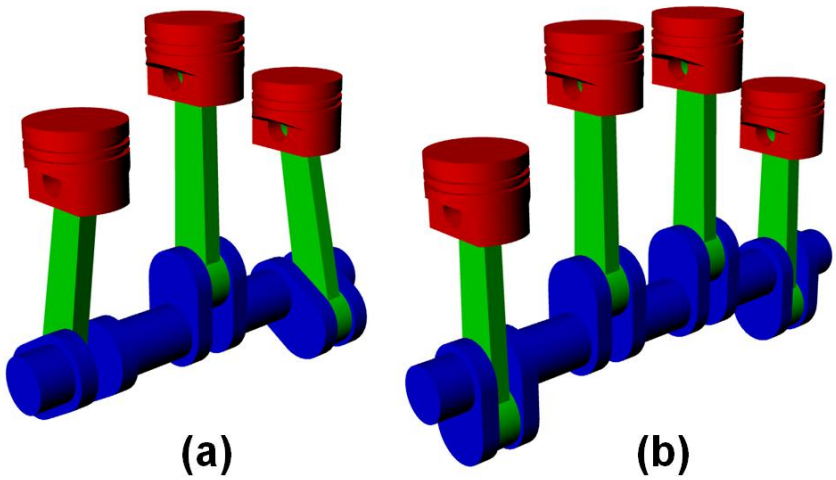

Figure 5.10. Even-firing inline-3 (a) and inline-4 (b) crankshaft designs

Generally, for inline REX engines, larger-displacement engines can benefit from the smoothness and flexibility afforded by more than two cylinders, especially if an even-firing design is desired. Smaller-displacement engines are more likely to benefit from the efficiency advantages of two-cylinder configurations, especially if odd-firing crankshafts are acceptable. This can change depending on the priorities of a specific application, however, which is why these comparisons are important, and why more streamlined modeling tools can be beneficial.

References

[1] Heywood, J, "Internal Combustion Engine Fundamentals," McGraw-Hill, New York, ISBN 978-1-25-900207-6, 1988.

[2] Richardson, D.V., "Handbook of Rotating Electric Machinery," Reston Publishing Company, Inc., Virginia, ISBN 0-8359-2759-8, 1980.

[3] Wu, W. and Ross, M., "Spark–Ignition Engine Fuel Consumption Modeling," SAE Technical Paper 1999-01-0554, 1999, doi:10.4271/1999-01-0554.

[4] Turner, J., Blake, D., Moore, J., Burke, P. et al., "The Lotus Range Extender Engine," SAE Int. J. Engines 3(2):318-351, 2010, doi:10.4271/2010-01-2208.

[5] Bassett, M., Thatcher, I., Bisordi, A., Hall, J. et al., "Design of a Dedicated Range Extender Engine," SAE Technical Paper 2011-01-0862, 2011, doi:10.4271/2011-01-0862.

Chapter 6. REX Case Study Analysis and Comparison

While true EREVs and REXs have yet to achieve broad market acceptance, they are not unprecedented. Both prototype and production REXs have been built, and their development has been well-documented. This presents opportunities for validation of the models developed here and the conclusions drawn from them, or for identification of areas that warrant improvement, based on comparisons to REX engines that have been designed using other tools and techniques.

This chapter presents three existing range extenders based on 4-stroke SI engines, and examines their designs in the context of the models and analyses presented in previous chapters. While they have many similarities, each REX discussed here also has some unique features and differing design priorities, providing a useful variety for comparative purposes.

6.1. Lotus Range Extender Engine

The Lotus Range Extender Engine is a purpose-designed genset ICE intended to meet the needs of a range of midsized D-segment and compact C-segment electric vehicles. A target maximum power output of 38 kW was selected based upon a road-load study that focused primarily on power requirements for high-speed cruising and gradeability, with allowances made for possible future EVs with larger and heavier battery designs. A modest maximum operating speed of 3500 RPM was selected to improve efficiency and limit unwanted NVH, leading to a required displacement of 1200 cm^3 in order to produce the desired power at a target BMEP of 1080 kPa. The engine is also capable of reducing its output by running at lower speeds [1].

Design priorities for this engine emphasized reduced parts count and manufacturing costs, modularity and flexibility, good NVH characteristics, and low weight. From the outset, Lotus engineers sought to pursue a narrow-bore design for a low-surface-area combustion chamber, optimized intake phenomena, improved tolerance of high compression ratios, and easy adjustment of the compression ratio. Pistons were initially manufactured for compression ratios of 10 and 11, and the design allows higher compression ratios to be explored for dedicated alcohol variants in the future.

Other design features include a monoblock construction that combines the cylinder head, block, and exhaust manifold into a single component, a separate crankcase for

improved modularity, a simplified SOHC valvetrain with two optimized valves per cylinder, and an even firing sequence to improve NVH and minimize intake contamination between neighboring cylinders [1].

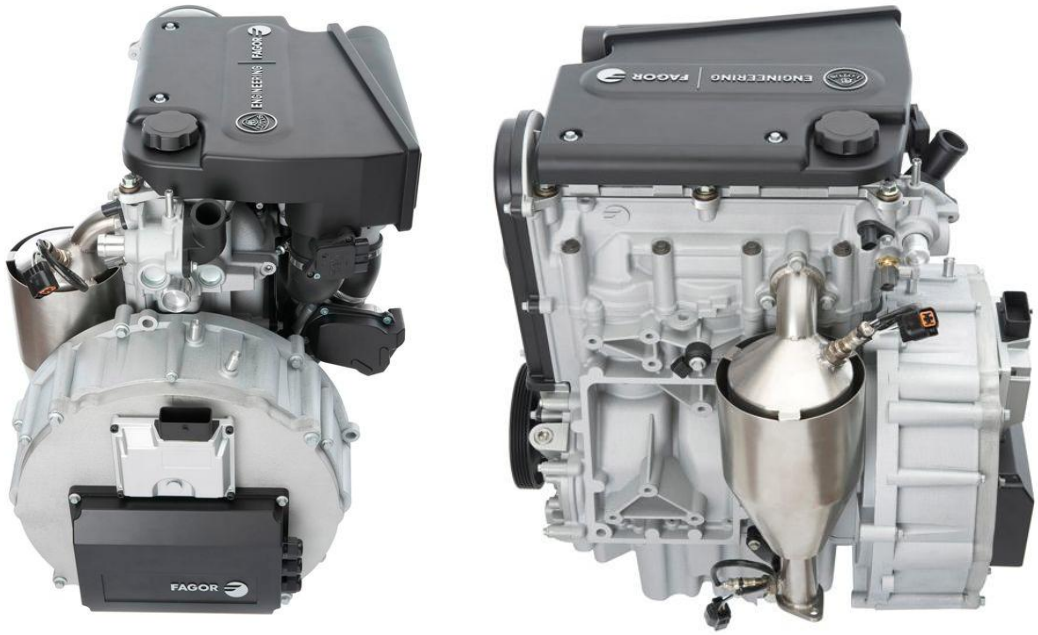

Figure 6.1. The Lotus Range Extender Engine fitted with a generator.

Lotus engineers performed a highly detailed parametric study comparing inline 2- and 3-cylinder configurations for this application. Using the engine model developed in chapter 4, estimated brake efficiency curves were generated based on the designs of the two proposed engines. These are shown in figure 6.2 below:

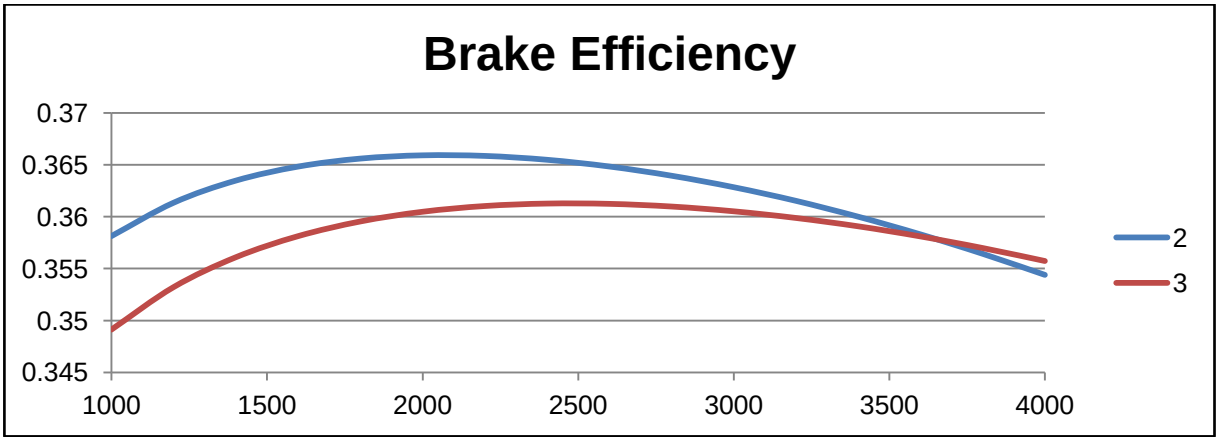

Figure 6.2. Estimated brake efficiency curves for the proposed 2- and 3-cylinder REX engines investigated by Lotus.

These curves suggest that while the brake efficiencies for each configuration are very similar at the target maximum operating speed of 3500 RPM, the 2-cylinder engine offers efficiency improvements at reduced output. Other advantages of the 2-cylinder engine, as discussed in the previous chapter, would have been reduced cost and a smaller package size.

While the size, cost, and thermodynamic advantages of the 2-cylinder were recognized, Lotus engineers ultimately selected the 3-cylinder configuration. A primary reason for this was the 3-cylinder engine's improved NVH characteristics. As mentioned in section 5.3, four-stroke even-firing inline-twos are highly unbalanced, and will produce harsh vertical out-of-balance forces that must be countered by a balance shaft system that would reduce mechanical efficiency and increase cost and weight. By comparison, an even-firing 3-cylinder engine's out-of-balance forces take the form of a rocking couple that results in less severe forces at the engine mounts (aided by the fact that the longer 3-cylinder block would naturally place the engine mounts further apart). Though the prototype 3-cylinder engine would also include a balance shaft system, it could be an optional feature, unlike the balance system for the 2-cylinder.

In addition, the 3-cylinder configuration resulted in reduced per-cylinder displacement for improved gas exchange behavior, and allowed for a narrower bore diameter with fewer manufacturing difficulties and a shorter engine block. Finally, by selecting a 3-cylinder design for the initial 1200 cm^3 engine, Lotus would be better able to develop a future family of range extenders that utilize the same bore and stroke, and share many parts. These include a supercharged 3-cylinder version producing up to 55 kW, and a two-cylinder, 800 cm^3, 24 kW variant for smaller vehicles [1].

The final 3-cylinder design utilized a 75 mm bore and a 90 mm stroke for a bore/stroke ratio of .8333; corresponding quite well to the .8 - .9 bore/stroke ratios recommended for high-displacement, lower-speed REX engines by the analysis in section 5.2.

6.2. MAHLE Compact Range Extender

The MAHLE Compact Range Extender was developed by UK-based MAHLE Powertrain to provide range extension in a compact and flexible package that could be easily integrated into new vehicle models or EREV conversions. The design of the MAHLE REX was based upon a detailed study of the power requirements of compact C-segment

European vehicles. This study simulated the performance and energy needs of typical C-segment EVs over a variety of driving cycles, and incorporated an in-depth analysis of American and European fleet data to better match standard drive-cycle predictions to real-world behavior. The study settled on a 30 kW engine output for the application [2].

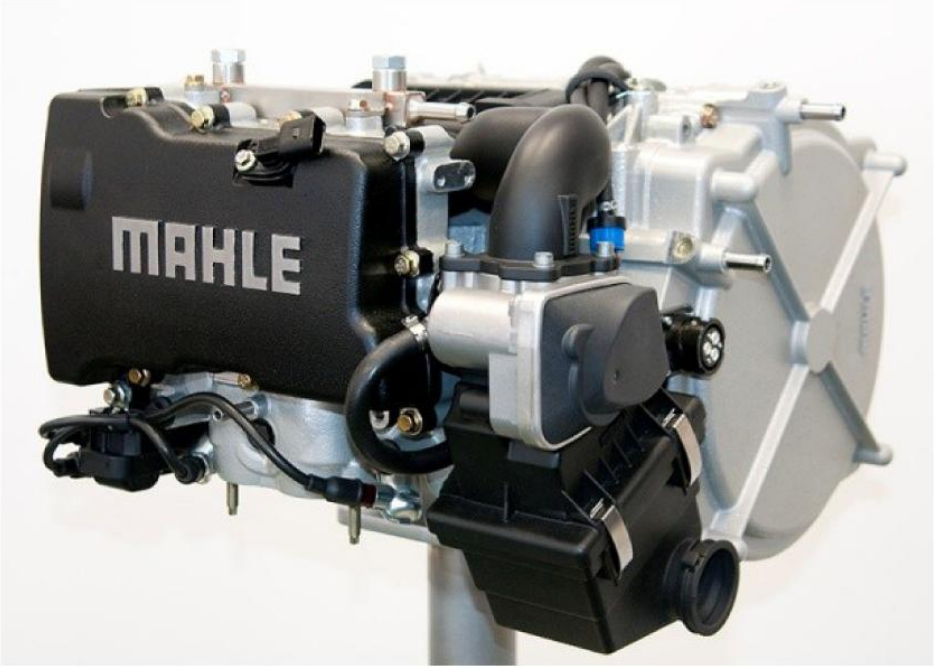

Figure 6.3. The MAHLE Compact Range Extender

With a target full-load BMEP of 1000 kPa, the engine displaces 900 cm^3 to provide the required power at a max-power operating speed of 4000 RPM. The speed can also be reduced to 2000 RPM to produce 15 kW of power with improved fuel conversion efficiency.

The engine uses an inline-two cylinder configuration, based on a parametric study that showed it offered reduced weight, cost, and package volume compared to inline three-cylinder, and V- and horizontally-opposed two-cylinder configurations. To avoid the negative design trade-offs of a balance shaft, an odd-firing 180-degree crankshaft was used to reduce the inherent out-of-balance forces to a counter-rotating couple that could be acceptably dampened by engine mounts. Though this limits tuning and results in some volumetric efficiency variations between the cylinders, MAHLE was still able to meet their BMEP target [3]. The array-based engine model from chapter 4 predicts improved efficiency with two cylinders (see figure 6.4 below), MAHLE's documentation indicates that the engine's size, cost, and weight were the driving factors in selecting this configuration.

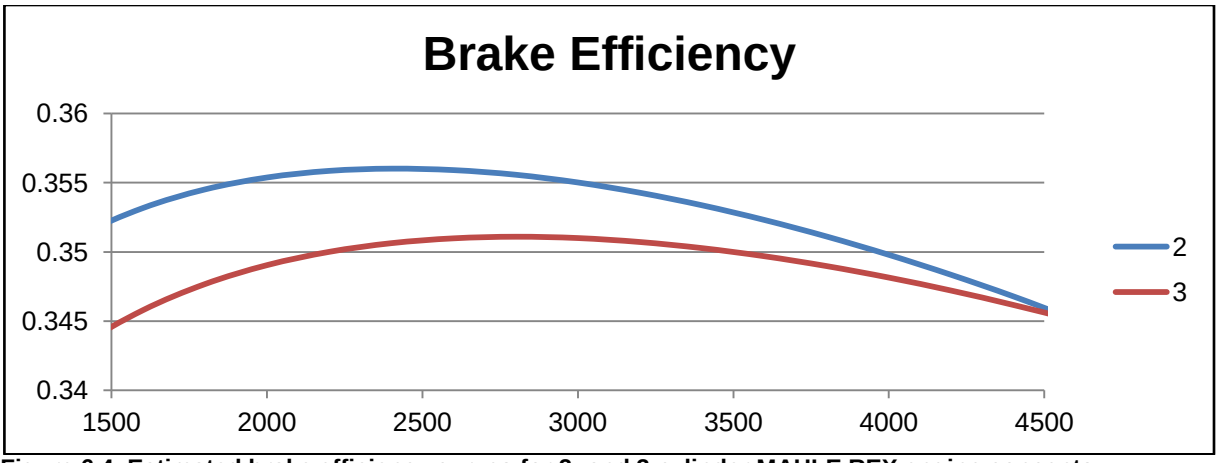

Figure 6.4. Estimated brake efficiency curves for 2- and 3-cylinder MAHLE REX engine concepts.

Because the MAHLE REX was designed with a special emphasis on minimal package volume and mounting flexibility, some design sacrifices were made in pursuit of this, including a less-than-optimal 83 mm square bore/stroke ratio and a modest compression ratio of 9.8 [3] [4]. Based on simulations with the engine model (shown in figure 6.5), an undersquare bore/stroke ratio would likely have improved the engine's efficiency at the reduced-output operating point where low fuel consumption was a priority, and permitted the use of a higher compression ratio.

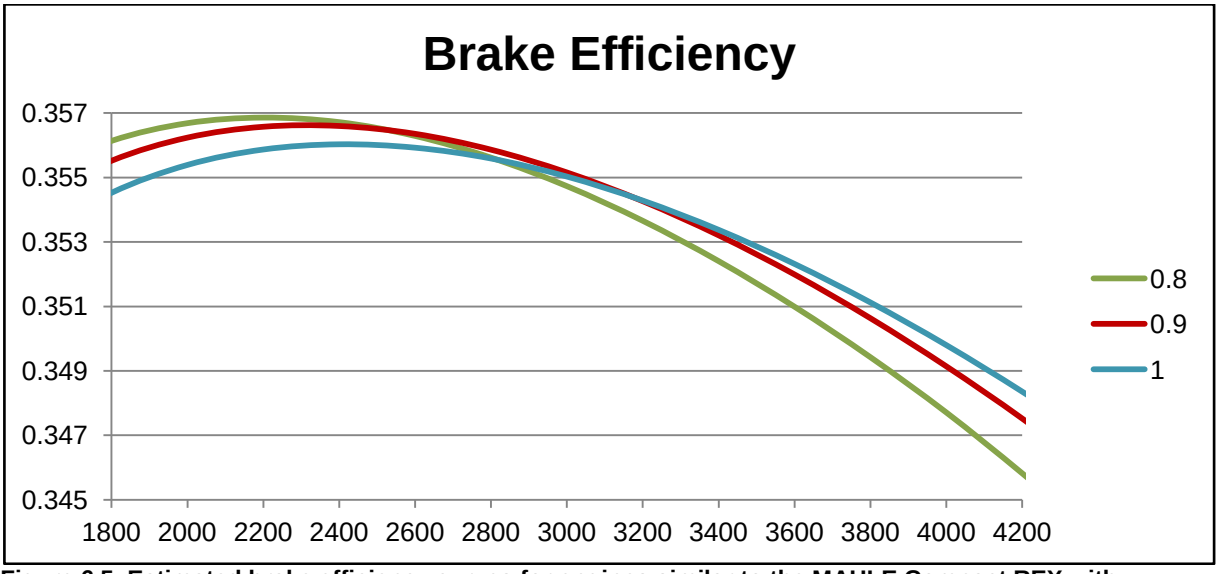

Figure 6.5. Estimated brake efficiency curves for engines similar to the MAHLE Compact REX with various bore/stroke ratios.

However, the curves shown in figure 6.5 suggest that the efficiency gains would be very minor, not enough to justify going against the project's primary design priorities of compactness and ease of integration.

And at this, the final REX design does quite well. With the generator installed, the unit has a mass of just 65 kg, and the block, heads, manifolds, and other integral systems have been arranged into a compact, roughly rectangular package that is 416 x 481 x 327 mm - comparable to a small suitcase. Its total installed mass in a vehicle with a controller, full 40-liter fuel tank, and other required systems is estimated to be 130 kg [5].

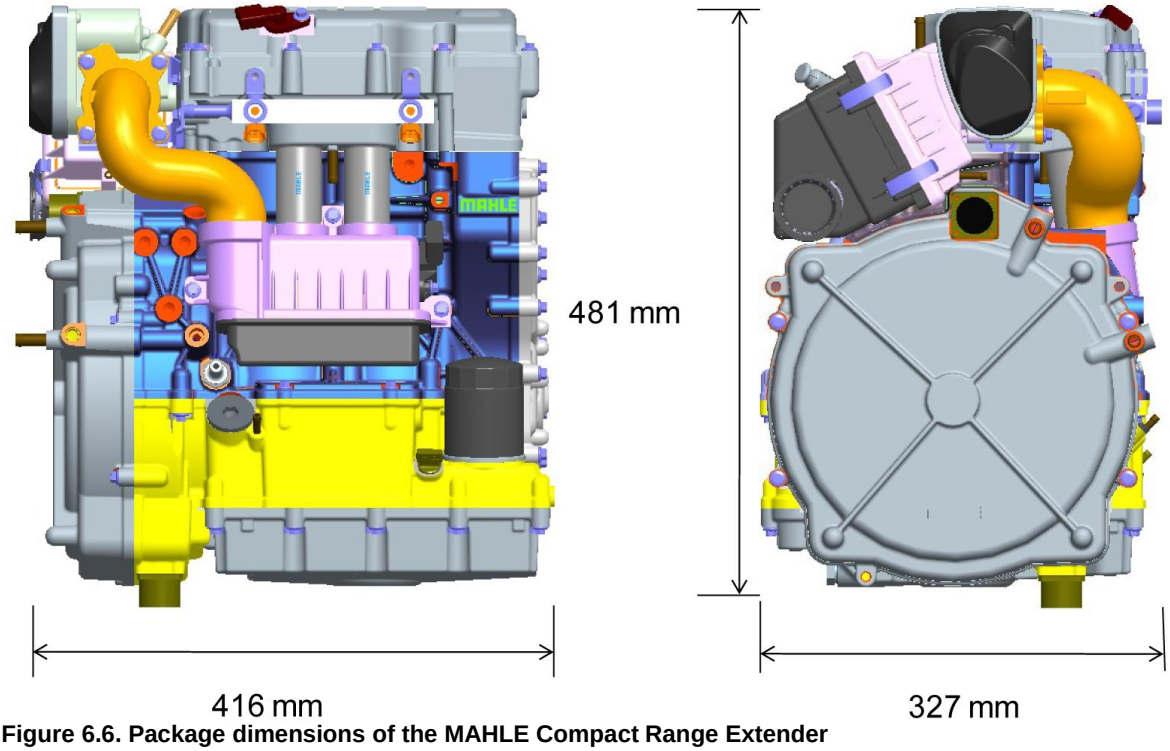

Figure 6.6. Package dimensions of the MAHLE Compact Range Extender

The MAHLE REX can be installed vertically or horizontally; all that needs to be changed is one part in the oil pickup system [4]. Other features include a short and simple two-bearing crankshaft with central flywheel placed between the cylinders, an optimized valve design with two valves per cylinder, roller cam followers to reduce start-up friction without the need for a specialized oil retention system, a very thin and lightweight axial flux generator with a rotor bolted directly to the crankshaft, and design considerations intended to make the prototype easily adaptable to more conventional mass-production manufacturing methods and materials [3]. Cost and complexity trade-offs are well-balanced by the ability to incorporate this REX into a wide variety of BEVs and BEV conversions without requiring the vehicle to be significantly redesigned or modified.

6.3. BMW i3

The BMW i3 is a compact EV that is significant for being a BEV that can be enhanced with an optional REX if desired by the individual buyer. The BEV and EREV versions of the i3 share the exact same electric drive system and battery pack, the only differences are the presence or absence of the REX unit, and some minor variations in trim and options. The base MSRP for the range-extended i3 for US customers is $3850 more than the base BEV i3.

Figure 6.7. The BMW i3 EREV.

When installed, the i3's REX sits next to the vehicle's drive motor between the rear wheels, replacing a structural brace present in the BEV i3. As a result, there is no loss in cargo or passenger space due to the addition of the REX, though it does of course add some mass. The range-extended i3 is approximately 120 kg heavier than the BEV model, and is fitted with slightly larger rear tires to support the additional weight over the rear axle. As a result, the range-extended i3 has a higher rated energy consumption per distance traveled, slightly reduced acceleration, and a shorter all-electric range over standard driving cycles. [6] [7]. These minor trade-offs are to be expected when adding a range-extender, however, and for the most part the BMW i3's REX is a well-done adaptation of an existing production engine.

The only major issue with the execution of the EREV i3 applies to the vehicles sold in the US, which do not allow drivers to employ high-SoC charge-sustaining driving strategies to improve performance and reduce battery wear during long trips. While the REXs in European i3s can be activated before the battery is depleted, this feature is locked out in the

US market in order to comply with California Air Resources Board (CARB) regulations that do not allow EREVs (labeled by CARB with the term BEVx) to be eligible for electric vehicle incentives unless the battery is depleted before the REX can be activated [8].

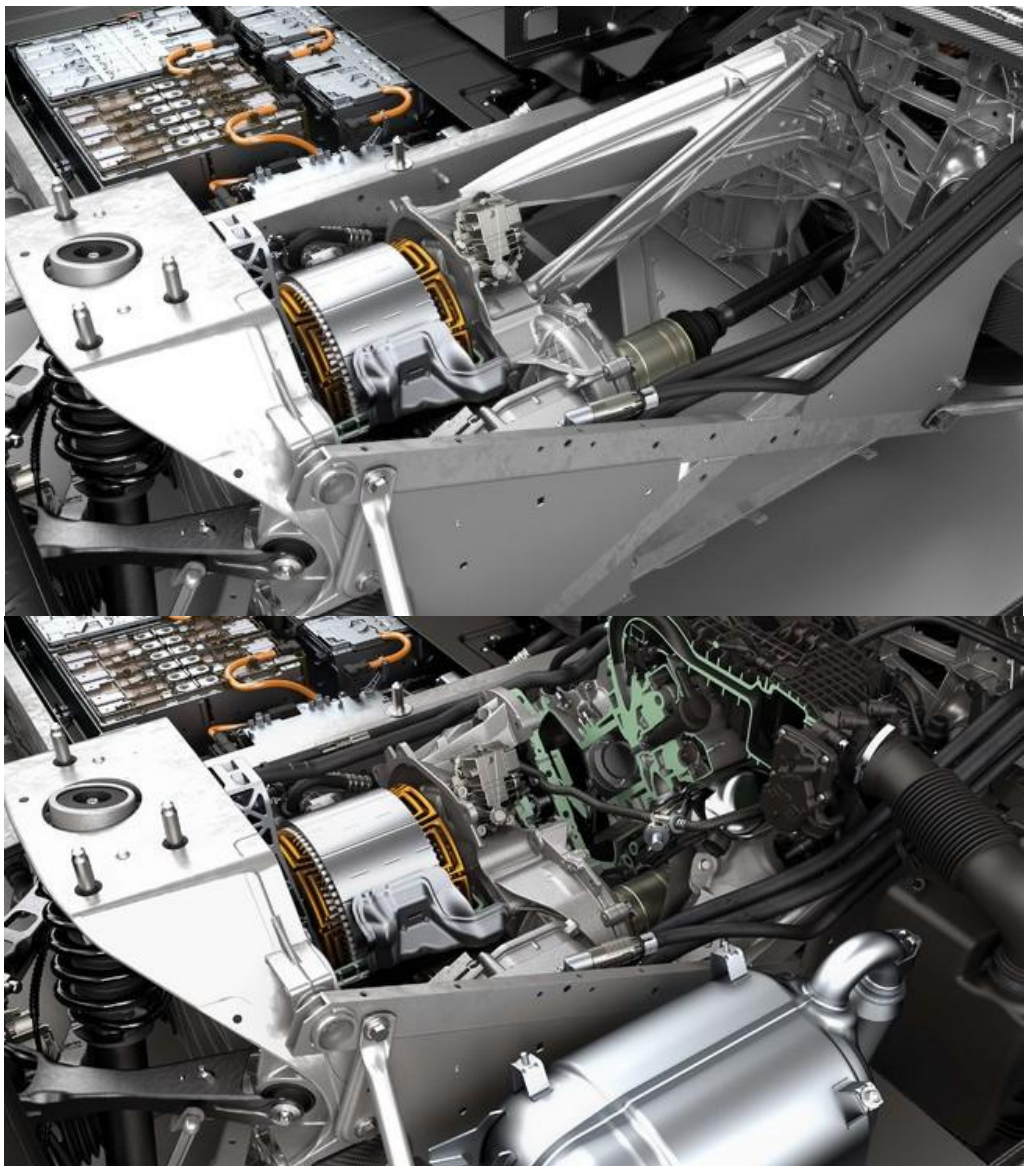

Figure 6.8. BMW i3 driveline for the BEV (top) and the EREV (bottom) variants.

The i3's REX is powered by an inline two-cylinder 647 cm^3 engine adapted from BMW's C600 and C650 GT maxi-scooters [9]. In the scooters, these engines have a compression ratio of 11.6 and produce up to 44 kW at 7500 RPM [9]. In the i3, the compression ratio is reduced to 10.6, and the engine is run at 4300 RPM to produce 25 kW (at an approximate BMEP of 1078 kPa). In both roles, the engines use a DOHC valvetrain and four valves per cylinder. The bore is 79 mm and the stroke is 66 mm, for an oversquare bore/stroke ratio of roughly 1.2. The scooter engines use an odd-firing 270-degree

crankshaft with twin balance shafts to dampen the out-of-balance forces [10]. This crank and balance shaft design is presumably retained in the i3.

Figure 6.9. BMW Motorrad C 650 GT scooter (left) and engine (right).

This engine is apparently a high-speed design that operates above its peak efficiency speed in order to achieve a small displacement. A square or oversquare bore/stroke ratio is beneficial for this type of operation due to the decreased mechanical friction and higher possible relative valve flow area; but results from the steady-state engine model suggest that a bore/stroke ratio closer to 1 would likely be more optimal in this role, since the engine isn't operating in excess of 7000 RPM as in the scooter. According to the model however, there should very little difference in total brake efficiency for bore/stroke ratios between 1 and 1.2 for this size and type of engine. The cost and production benefits of the common parts and shared manufacturing would likely do more for the REX's marketability than a fraction of a percent change in the engine's theoretical brake efficiency.

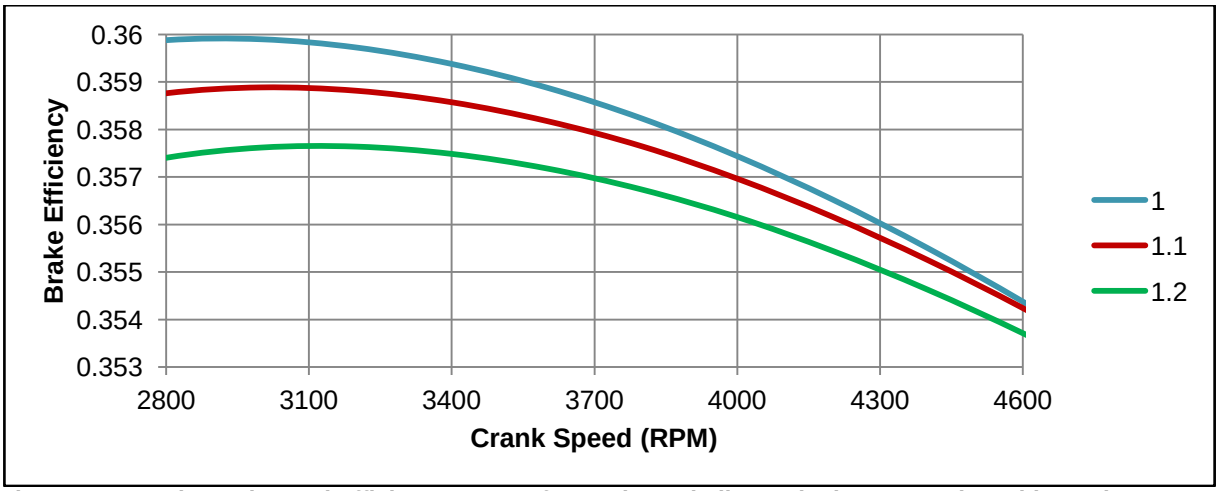

Figure 6.10. Estimated speed-efficiency curves for engines similar to the i3 REX engine with varying bore/stroke ratios.

The same goes for the engine's valvetrain. The 4-valve DOHC valvetrain designed for quick response and peak power at speeds up to 7500 RPM in a high-performance scooter is likely unnecessary for constant-speed operation at 4300 RPM, especially given the engine's wide bore and low displacement. A SOHC design with two properly-sized valves per cylinder should reduce mass, friction, and complexity while still providing an optimal flow area. Once again though, the differences in total mass and overall efficiency are likely minor at best, and would be outweighed by the production benefits.

So while the scooter engine is somewhat more complex than necessary, the potential efficiency gains that could be achieved with a new, purpose-designed engine are likely minor at best, and there are obvious production advantages to using an existing engine. This makes the adapted scooter engine a good choice, especially with the fact that the i3 is not intended for frequent operation outside its EV range, or very long-distance travel.

References

[1] L Turner, J., Blake, D., Moore, J., Burke, P. et al., "The Lotus Range Extender Engine," SAE Int. J. Engines 3(2):318-351, 2010, doi:10.4271/2010-01-2208.

[2] Bassett, M., Fraser, N., Brooks, T., Taylor, G. et al., "A Study of Fuel Converter Requirements for an Extended-Range Electric Vehicle," SAE Int. J. Engines 3(1):631-654, 2010, doi:10.4271/2010-01-0832.

[3] Bassett, M., Thatcher, I., Bisordi, A., Hall, J. et al., "Design of a Dedicated Range Extender Engine," SAE Technical Paper 2011-01-0862, 2011, doi:10.4271/2011-01-0862.

[4] Bassett, M., Hall, J., OudeNijeweme, D., Darkes, D. et al., "The Development of a Dedicated Range Extender Engine," SAE Technical Paper 2012-01-1002, 2012, doi:10.4271/2012-01-1002.

[5] Christoffel, J., SAE International, "MAHLE Unveils Compact 30-kW Range Extender for EVs," http://articles.sae.org/10227, Sep. 2011.

[6] BMW, "BMW i3 product page," http://www.bmw.com/com/en/newvehicles/i/i3/2013/showroom/index.html, 2014.

[7] Cole, J., Inside EVs, "BMW i3 Range Extender To Offer Up to 87 More Miles, Decreases Performance," http://insideevs.com/bmw-i3-range-extender-to-offer-up-to-87-more-miles-decreases-performance/, July 2013.

[8] Voelcker, J., Green Car Reports, "2014 BMW i3 Electric Car: Why California Set Range Requirements, Engine Limits," http://www.greencarreports.com/news/1087888_2014-bmw-i3-electric-car-why-california-set-range-requirements-engine-limits, Oct. 2013.

[9] BMW Motorrad, "Urban Mobility," http://www.bmwmotorcycles.com/us/en/index.html?content=http://www.bmwmotorcycles.com/us/en/urban_mobility/c650gt_2012/c650gt_overview.html&notrack=1, 2014.

[10] Boeriu, H., BMW Blog, "BMW C 600 Sport and BMW C 650 GT - New BMW Scooters," http://www.bmwblog.com/2011/11/09/bmw-c-600-sport-and-bmw-c-650-gt-new-bmw-scooters/, Nov. 2011.

Chapter 7. Conclusions and Recommended Future Work

This paper presented a thorough investigation of the design and operation of EREVs and range extenders. Taking advantage of the relatively straightforward operating nature of REX engines, simplified math-based models were developed to aid in the sizing and configuration of 4-stroke spark-ignition engines intended for this role. These models were then used to study the impact of engine design parameters on performance and efficiency, and the conclusions from that study were compared to the design decisions made for existing REXs

7.1. Conclusions

The validations and comparisons in the previous chapters show that the models developed in this paper produce realistic results based on very simple inputs and relatively straightforward computational structures.

The sizing model predicts maximum REX power requirements for typical passenger vehicles by applying well-known road-load power relationships in such a way that they can be employed using simple algebraic calculations.

The steady-state engine performance model is, in its current state, able to assist in making qualitative decisions regarding various aspects of ICE configurations. It can help identify optimal values for various design variables, and also - as revealed in chapter 6 - identify when selecting a non-optimal value for a design variable would be an acceptable trade-off in order to improve other aspects of an engine's design.

7.2. Recommended Future Work

The models and conclusions developed and presented here are intended as starting points toward the development of streamlined tools specifically intended to be used in the design of REX engines. Further development and refinement of these concepts and methods will increase their usefulness and allow them to adapt as REXs become more widespread and refined.

7.2.1. REX Sizing Model

The sizing model developed here is not intended to replace existing drive-cycle analysis techniques; it is meant to be a simplified and streamlined way to examine constant-speed operation and estimate the maximum output required from a REX. In its current state, it accomplishes this goal for EREVs.

However, this steady-state modeling approach could be used to examine some additional operating phenomena. It would not be difficult to calculate the required REX duty cycle to meet a certain power demand at a given speed, and for a given duty cycle and cycle period, the extent to which the battery is cycled and the energy lost to charging/discharging losses could also be approximated with some additional inputs.

This model could also be expanded to more accurately model REX trailers. The principles of rolling resistance, weight, and aerodynamic drag forces for constant-speed operation of an EREV also apply to the combined system of a BEV and REX trailer, but the application of those concepts is not as simple.

The added mass of a trailer will affect gradeability and inertia much as the added mass of an integrated REX will (though a trailer will obviously be significantly heavier), but the effect of the trailer on rolling resistance and drag is rather more complex. The weight of the trailer is supported by both its own wheels and suspension, and those of the tow vehicle, and each will have different rolling resistance coefficients. The distribution of the trailer's weight between the two will depend on the design of both the trailer and the tow vehicle, and possibly even dynamic elements such as the state of the trailer's fuel tank. Likewise, the aerodynamic interactions between a tow vehicle and trailer can be complex, and their combined drag coefficients will have to be studied on a case-by-case basis.

Tests, simulations, and design studies of various combinations of BEVs and REX trailers would be necessary in order to identify exactly how the maximum output requirements of a trailer-mounted REX differ from those of an integral REX.

7.2.2. REX Engine Model

The flexibility and usefulness of array-based engine modeling has already been discussed in chapter 4. The model developed and analyzed in this work was found to be adequate for its intended use of comparing different engine configurations, but as this is a first attempt, there is some room for improvement.

As discussed in section 4.3, the relations used to calculate manifold pressures and scale the size of the valves are fairly general and simplistic. While throttling PMEP is generally not a major concern for REX engines, valve flow work and other gas exchange phenomena are important considerations that should play into the selection of engine configuration. Even for use in general configuration comparisons, it would be beneficial to refine the model, and allow it to more realistically calculate manifold pressure, and predict the effect of valve size and arrangement on pumping work, volumetric efficiency, and indicated performance.

The friction model used here is robust and capable of general qualitative comparisons, but there are still some simplifications and assumptions that could be improved upon, especially with regard to bearing losses. Also, the correlations used in this model are not all based on the current state of the art, and are largely derived from tests with larger-displacement CV engines that were not specifically designed to be prime movers in a genset. Additional development based on tests with more relevant engines could allow this friction model to produce more reliable quantitative information while still retaining its functional advantages over more specialized and complicated engine simulation software.

Finally, this model could be expanded to include secondary operating phenomena that vary with speed and load. The comparisons in chapter 6 demonstrated that considerations such as weight, size, and balance were often of more importance than idealized efficiency. With the proper inputs and assumptions, the frequency and magnitude of noise and vibration could be estimated at different brake operating points the same way other performance parameters are. Exact NVH figures may be difficult to calculate, but it should be possible to obtain estimates that are sufficient for comparing different configurations of engines of a similar design. This would greatly increase the usefulness of this model as a design tool.

Appendix A

Speed-Efficiency Curves for Engines with Varying Bore/Stroke Ratios

500 cm^3, 2-Cylinder

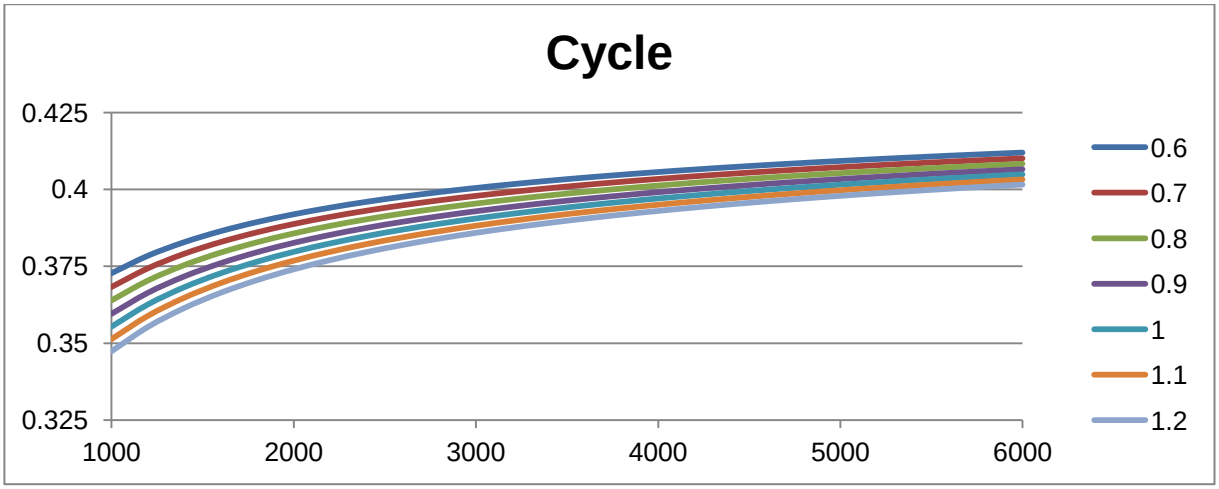

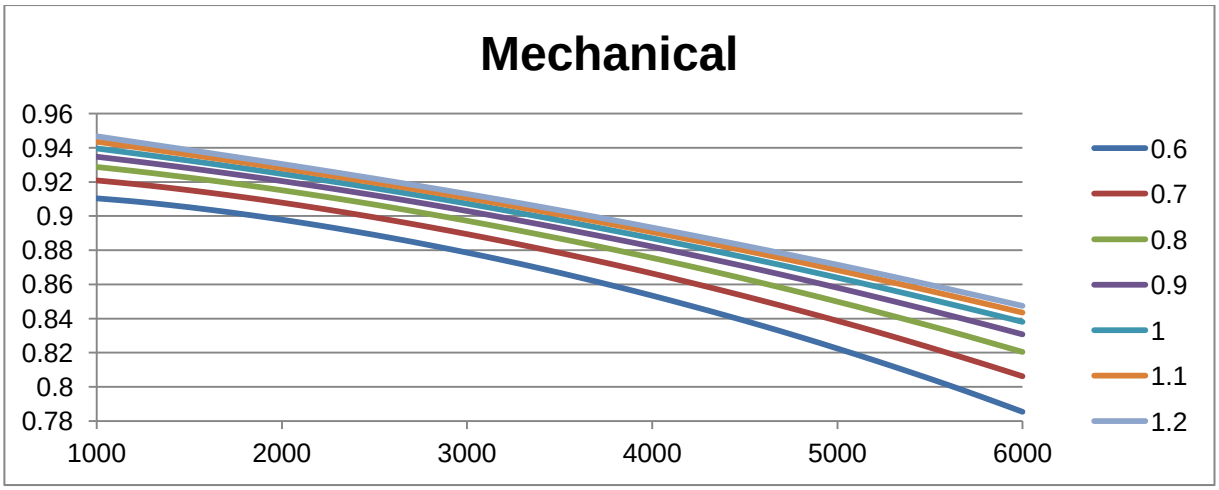

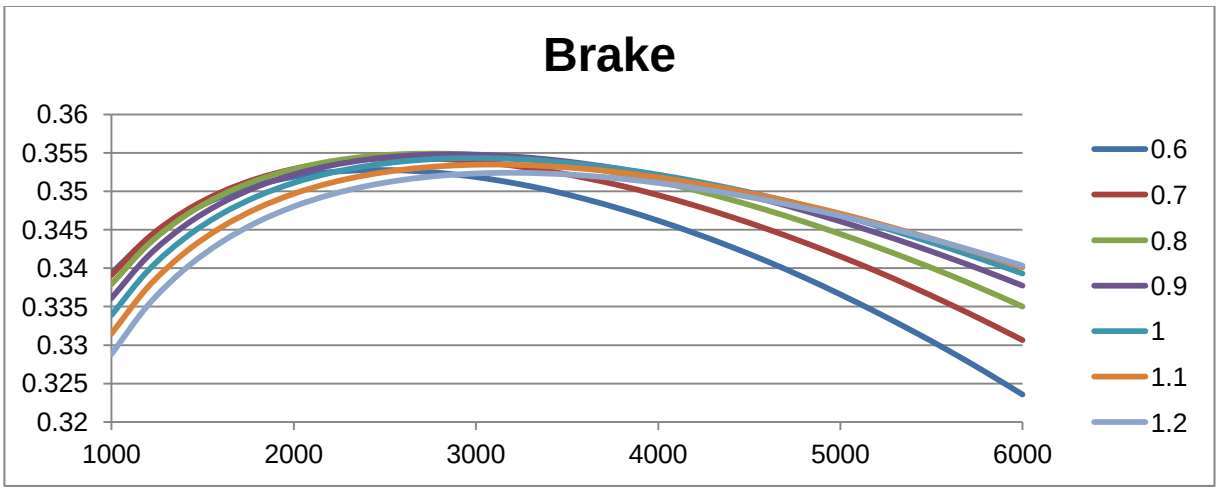

500 cm^3, 3-Cylinder

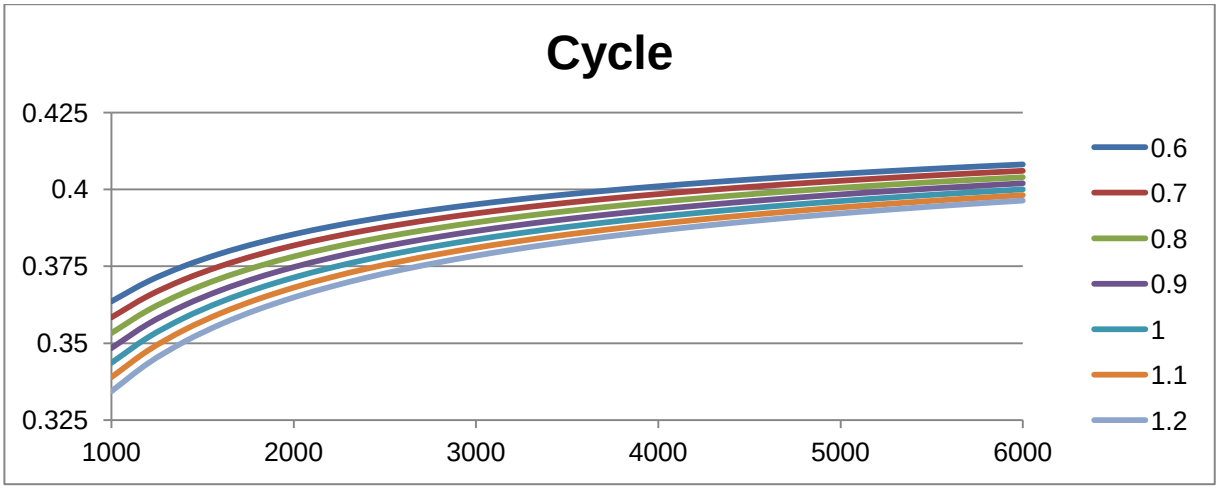

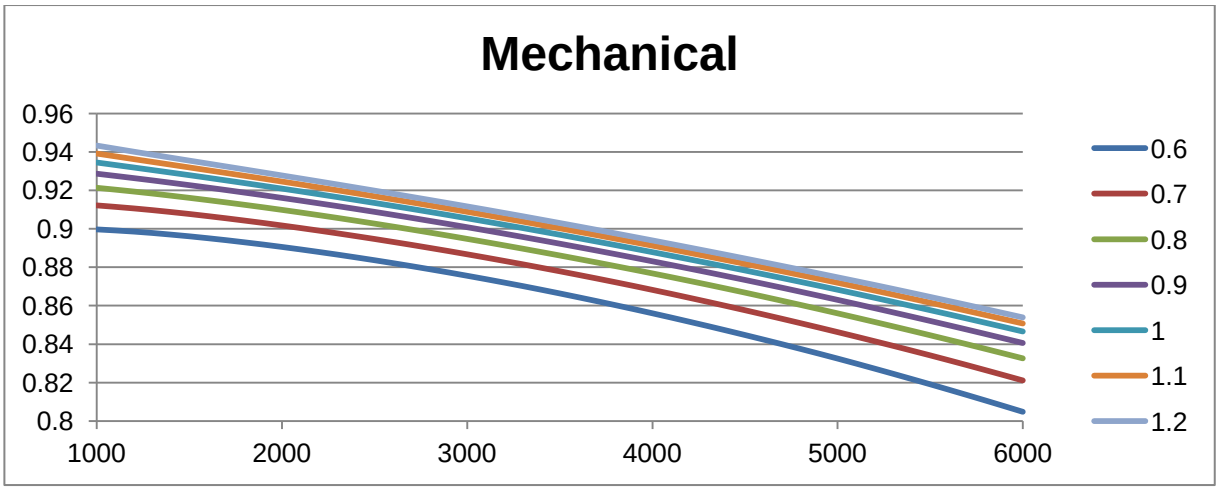

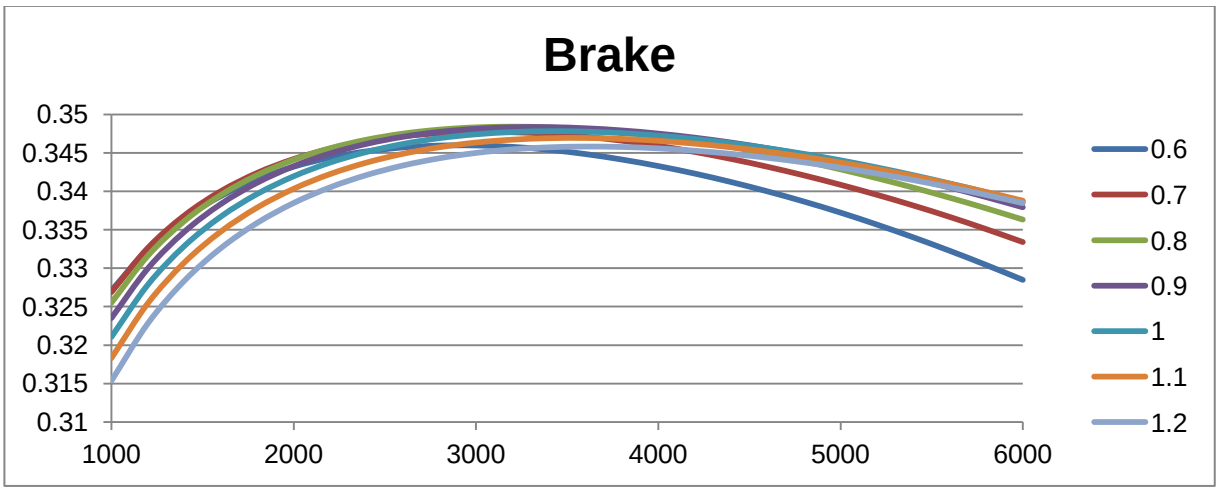

500 cm^3, 4-Cylinder

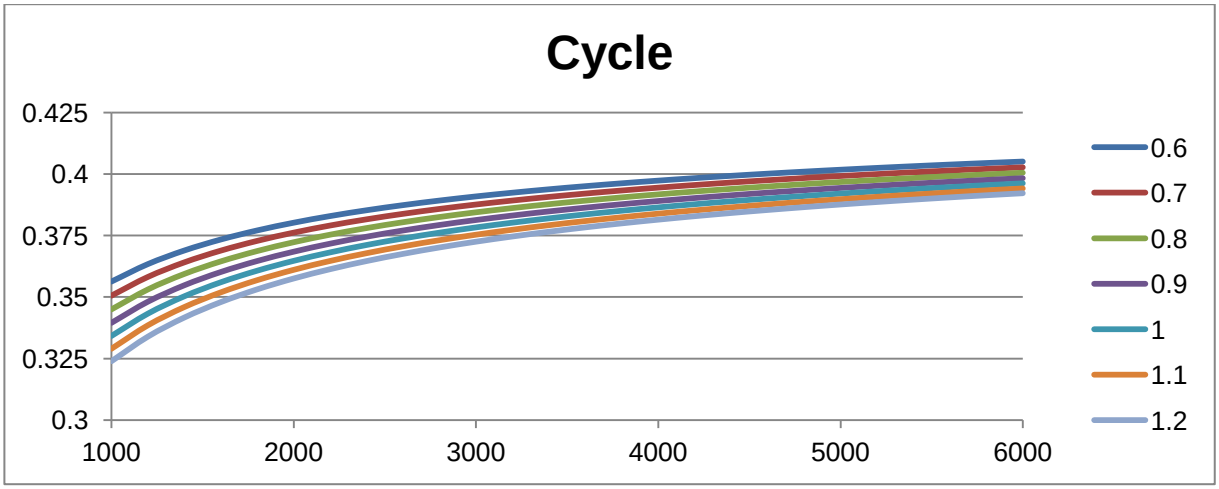

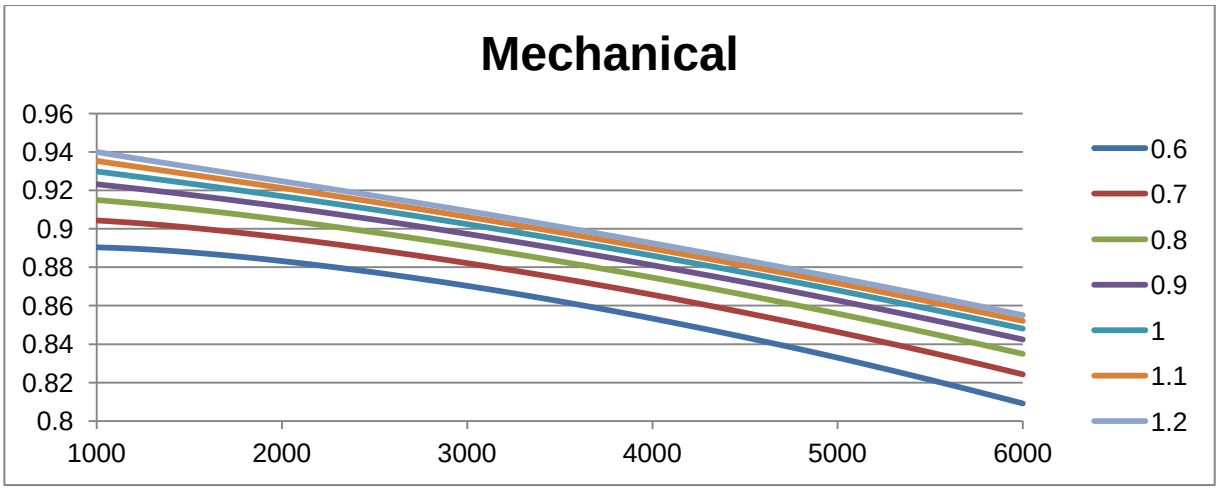

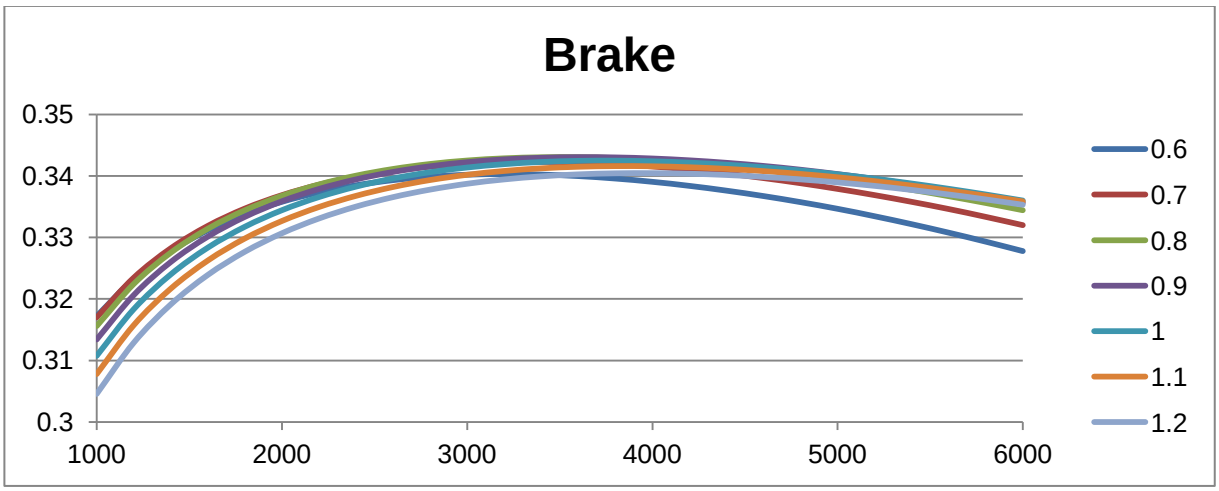

600 cm^3, 2-Cylinder

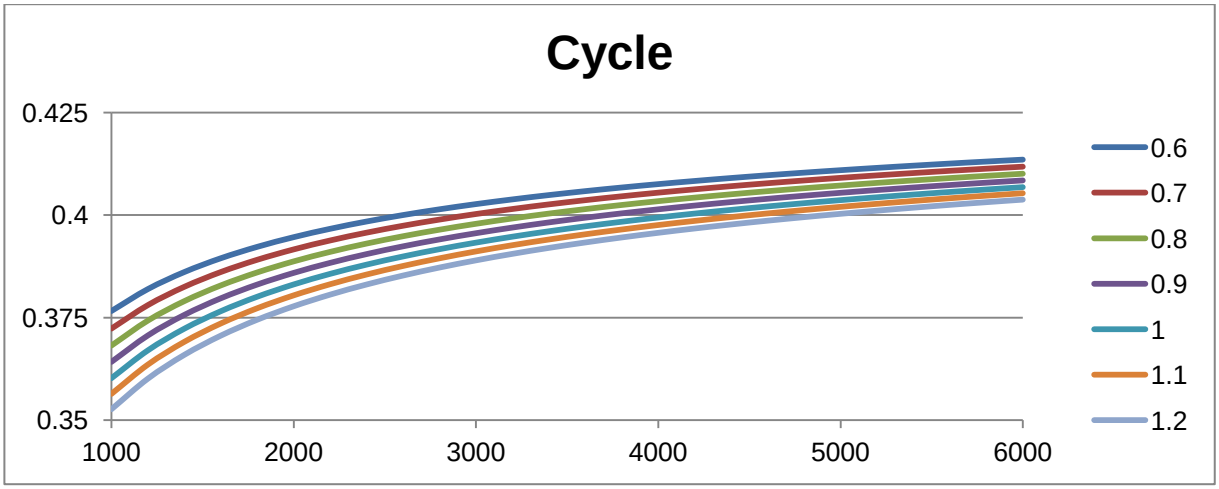

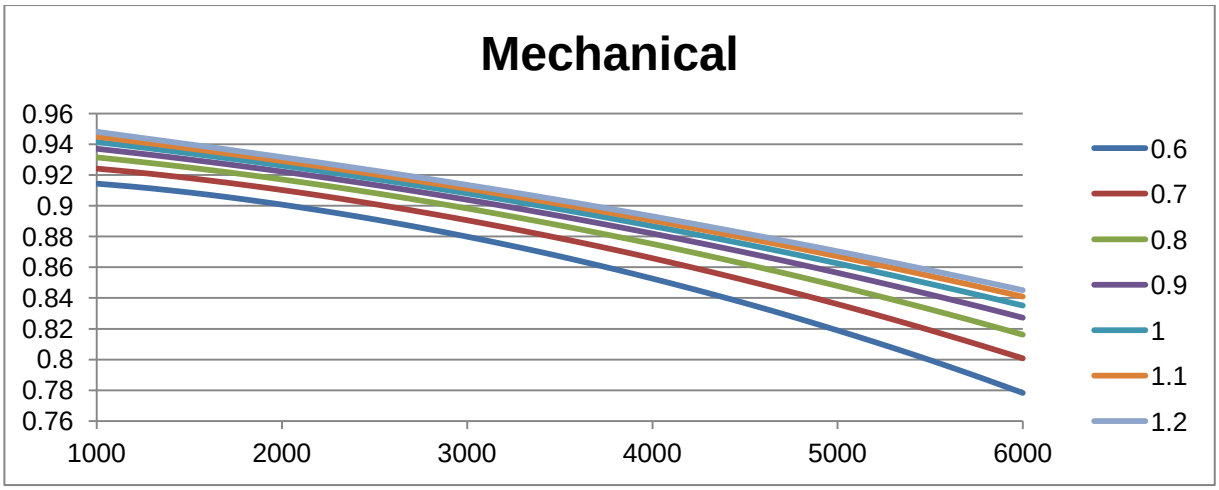

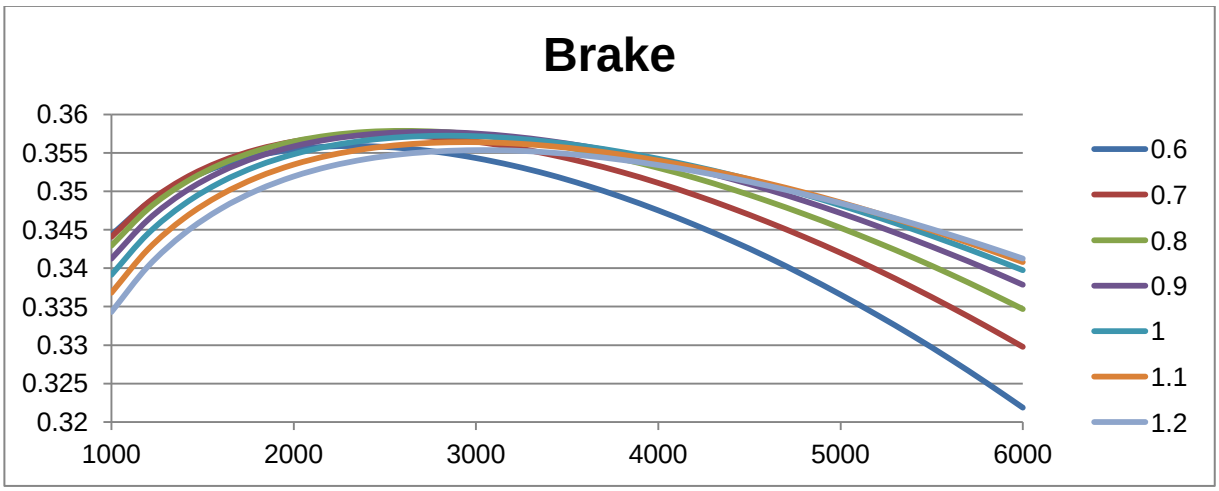

600 cm^3, 3-Cylinder

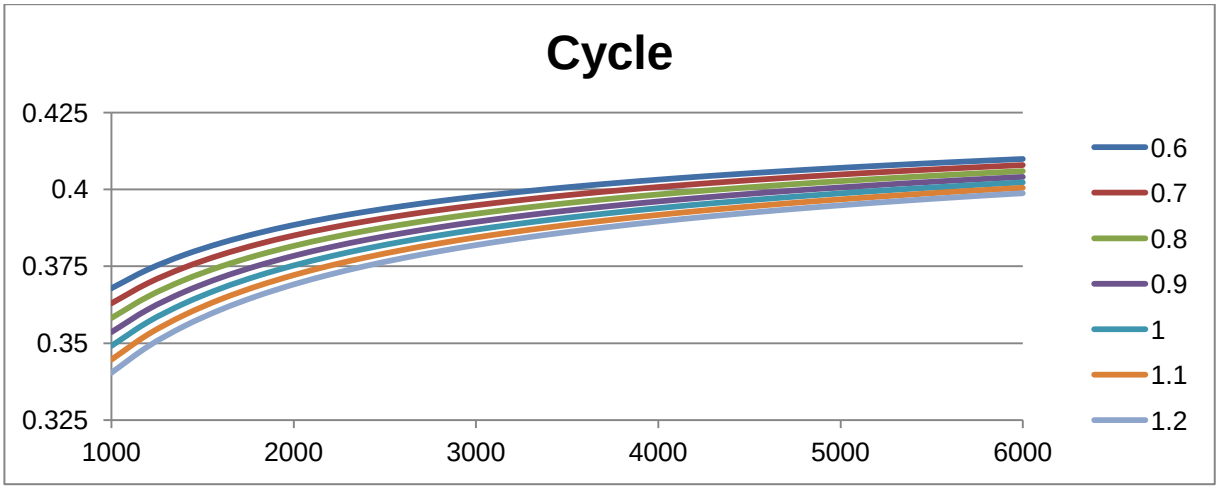

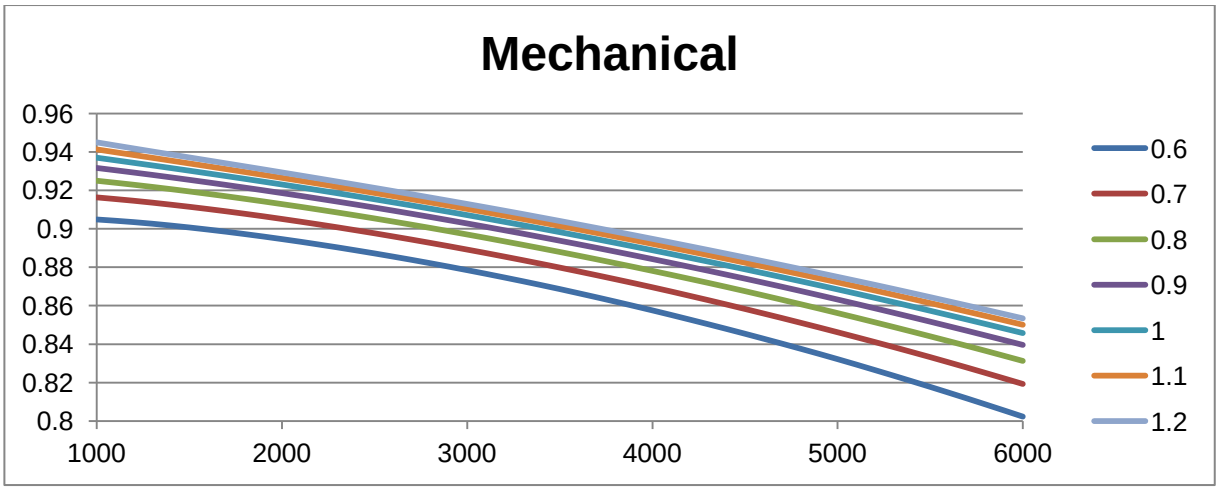

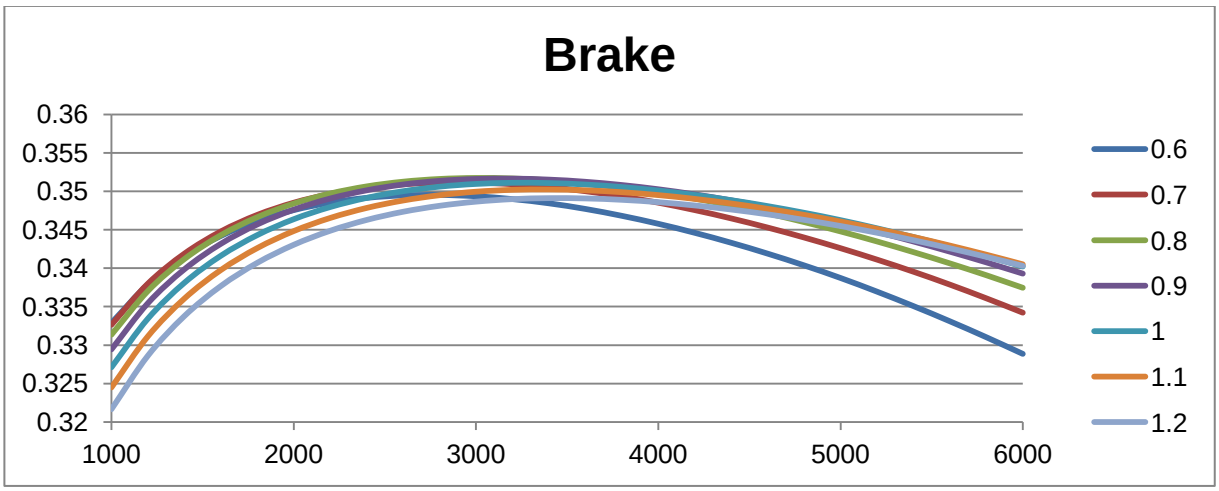

600 cm^3, 4-Cylinder

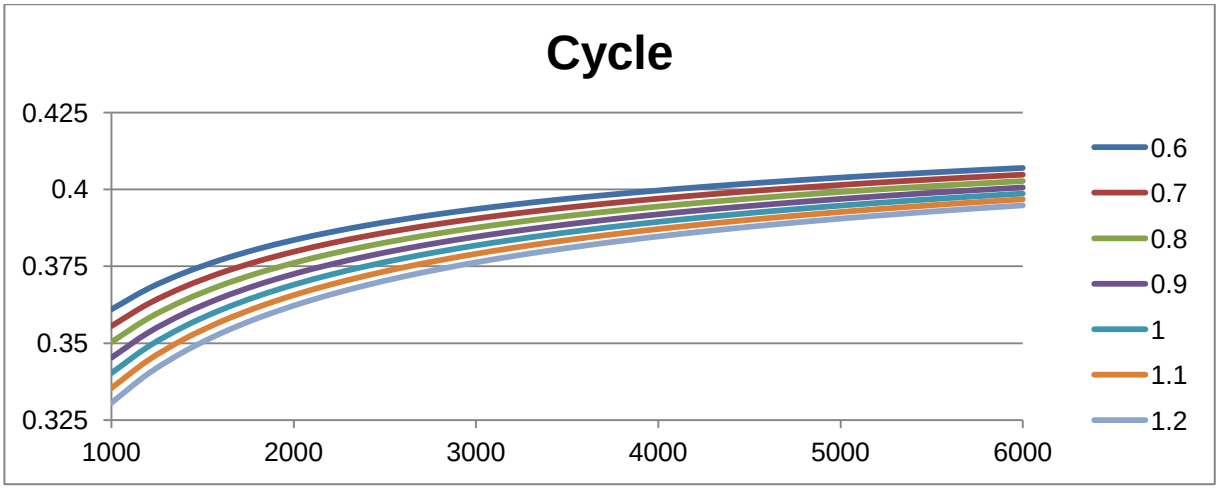

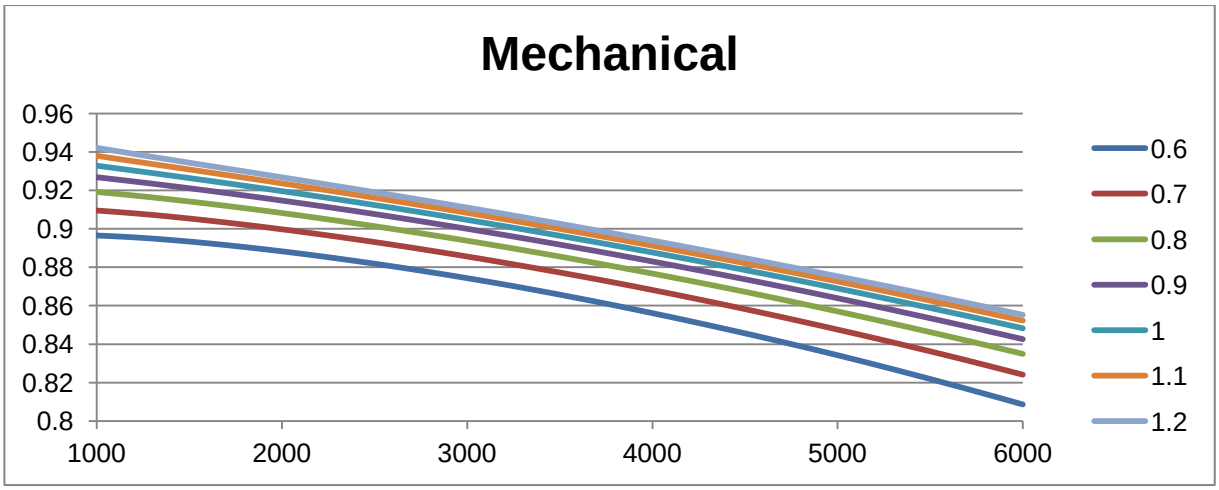

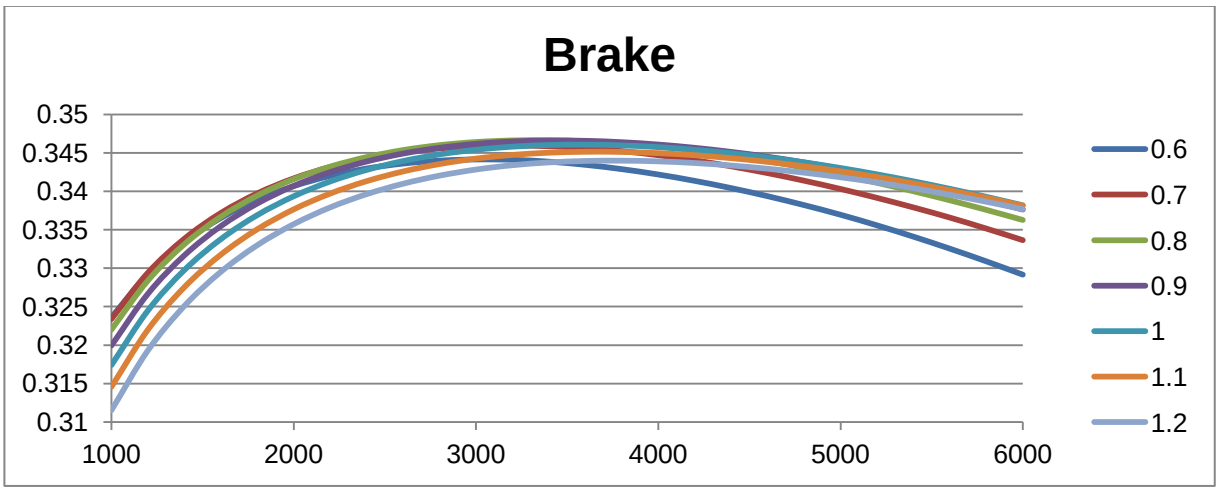

700 cm^3, 2-Cylinder

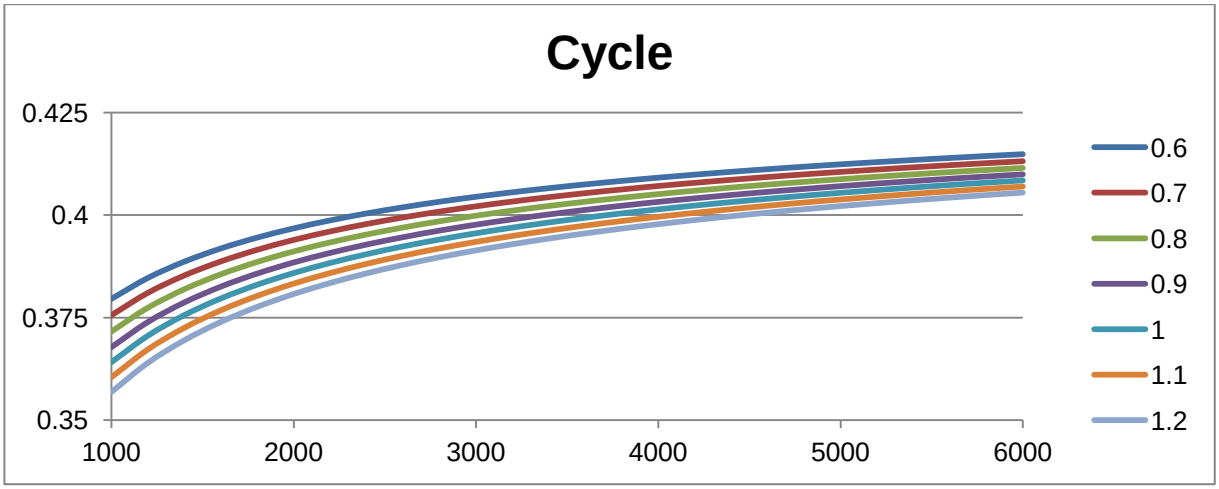

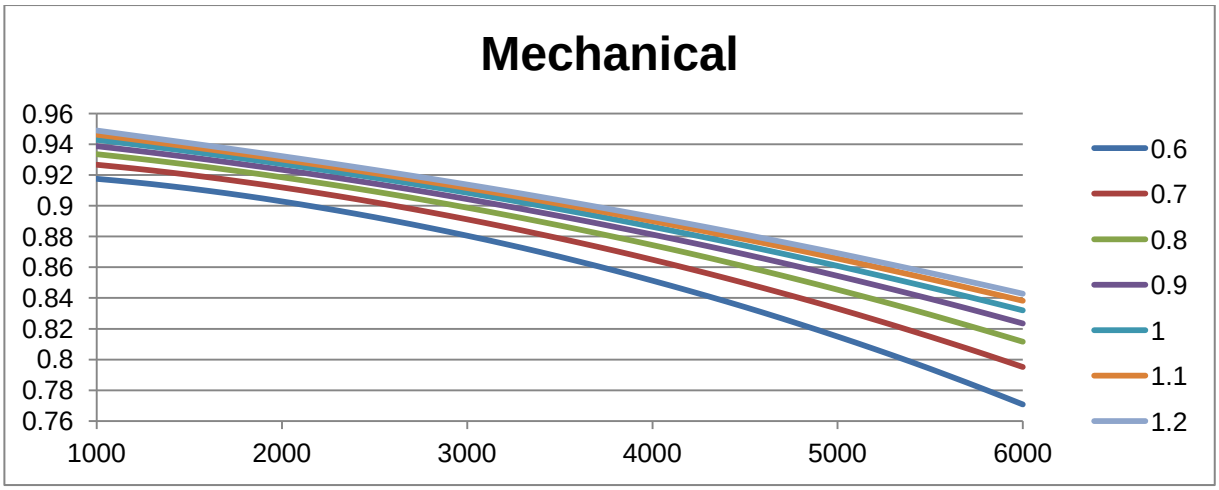

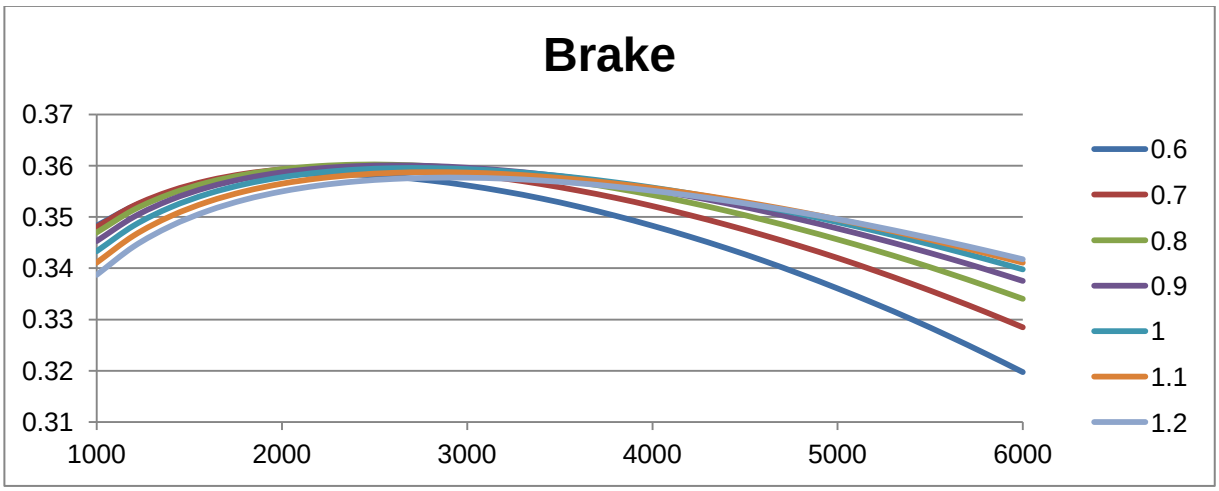

700 cm^3, 3-Cylinder

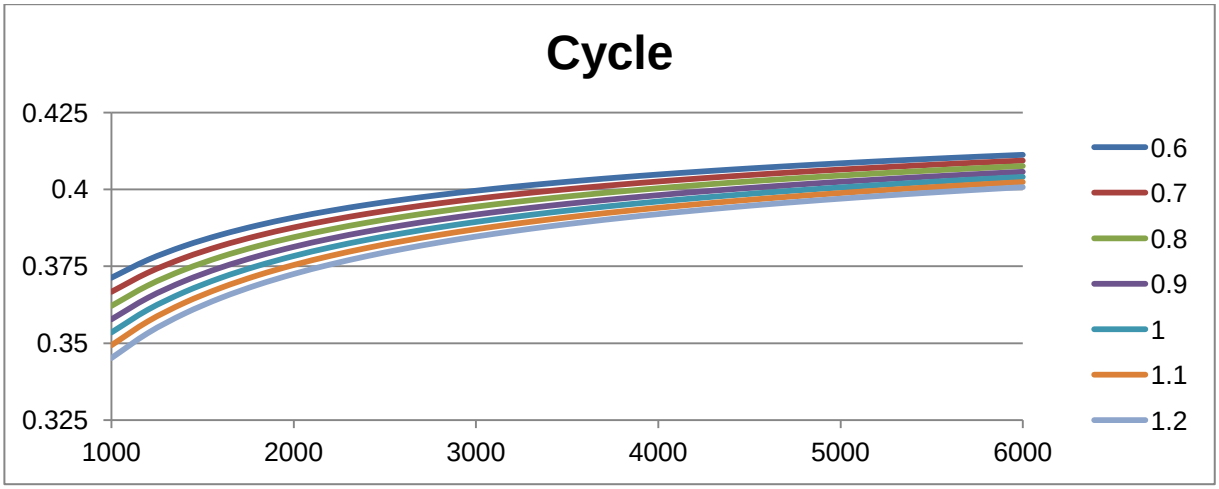

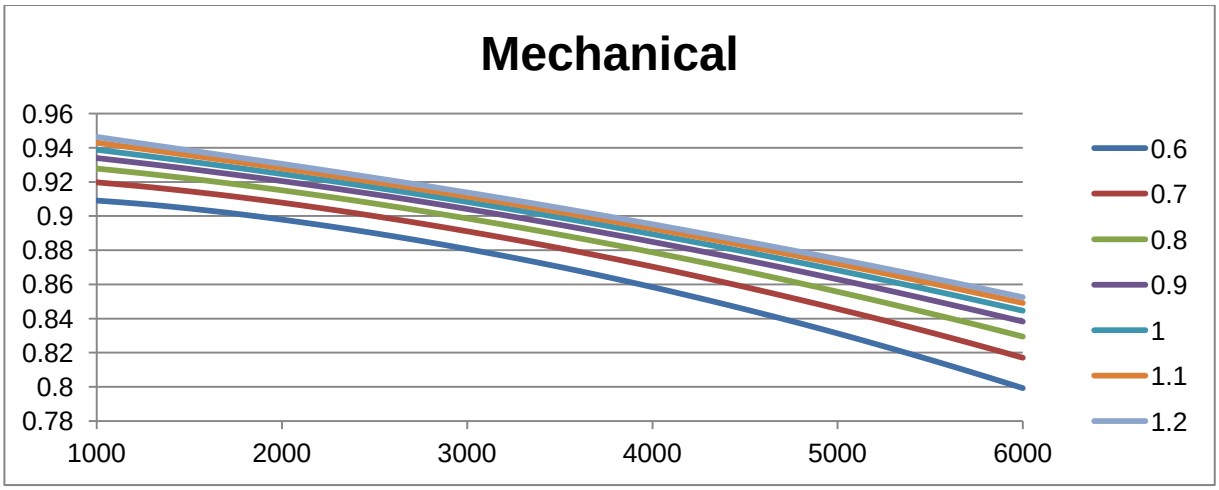

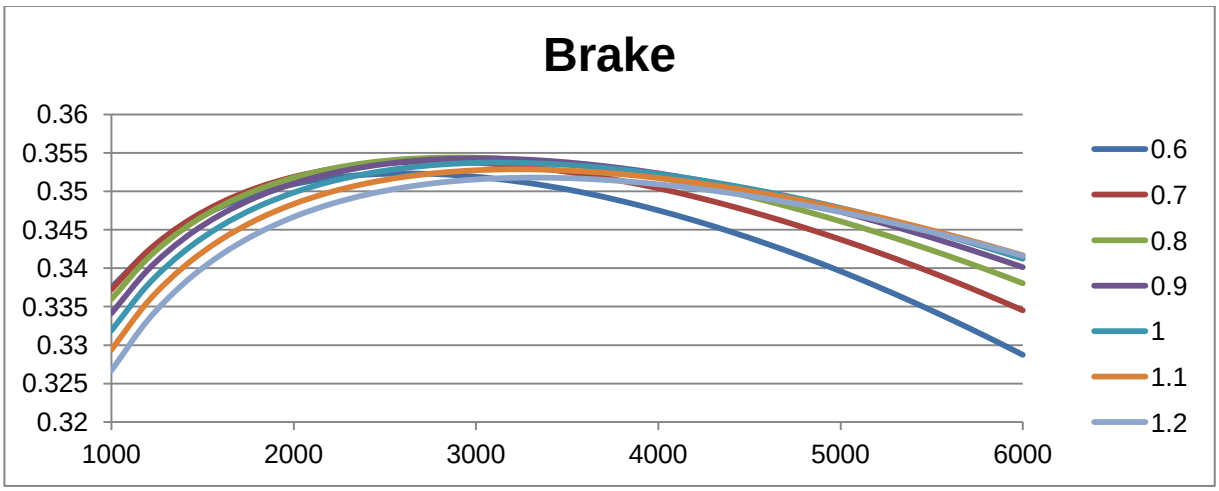

700 cm^3, 4-Cylinder

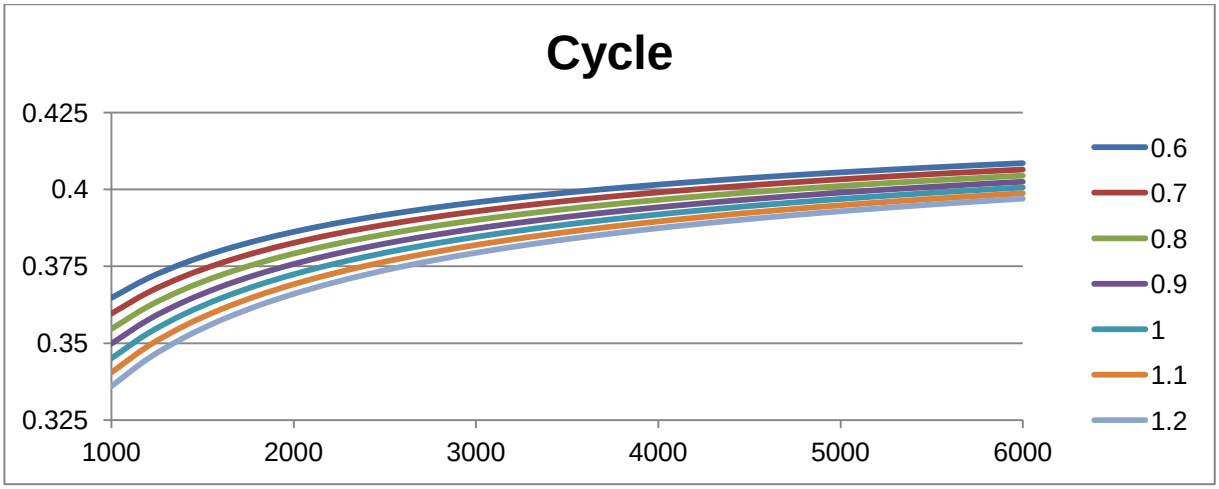

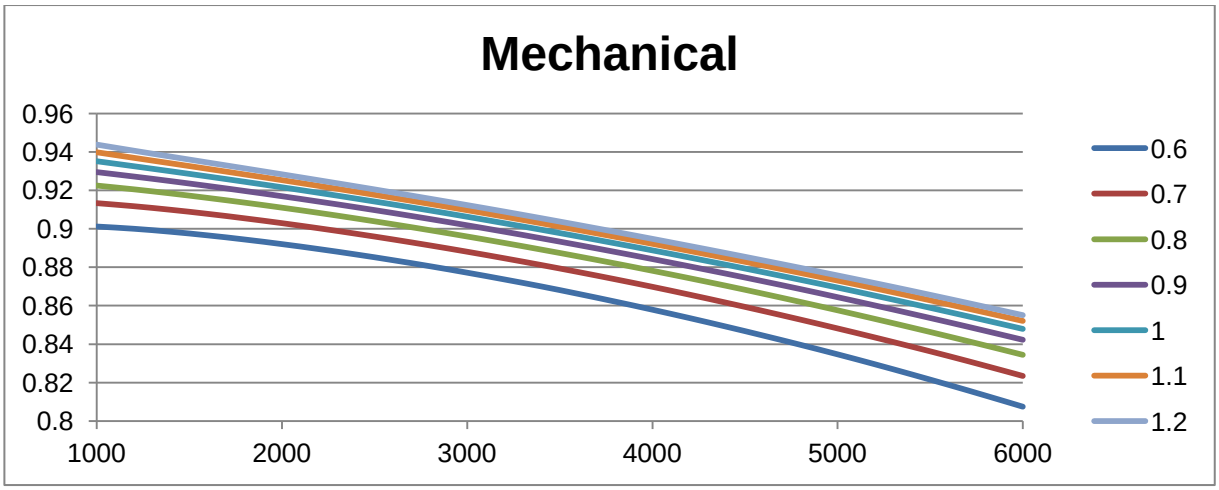

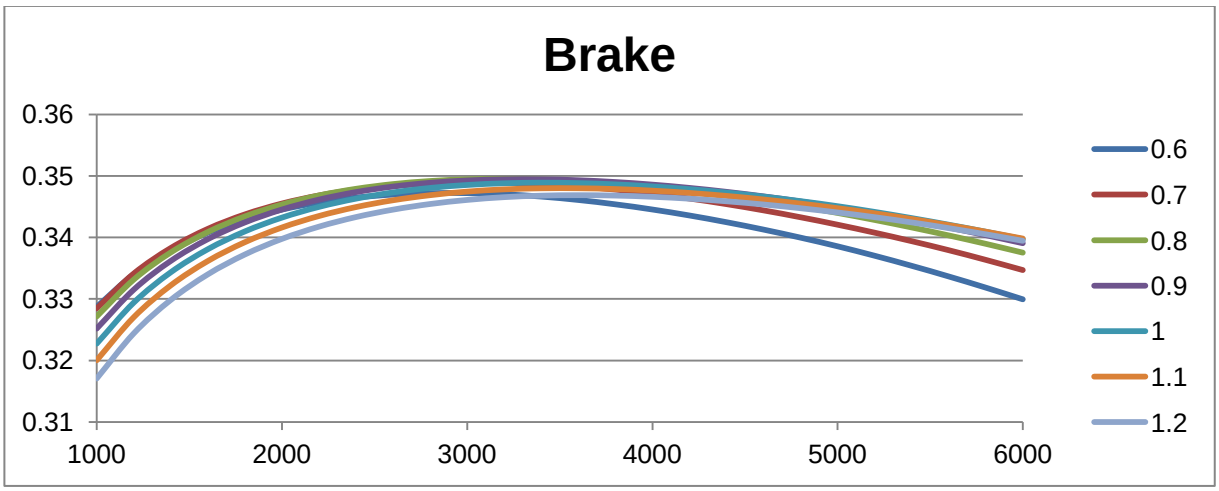

800 cm^3, 2-Cylinder

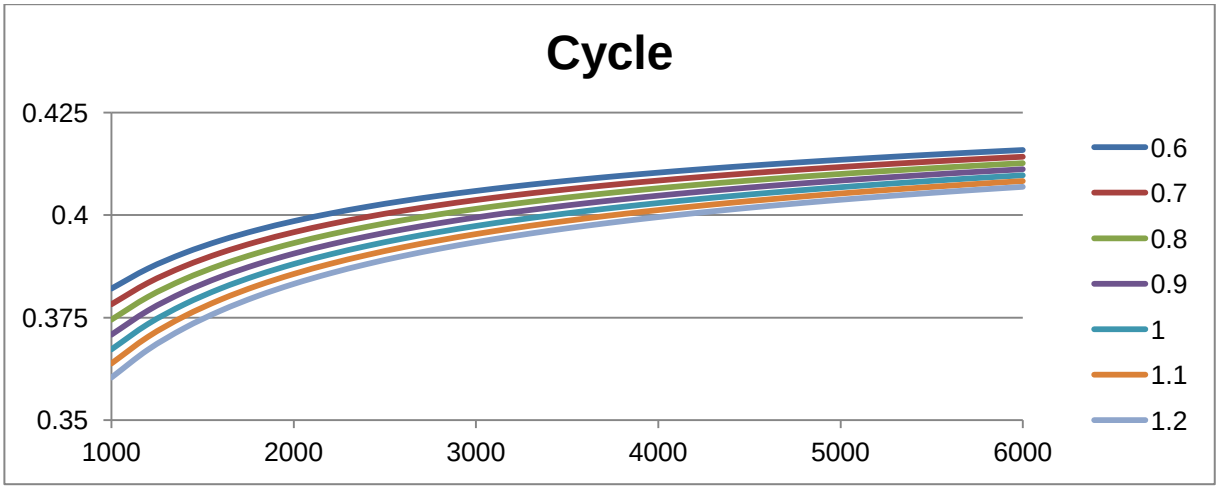

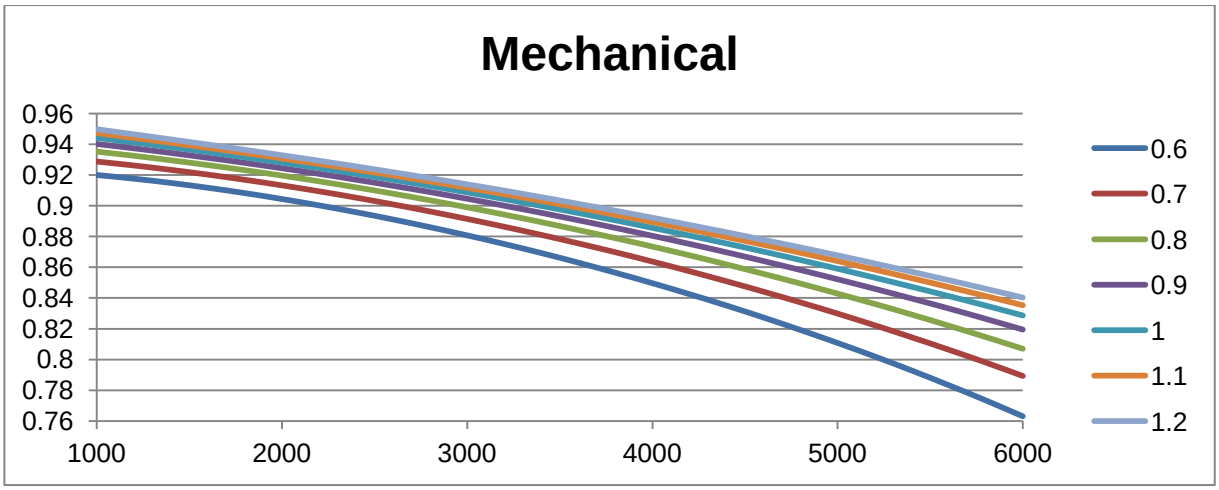

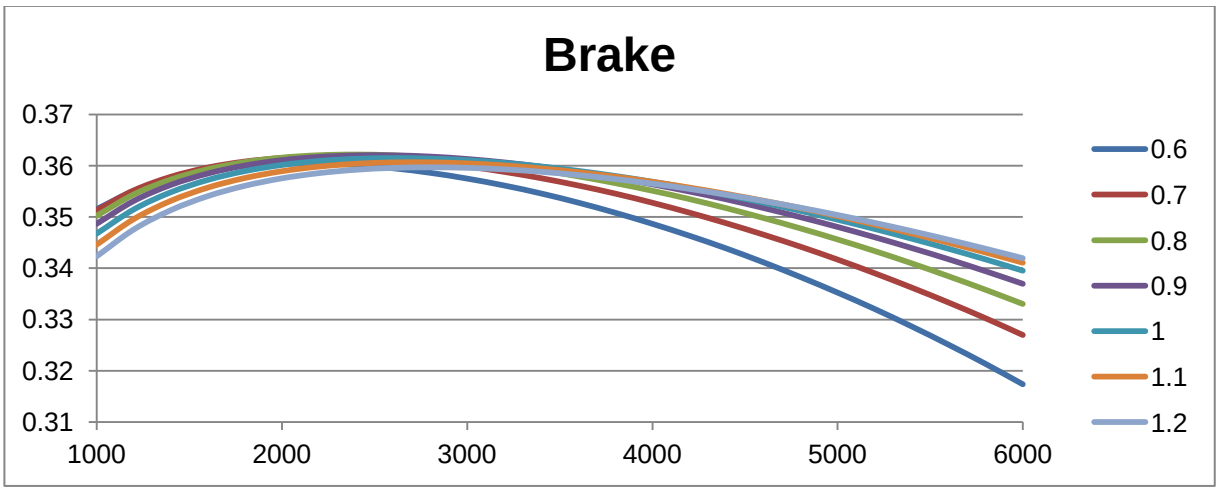

800 cm^3, 3-Cylinder

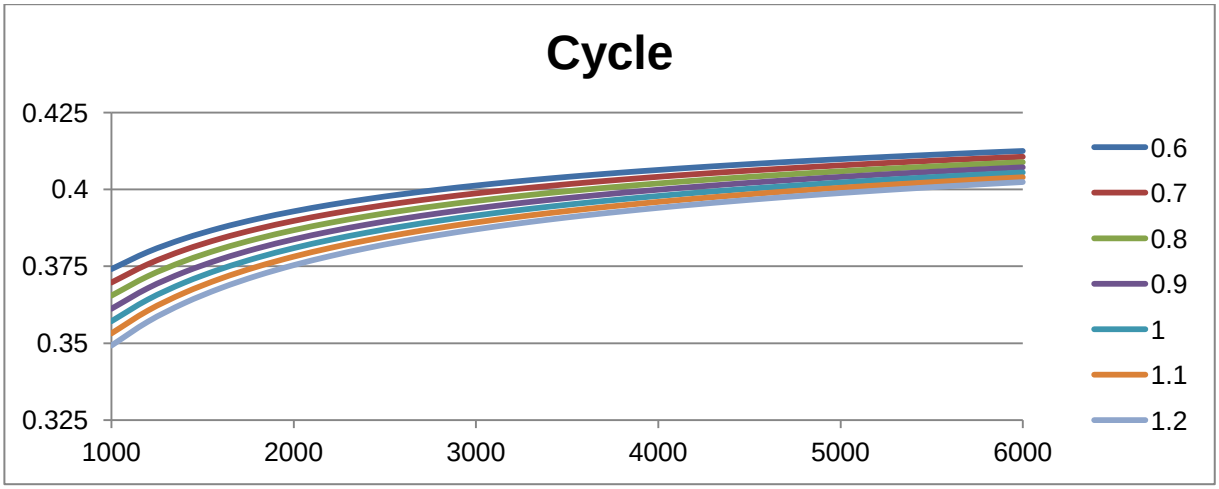

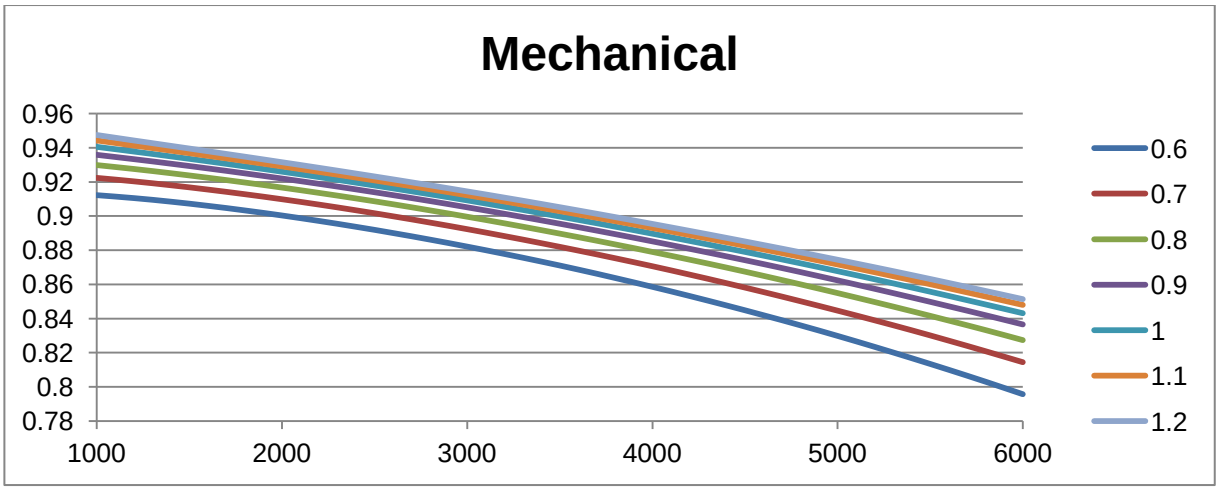

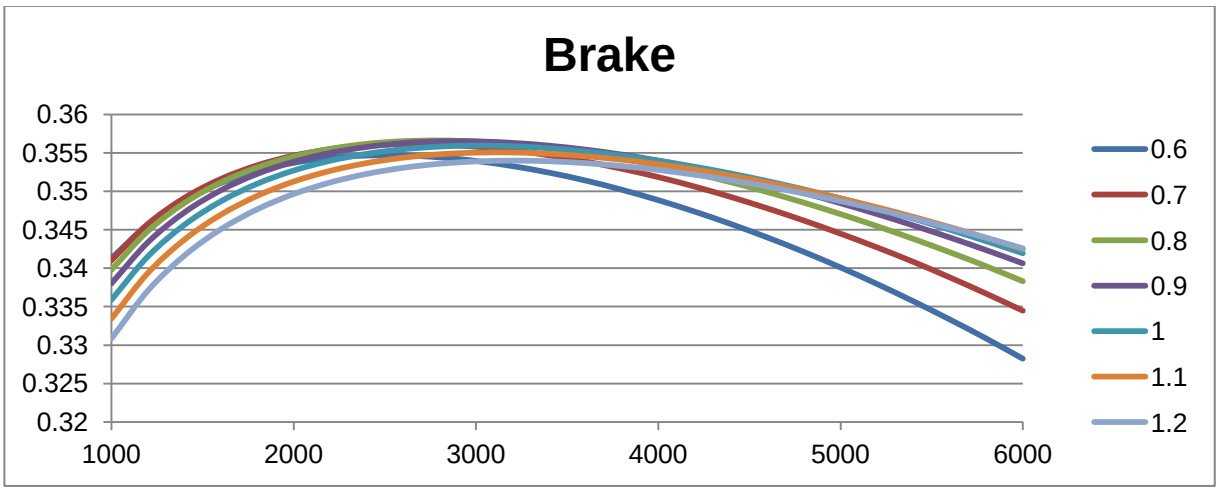

800 cm^3, 4-Cylinder

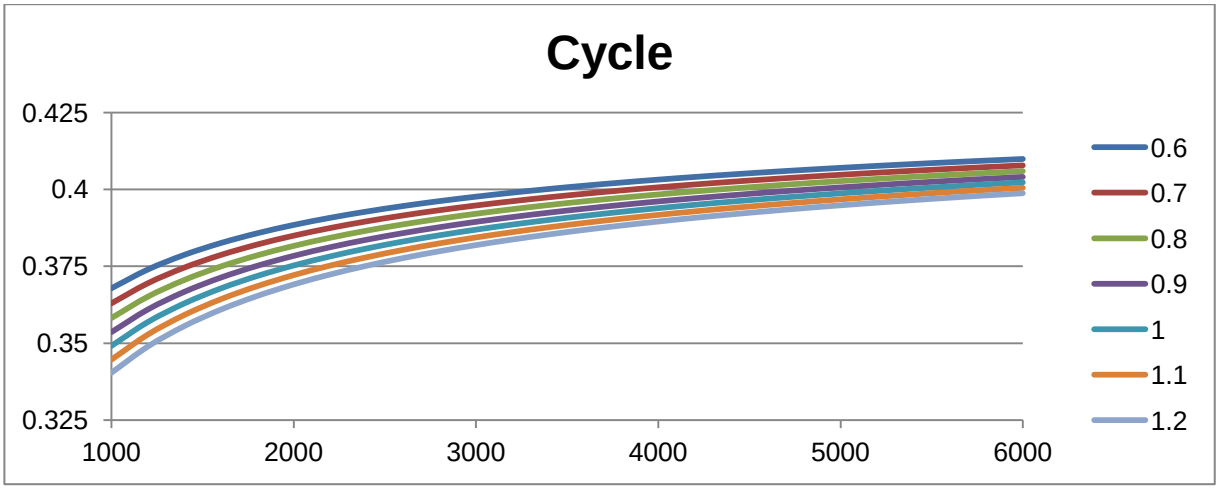

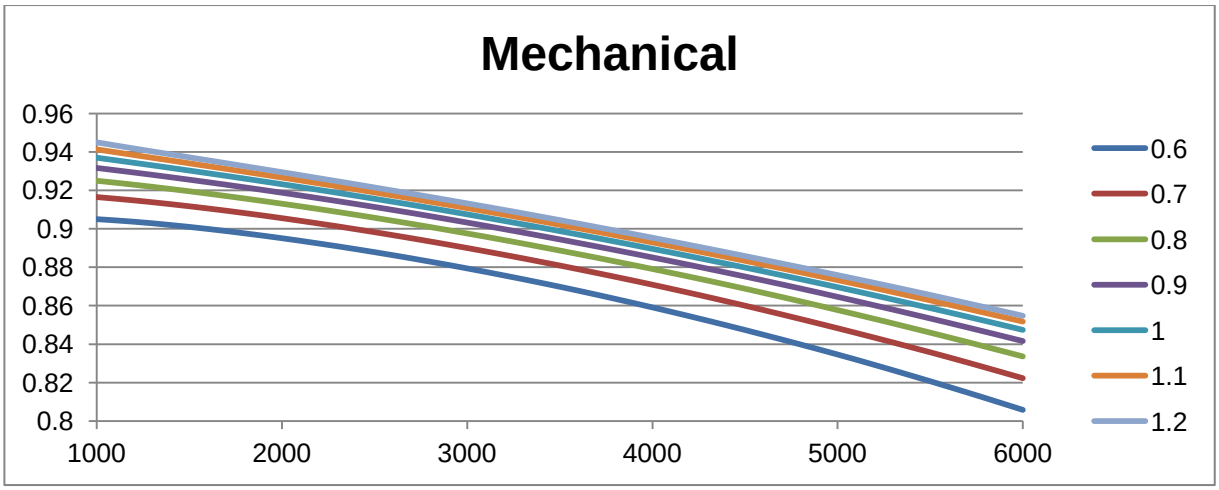

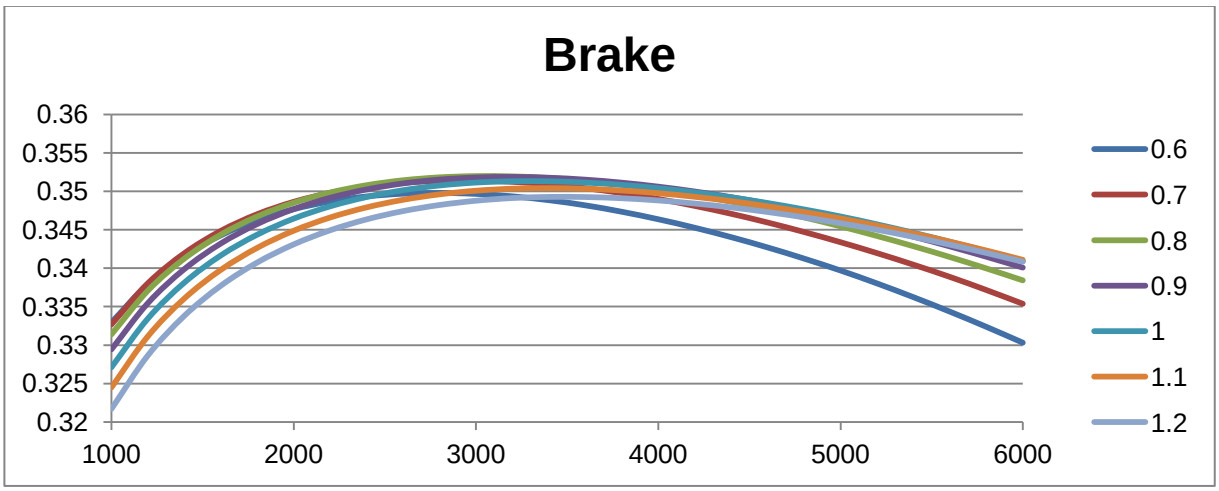

900 cm^3, 2-Cylinder

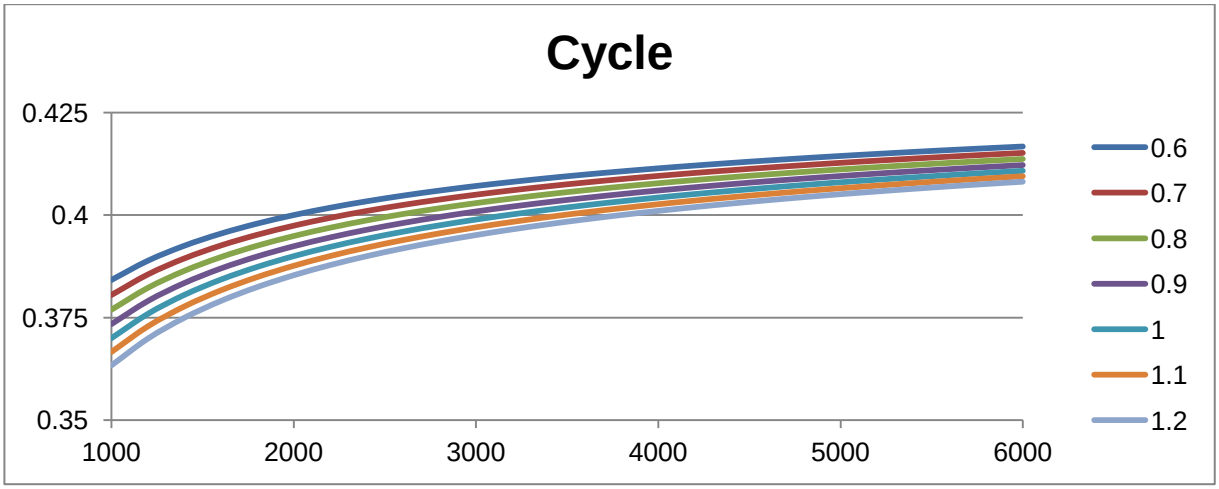

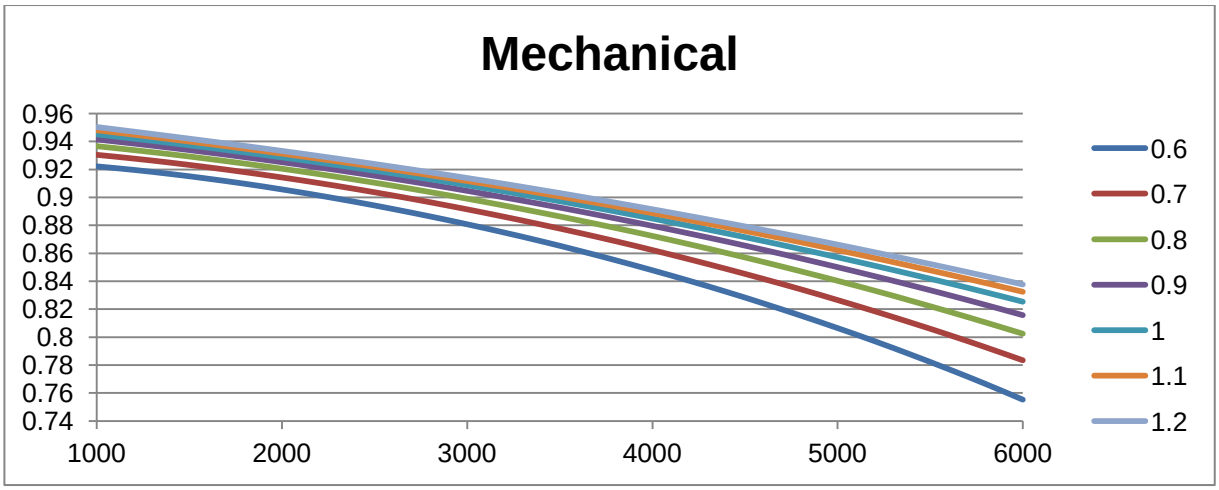

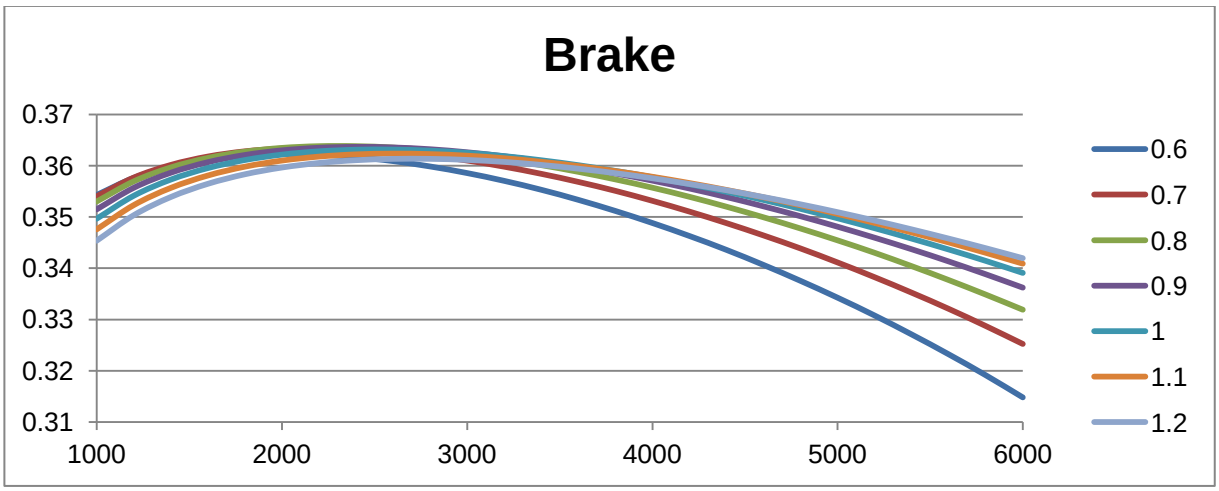

900 cm^3, 3-Cylinder

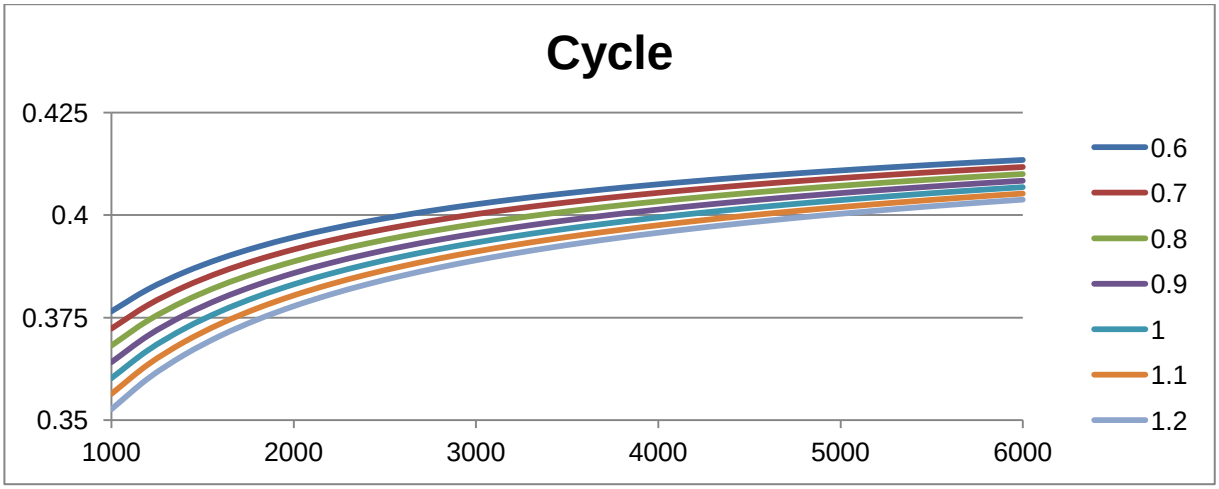

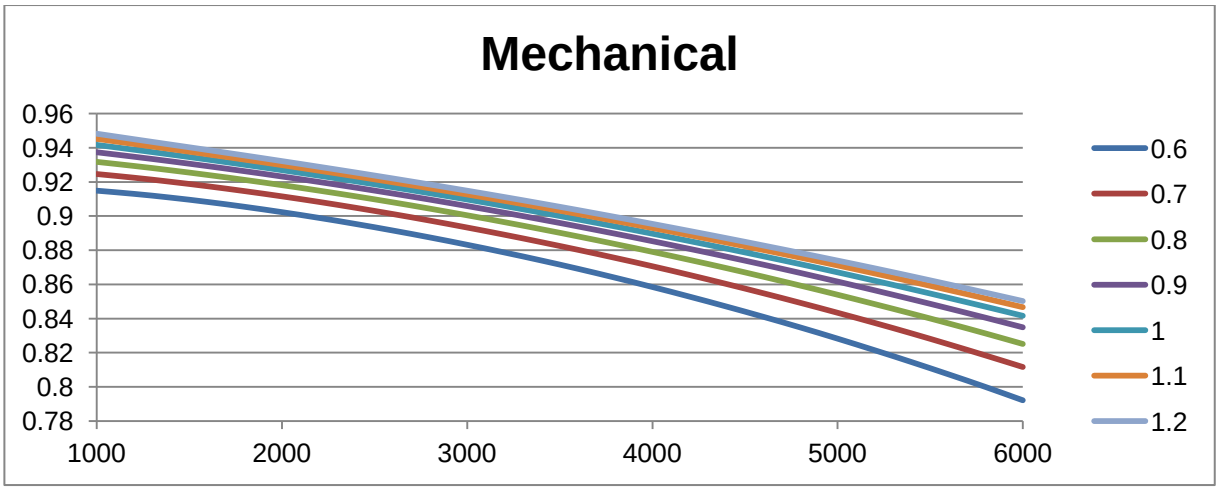

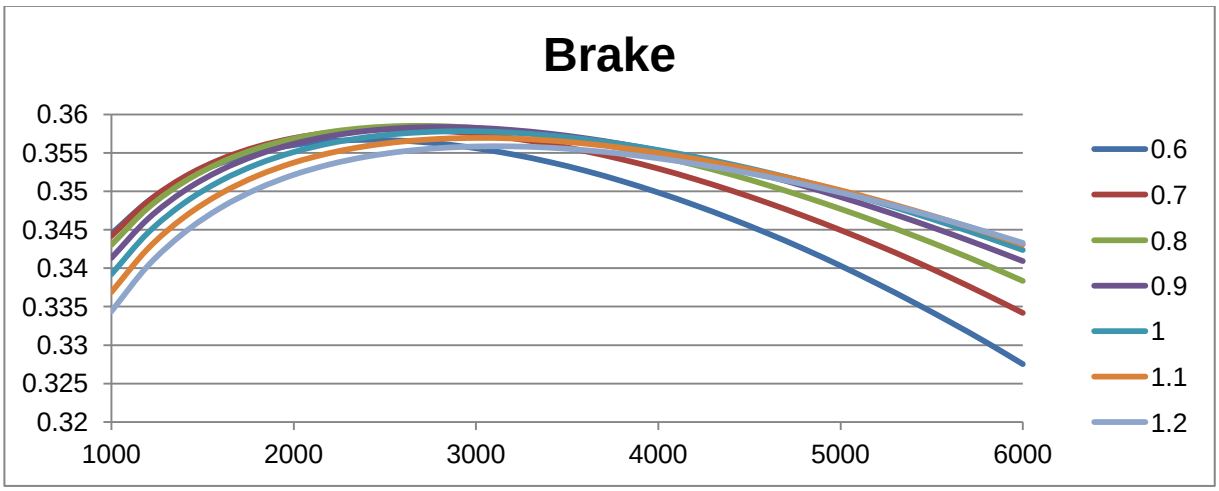

900 cm^3, 4-Cylinder

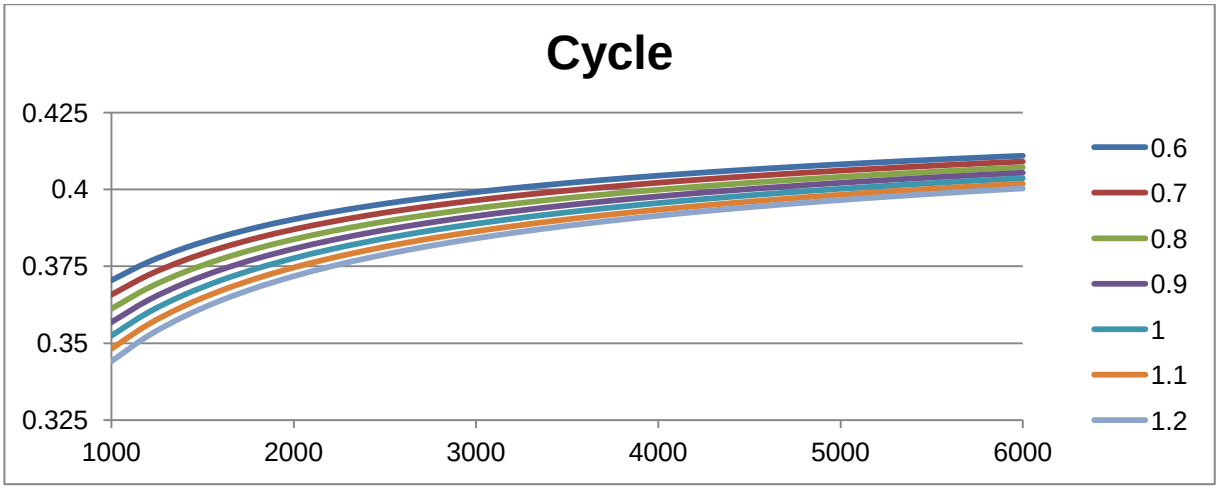

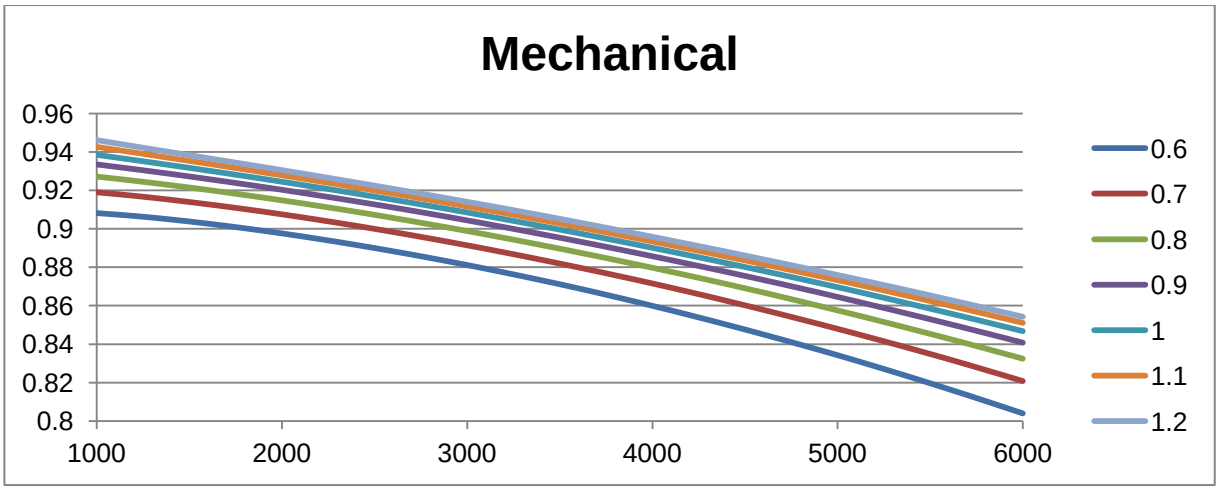

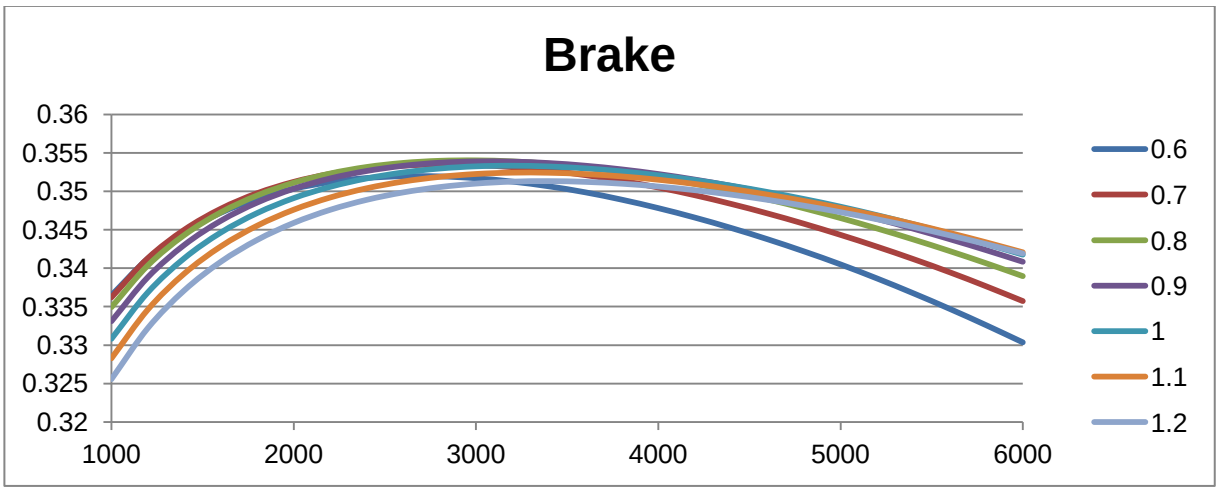

1000 cm^3, 2-Cylinder

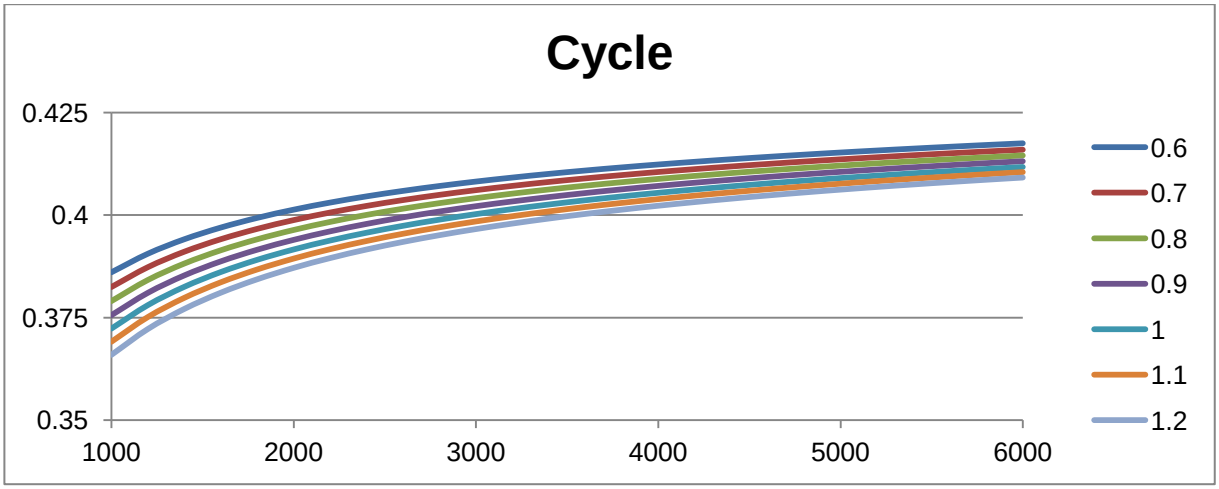

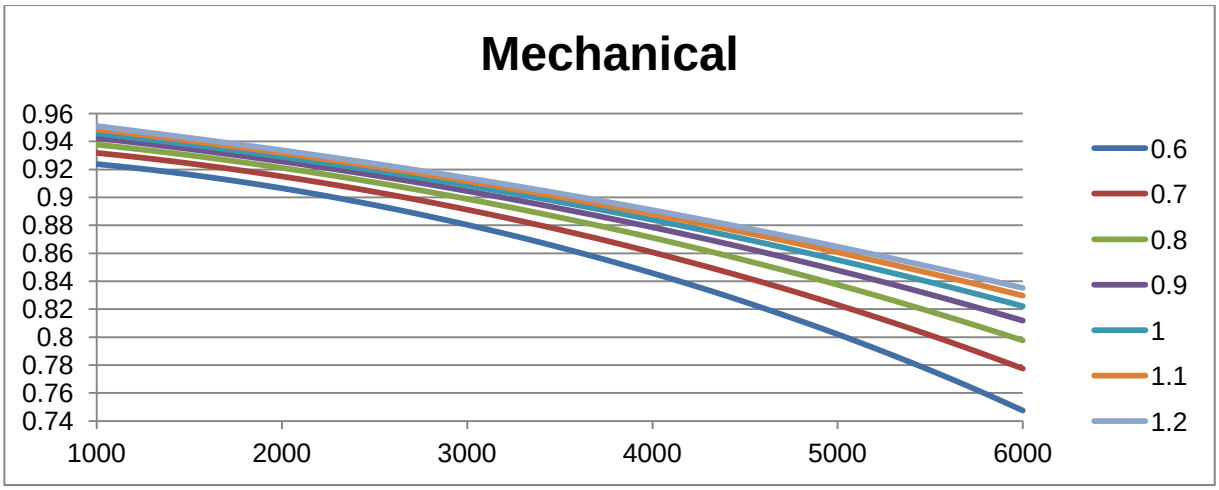

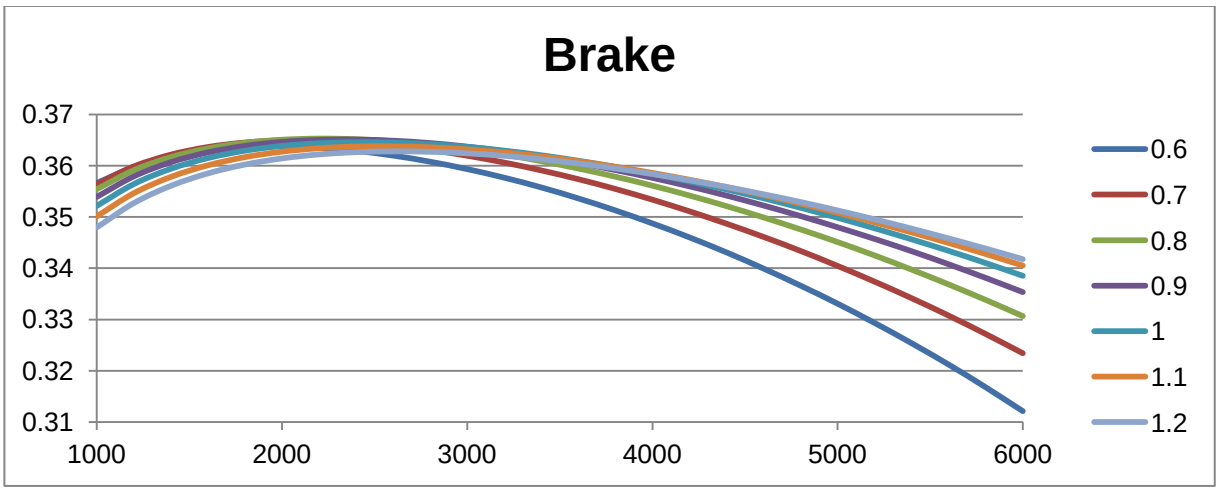

1000 cm^3, 3-Cylinder

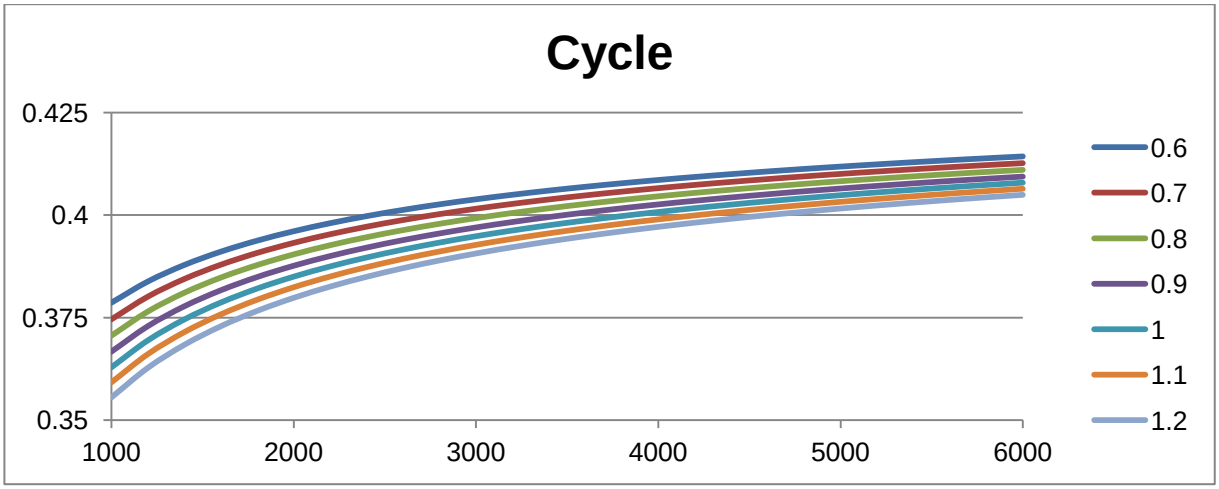

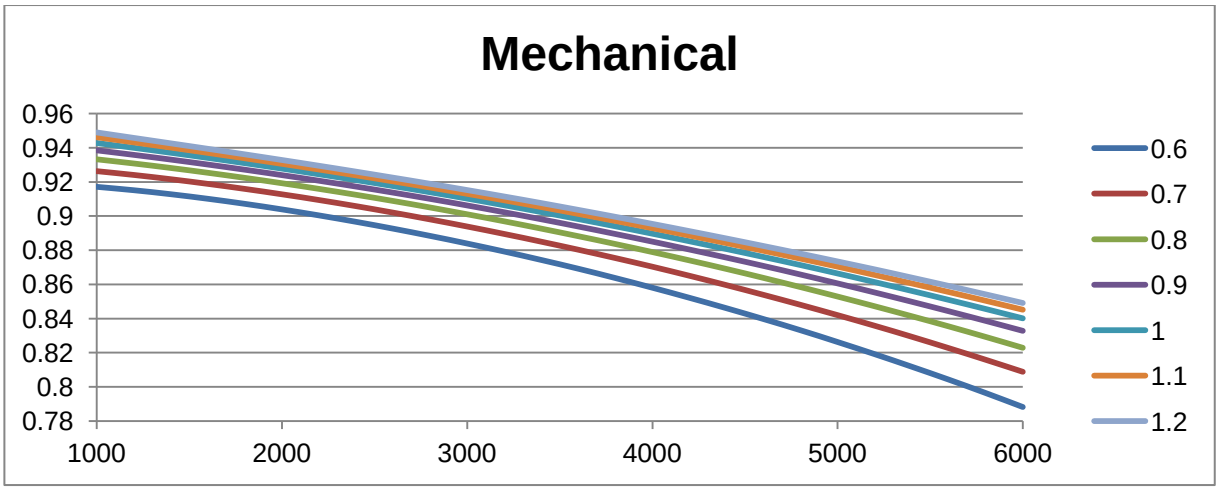

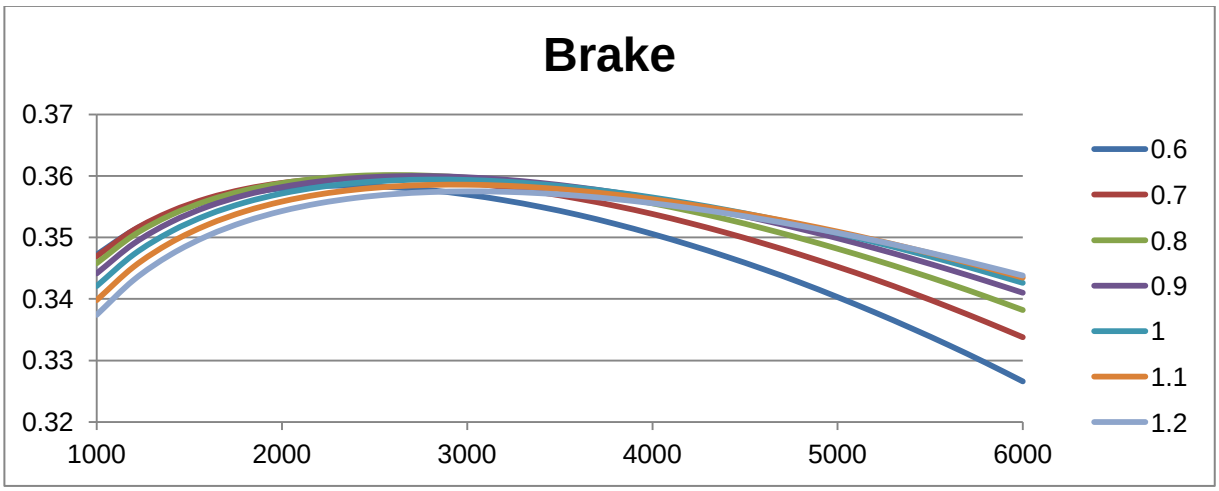

1000 cm^3, 4-Cylinder

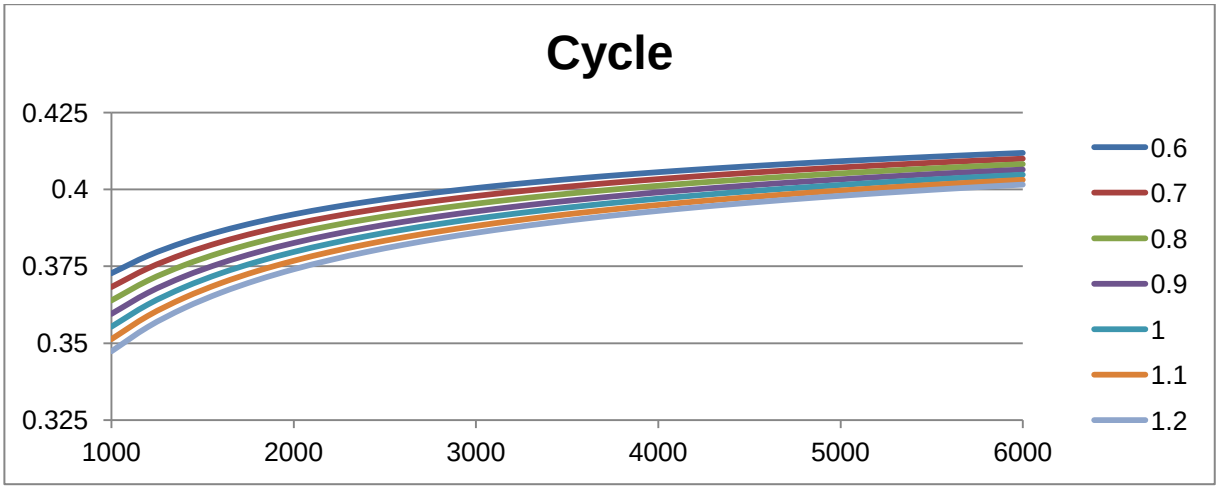

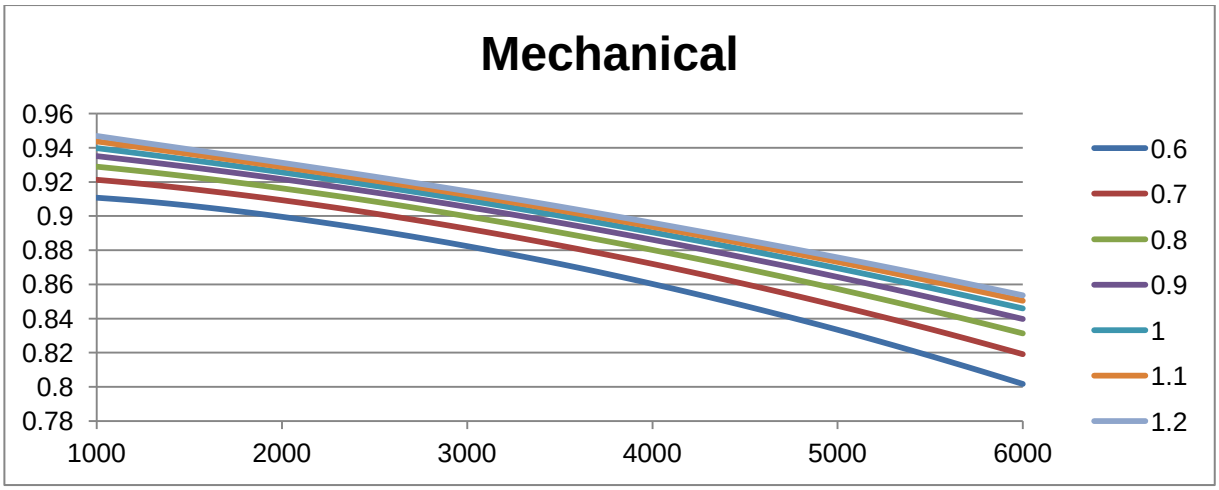

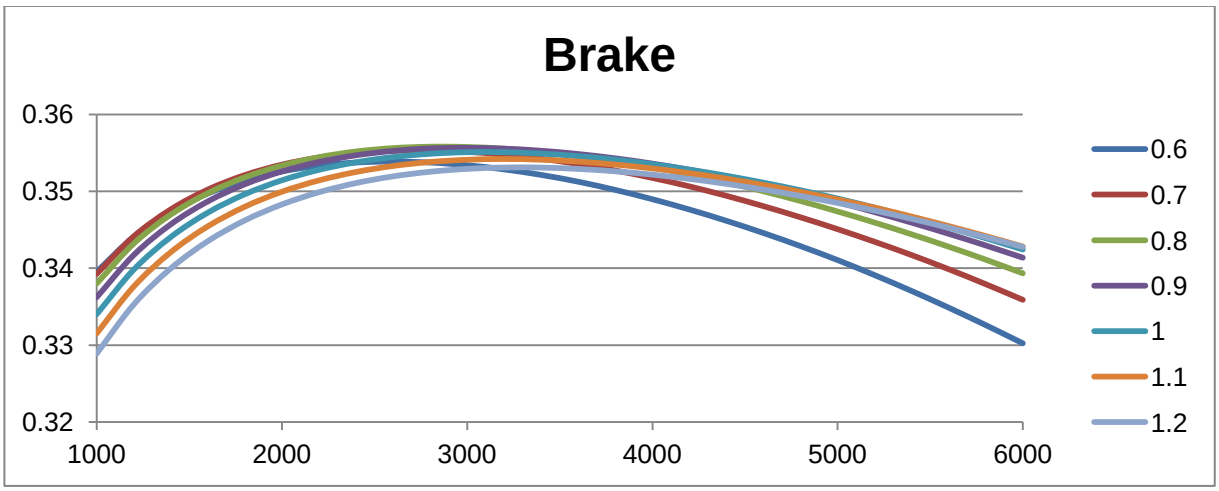

Appendix B

Speed-Efficiency Curves for Engines with Varying Numbers of Cylinders

500 cm^3

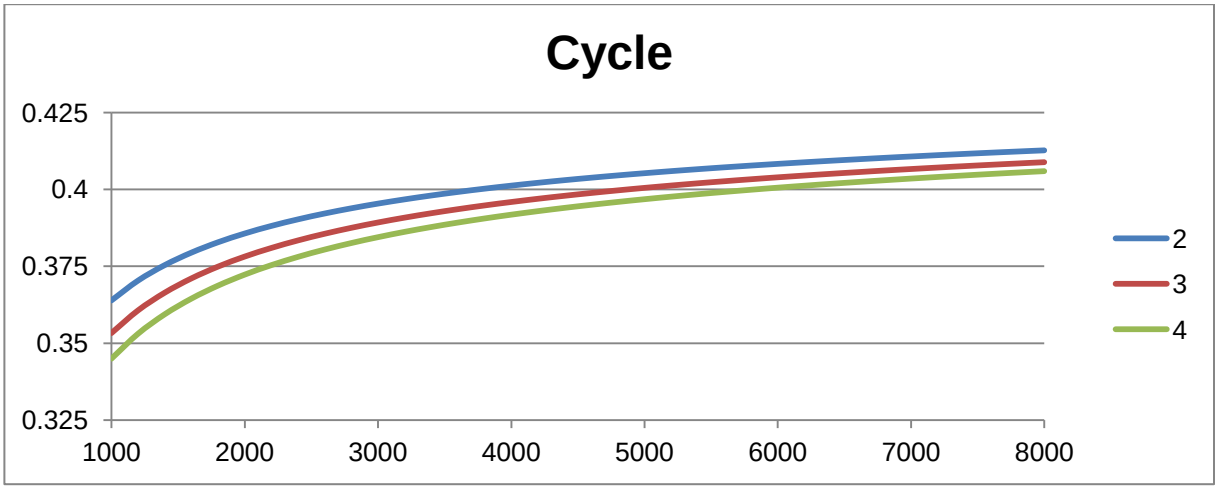
Cycle
0.425
0.4
0.375
0.35
0.325
1000
2000
3000
4000
5000
6000
7000
8000
2
3
4

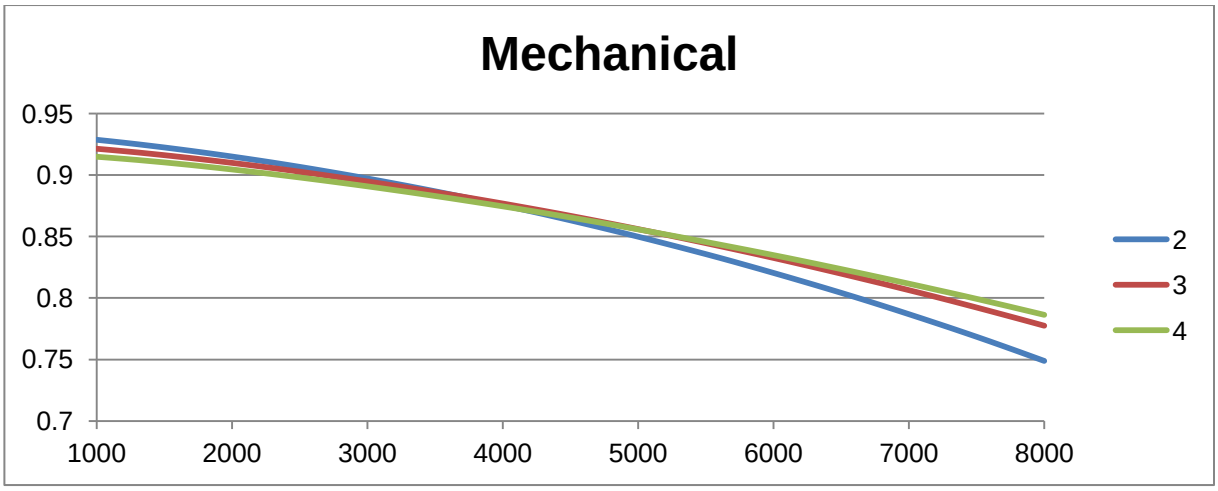
Mechanical
0.95
0.9
0.85
0.8
0.75
0.7
1000
2000
3000
4000
5000
6000
7000
8000
2
3
4

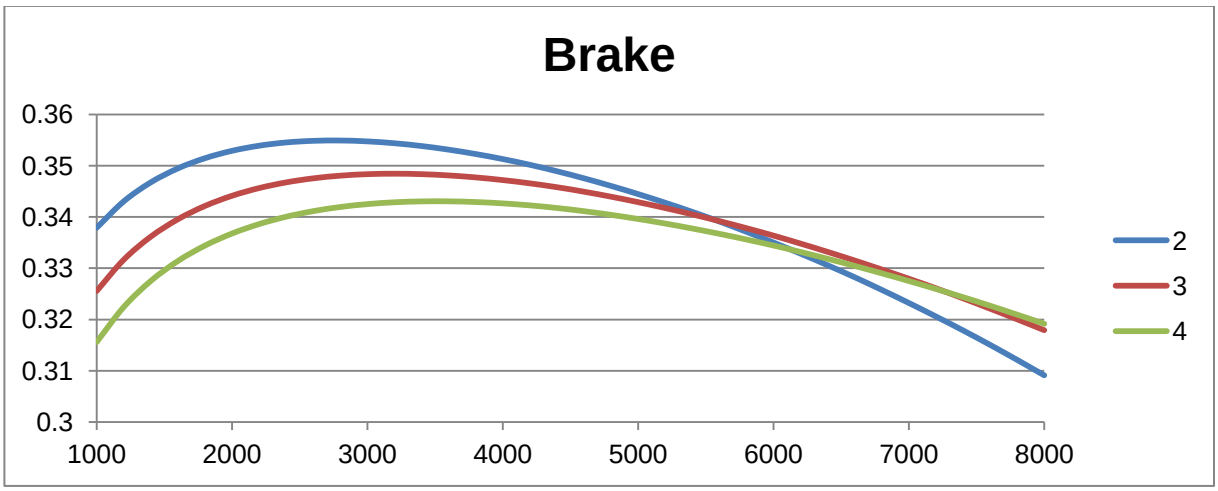
Brake
0.36
0.35
0.34
0.33
0.32
0.31
0.3
1000
2000
3000
4000
5000
6000
7000
8000
2
3
4

600 cm^3

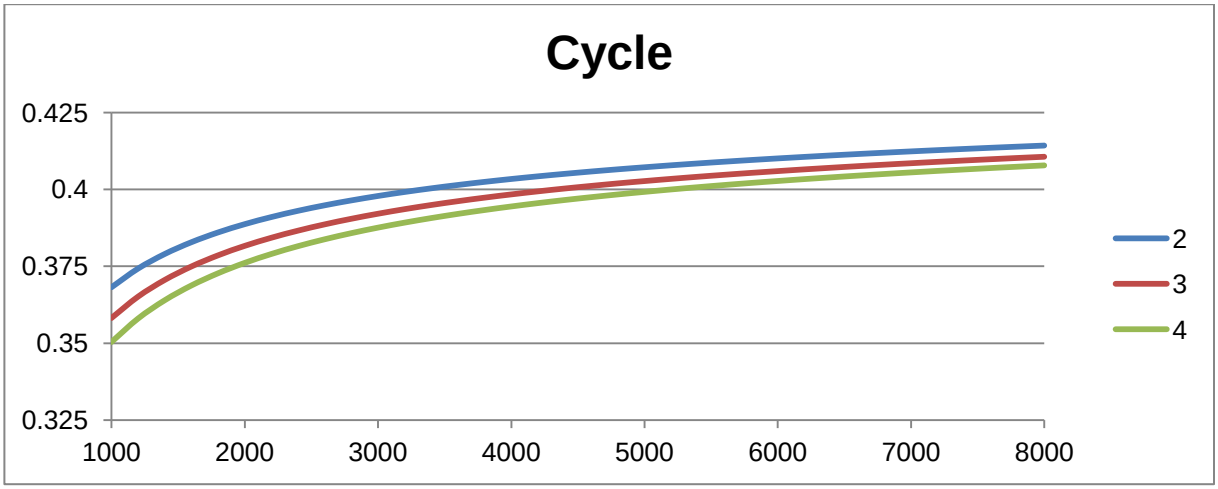
Cycle
0.425
0.4
0.375
0.35
0.325
1000
2000
3000
4000
5000
6000
7000
8000
2
3
4

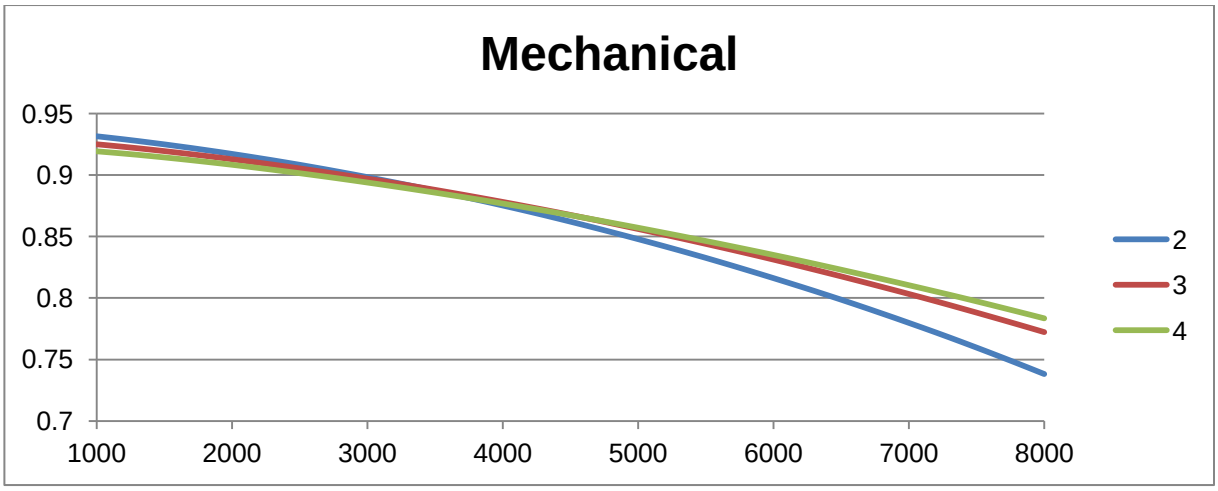
Mechanical
0.95
0.9
0.85
0.8
0.75
0.7
1000
2000
3000
4000
5000
6000
7000
8000
2
3
4

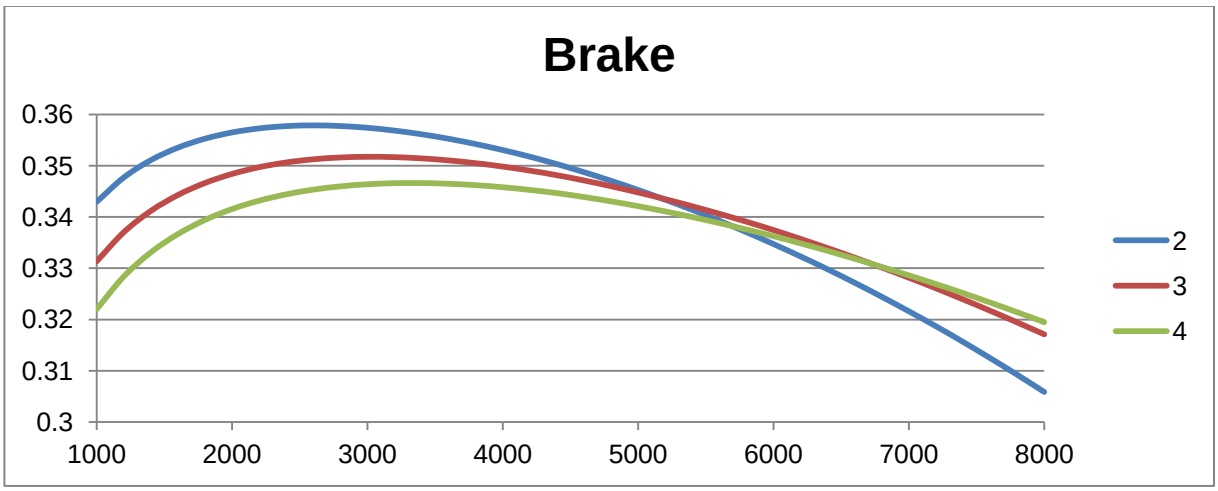
Brake
0.36
0.35
0.34
0.33
0.32
0.31
0.3
1000
2000
3000
4000
5000
6000
7000
8000
2
3
4

700 cm^3

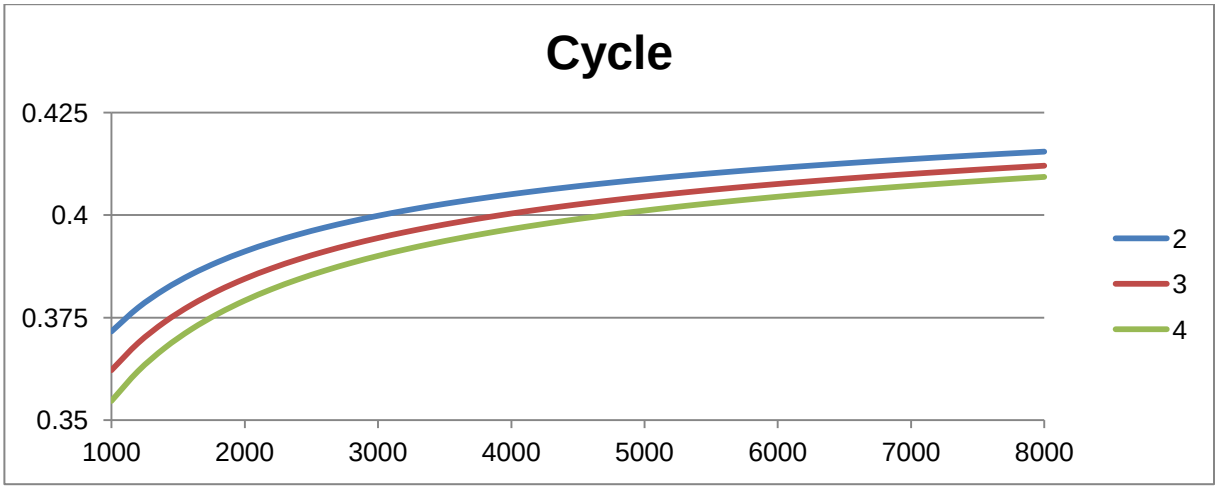
Cycle
0.425
0.4
0.375
0.35
1000
2000
3000
4000
5000
6000
7000
8000
2
3
4

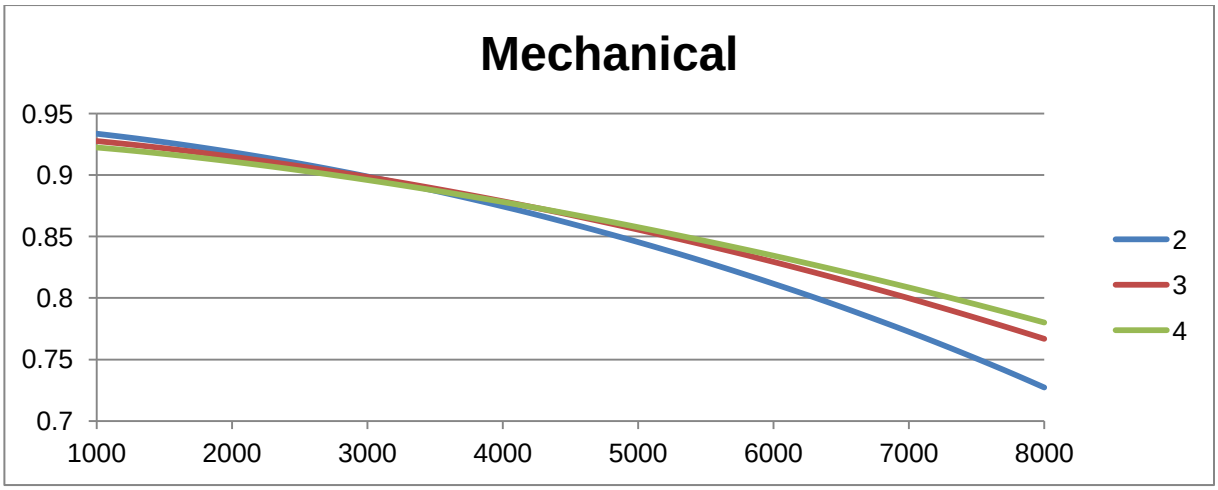
Mechanical
0.95
0.9
0.85
0.8
0.75
0.7
1000
2000
3000
4000
5000
6000
7000
8000
2
3
4

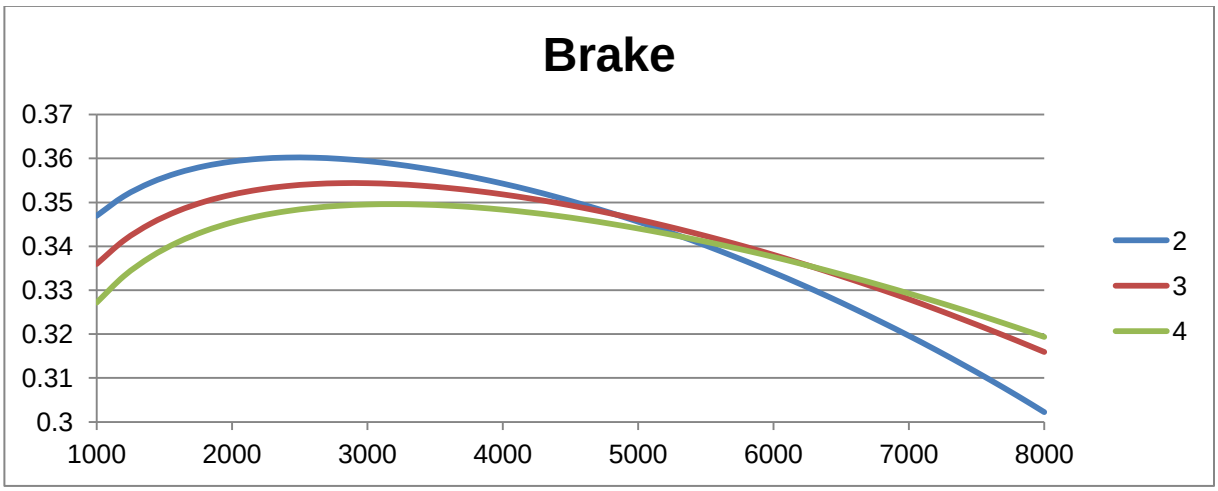
Brake
0.37
0.36
0.35
0.34
0.33
0.32
0.31
0.3
1000
2000
3000
4000
5000
6000
7000
8000
2
3
4

800 cm^3

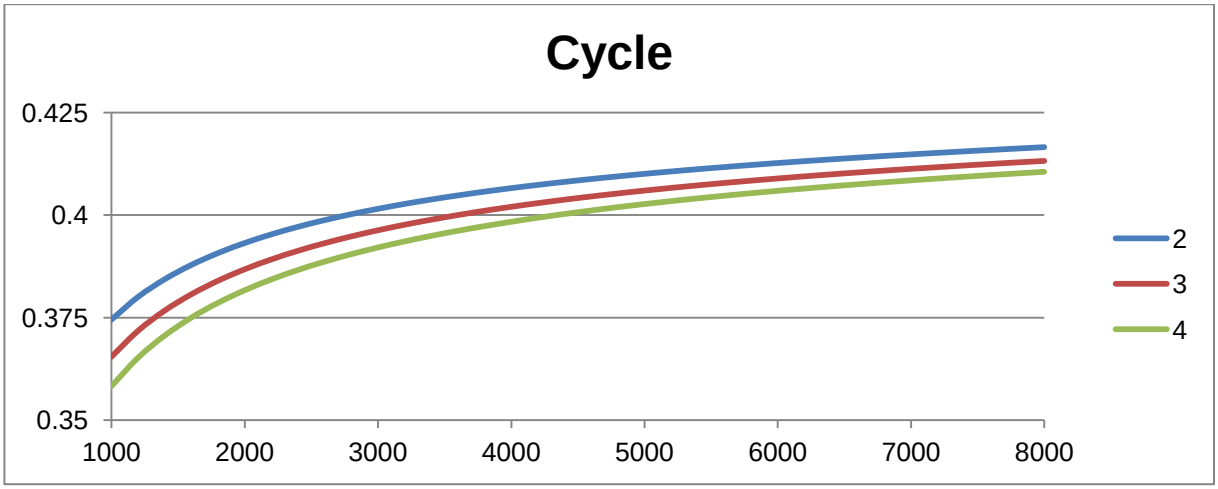
Cycle
0.425
0.4
0.375
0.35
1000
2000
3000
4000
5000
6000
7000
8000
2
3
4

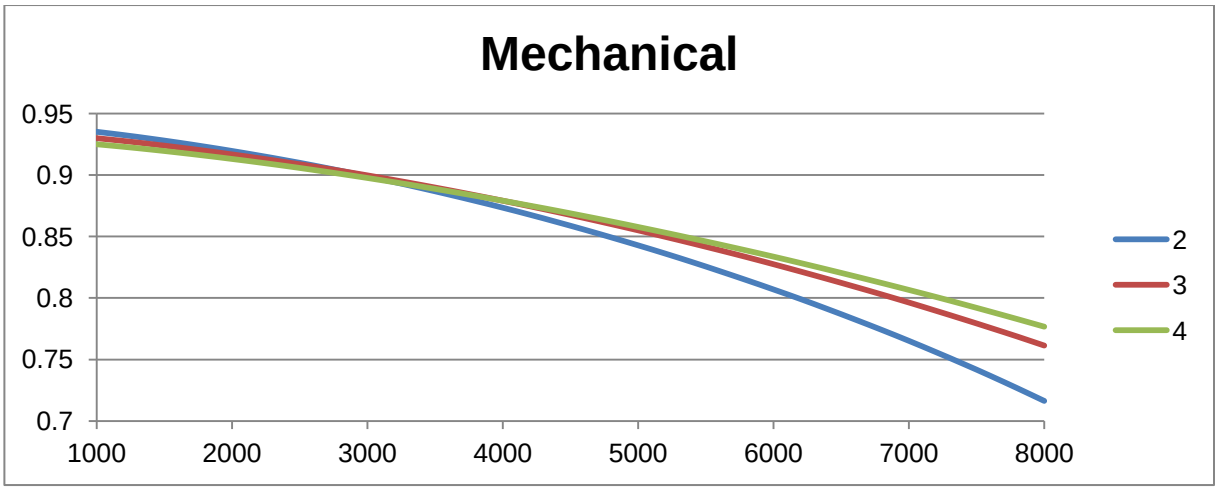
Mechanical
0.95
0.9
0.85
0.8
0.75
0.7
1000
2000
3000
4000
5000
6000
7000
8000
2
3
4

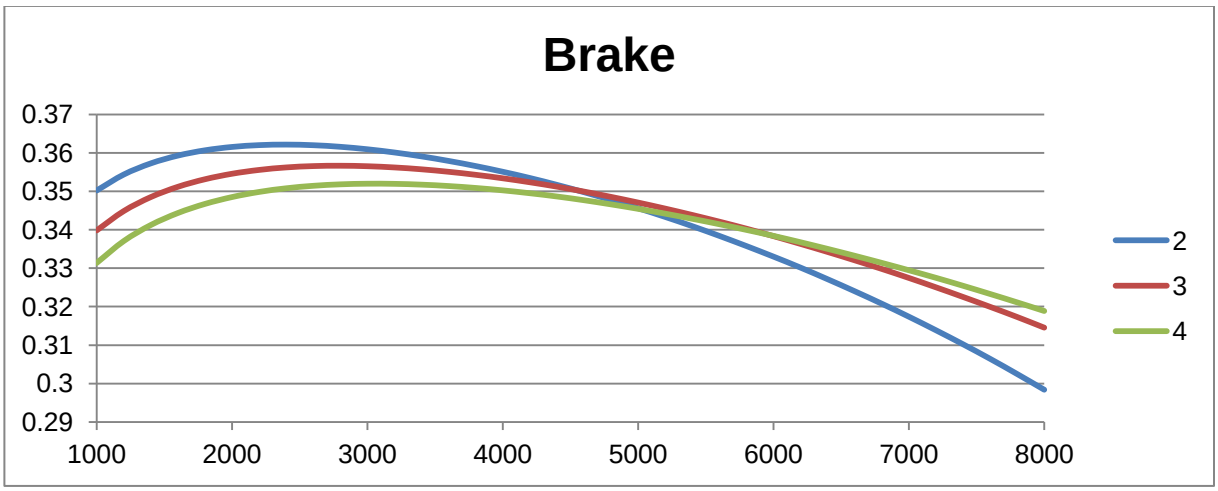
Brake
0.37
0.36
0.35
0.34
0.33
0.32
0.31
0.3
0.29
1000
2000
3000
4000
5000
6000
7000
8000
2
3
4

900 cm^3

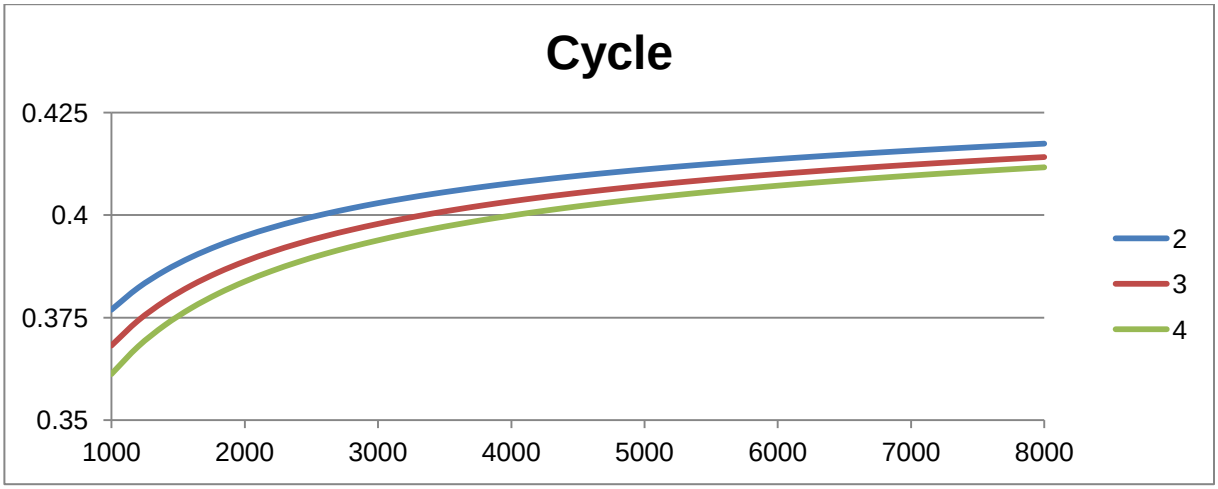
Cycle
0.425
0.4
0.375
0.35
1000
2000
3000
4000
5000
6000
7000
8000
2
3
4

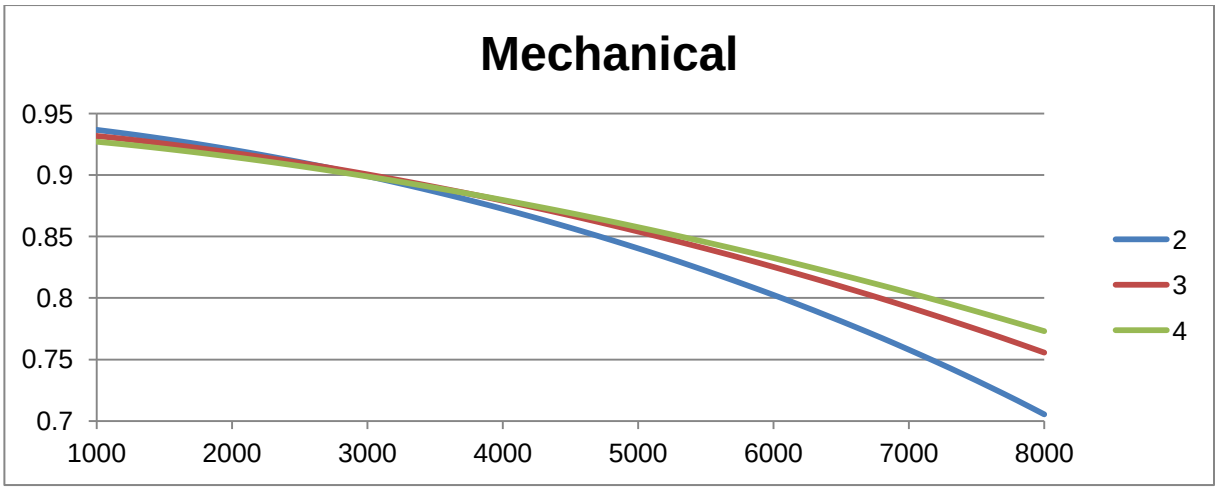
Mechanical
0.95
0.9
0.85
0.8
0.75
0.7
1000
2000
3000
4000
5000
6000
7000
8000
2
3
4

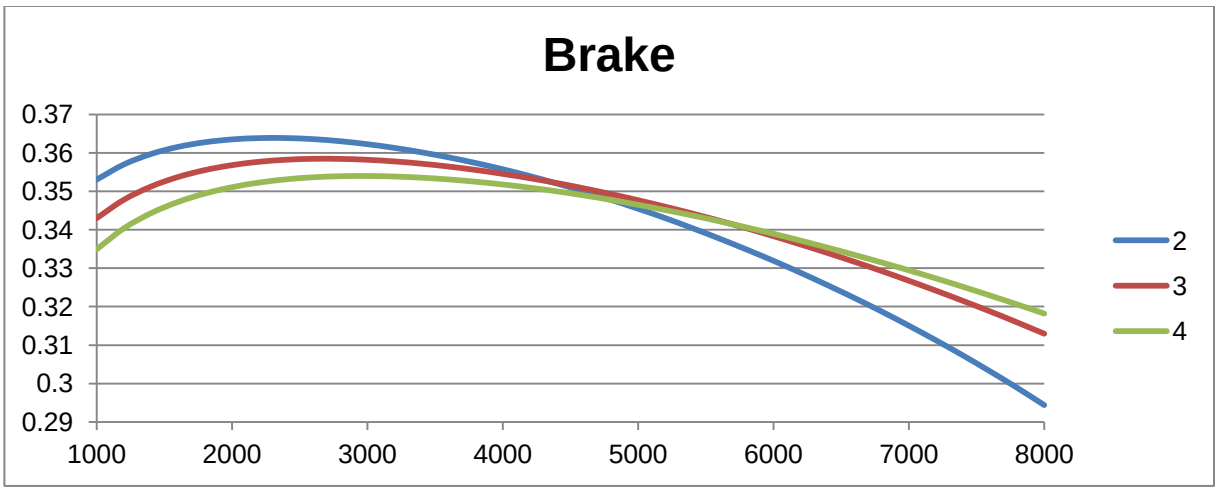
Brake
0.37
0.36
0.35
0.34
0.33
0.32
0.31
0.3
0.29
1000
2000
3000
4000
5000
6000
7000
8000
2
3
4

1000 cm^3

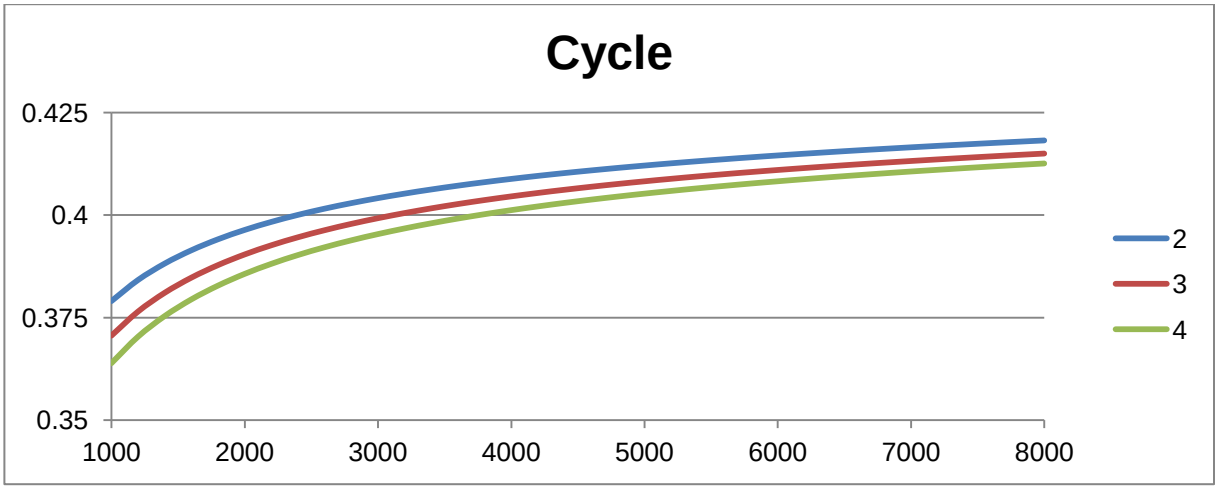
Cycle
0.425
0.4
0.375
0.35
1000
2000
3000
4000
5000
6000
7000
8000
2
3
4

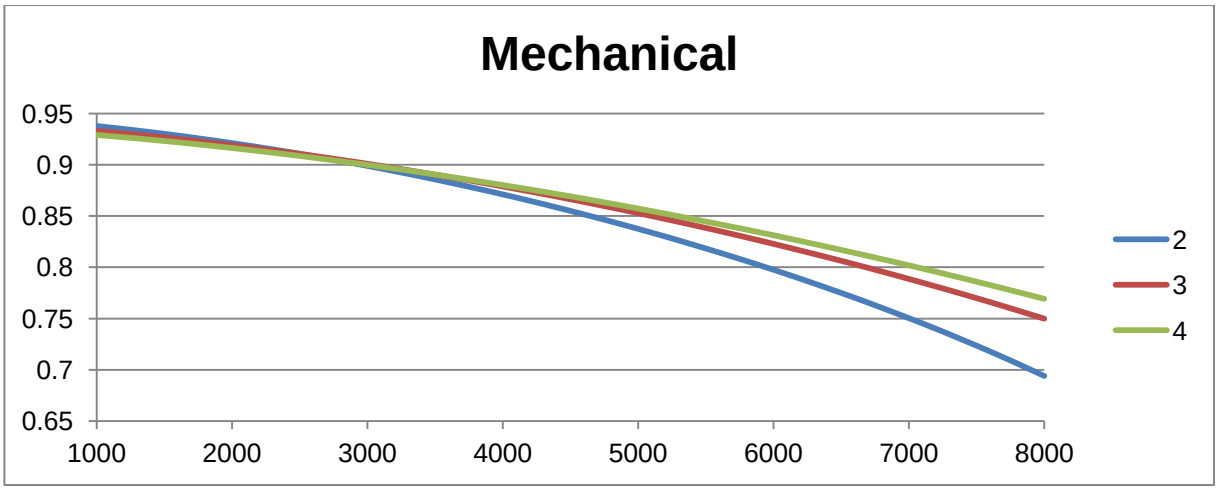
Mechanical
0.95
0.9
0.85
0.8
0.75
0.7
0.65
1000
2000
3000
4000
5000
6000
7000
8000
2
3
4

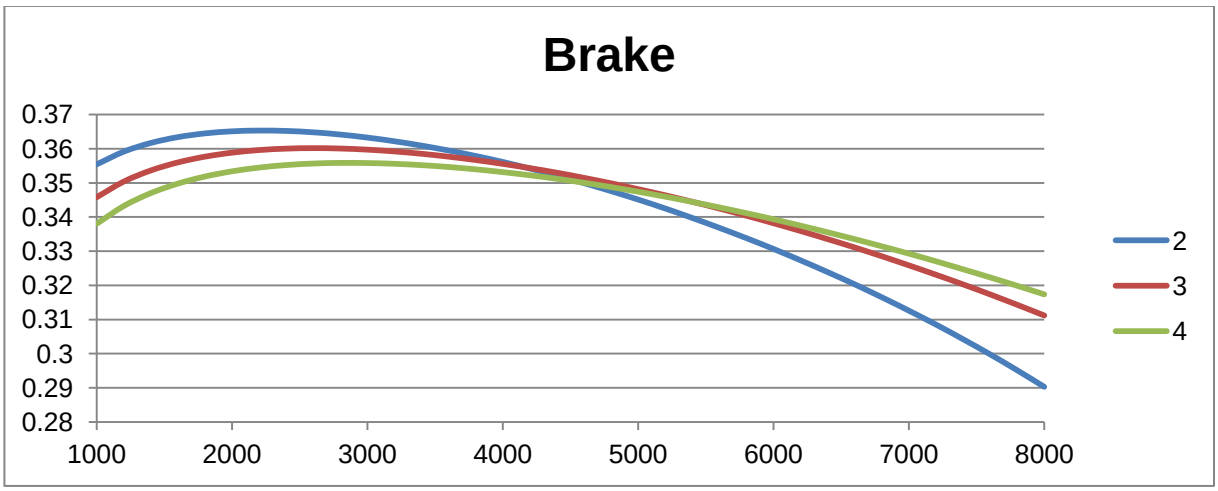
Brake
0.37
0.36
0.35
0.34
0.33
0.32
0.31
0.3
0.29
0.28
1000
2000
3000
4000
5000
6000
7000
8000
2
3
4

1100 cm^3

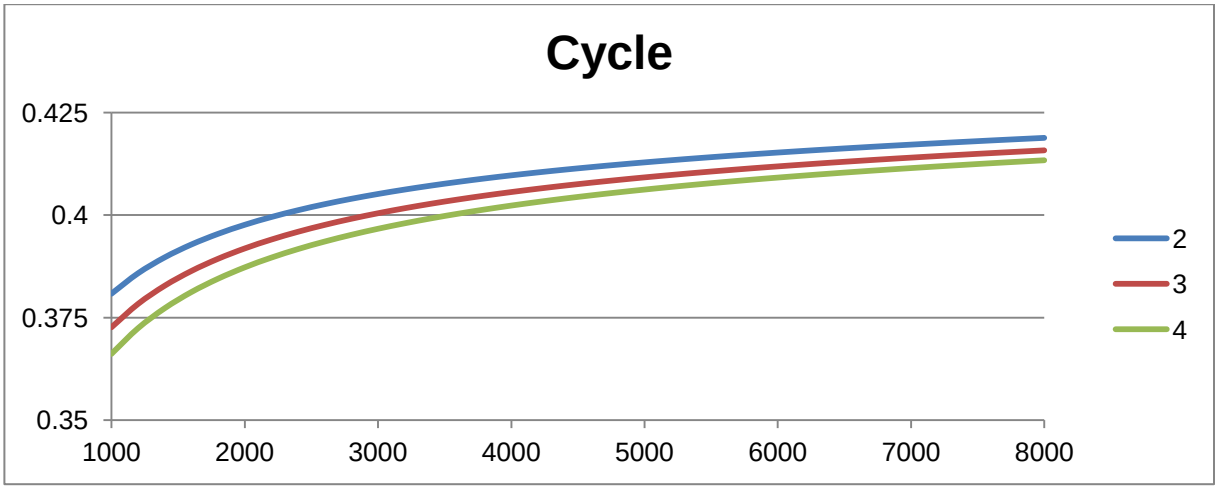
Cycle
0.425
0.4
0.375
0.35
1000
2000
3000
4000
5000
6000
7000
8000
2
3
4

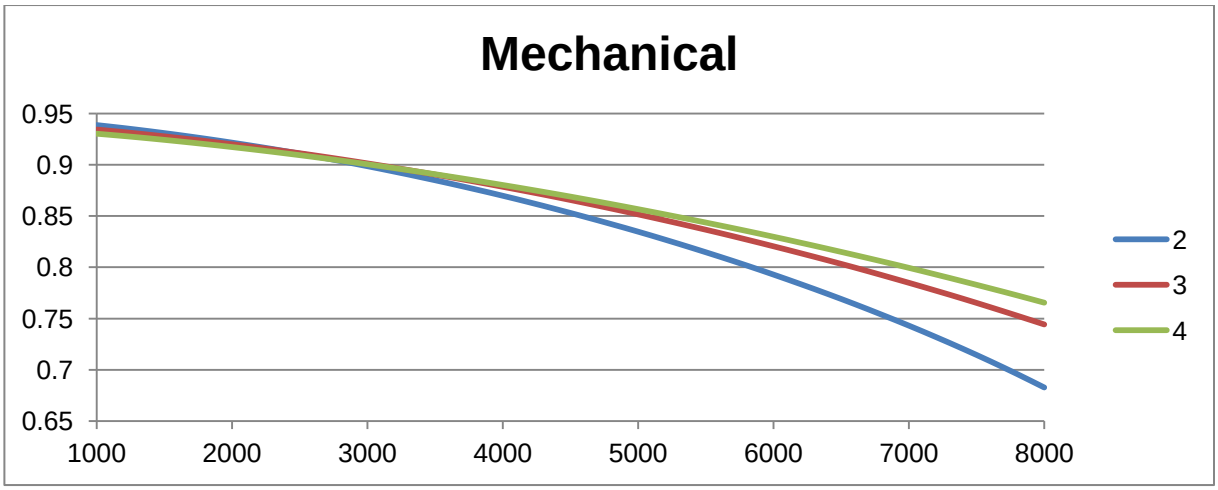
Mechanical
0.95
0.9
0.85
0.8
0.75
0.7
0.65
1000
2000
3000
4000
5000
6000
7000
8000
2
3
4

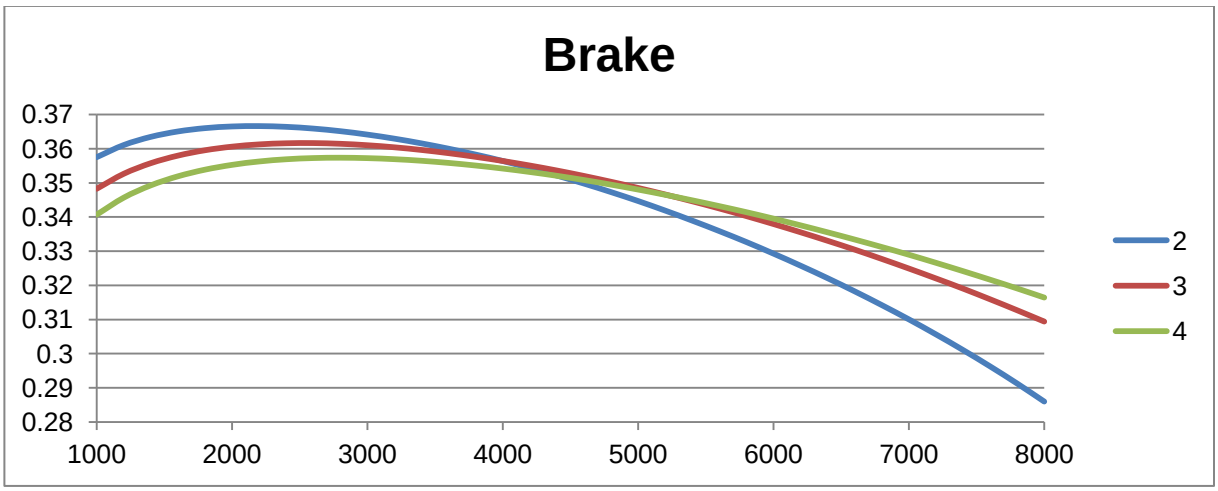
Brake
0.37
0.36
0.35
0.34
0.33
0.32
0.31
0.3
0.29
0.28
1000
2000
3000
4000
5000
6000
7000
8000
2
3
4

1200 cm^3

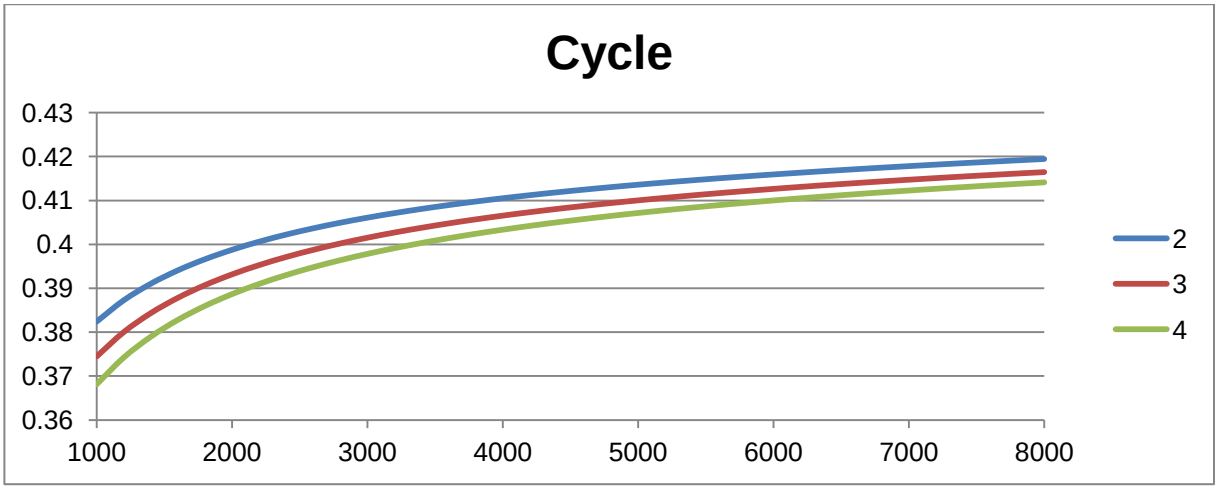
Cycle
0.43
0.42
0.41
0.4
0.39
0.38
0.37
0.36
1000
2000
3000
4000
5000
6000
7000
8000
2
3
4

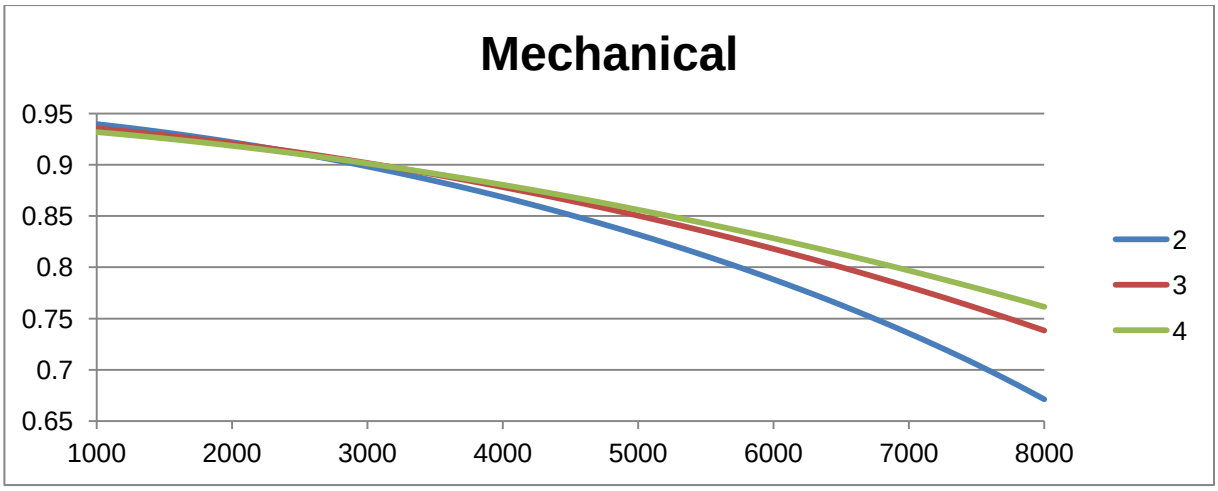
Mechanical
0.95
0.9
0.85
0.8
0.75
0.7
0.65
1000
2000
3000
4000
5000
6000
7000
8000
2
3
4

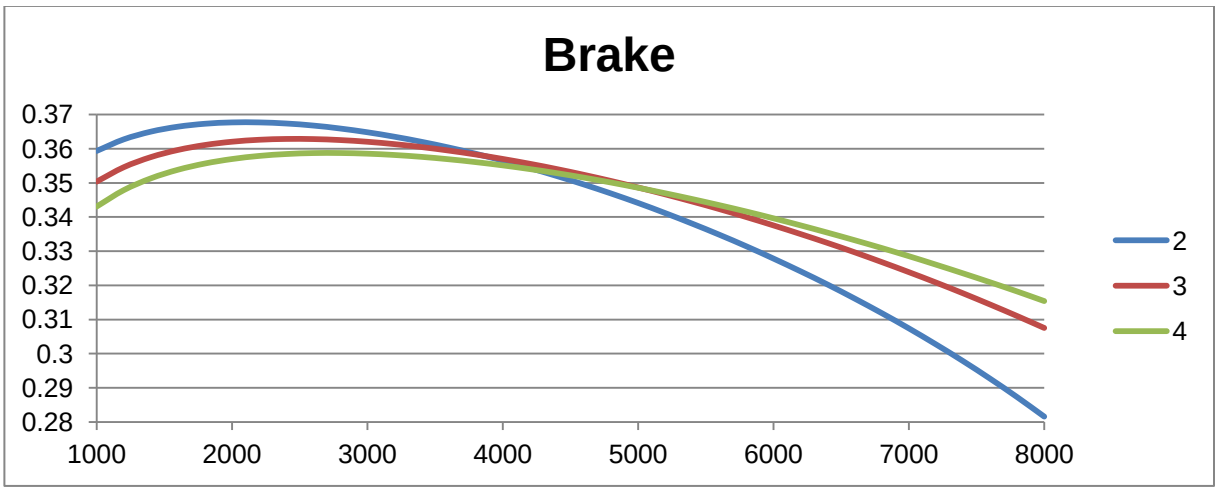
Brake
0.37
0.36
0.35
0.34
0.33
0.32
0.31
0.3
0.29
0.28
1000
2000
3000
4000
5000
6000
7000
8000
2
3
4